AN ABSTRACT OF THE THESIS OF

FRANK SAMUEL MATHEWS for the DOCTOR OF PHILOSOPHY
             (Name)   (Degree)

in   GEOPHYSICS   presented on   July 18, 1969
       (Major)   (Date)

Title: THE ELECTRICAL CONDUCTIVITY OF ATLANTIC TYPE

        PYROMAGMAS FROM MOUNT ETNA, SICILY

Abstract approved: Redacted for Privacy

The electrical conductivity of the pyromagmas from the North-

east Crater of Mount Etna, Sicily was measured over the temperature

range 1032°C to 1071°C and over the frequency range 1 kHz to

400 kHz. Measurements were made using a four-terminal Wenner

array in conjunction with a Wavetek Model 110B portable signal gen-

erator and Hewlett Packard Model 731 portable electronic voltmeters.

The electrical conductivity is of the order of 0.4 mhos/m with

less than 20% dispersion over the frequency range. Over the 40

degree temperature interval the temperature coefficient of resistance

corresponds to an activation energy of 1.5 ± 0.5 eV. The value for

the electrical conductivity of the gas-charged pyromagma is related

to values determined in the laboratory for gas-free melts of lava and

for glasses and slags of similar chemical composition. An original

design of semi-expendable graphite-molybdenum electrode

contributed greatly to the reliability of the measurements.

A chromatographic analysis of the vent gases, and a silicate analysis, a modal analysis and a normal analysis of the lavas are included for completeness. Finally, as an aid to future electromagnetic probing activity, an analysis and estimate are made of the variation of electrical conductivity of pyromagma with depth in a volcanic conduit.

The Electrical Conductivity of Atlantic Type
Pyromagmas From Mount Etna, Sicily

by

Frank Samuel Mathews

A THESIS

submitted to

Oregon State University

in partial fulfillment of
the requirements for the
degree of

Doctor of Philosophy

June 1970

APPROVED:

Professor of Mathematics and Oceanography

in charge of major

Chairman of Department of Oceanography

Dean of Graduate School

Date thesis is presented _____July 18, 1969_____

Typed by Clover Redfern for _____Frank Samuel Mathews_____

ACKNOWLEDGMENTS

facilities in Catania and on Mount Etna.

Finally, the author is most appreciative of the patience, under-standing and encouragement given him by his family during these investigations.

TABLE OF CONTENTS

LIST OF FIGURES

THE ELECTRICAL CONDUCTIVITY OF ATLANTIC TYPE
PYROMAGMAS. FROM MOUNT ETNA, SICILY

INTRODUCTION

Importance of Electrical Conductivity Measurements

In seeking to determine the physical conditions existing within

the earth and the nature of materials present at depth in the earth,

the geophysicist must of necessity use indirect methods since the site

under study is so completely inaccessible.

One of the most powerful approaches to the examination of the

earth's interior is to study the propagation, attenuation, dispersion,

refraction and reflection of waves within these regions. If the waves

being studied are mechanical waves such as those from earthquakes

or from explosions, they provide data on essentially mechanical prop-

erties such as the density and the elastic constants of earth materials.

If, on the other hand, electromagnetic waves are used, they in turn

yield information on the electromagnetic properties of earth mater-

ials, and, in particular, information on their electrical conductivity.

In general, electromagnetic waves attenuate in earth material much

more rapidly than do mechanical waves and thus would appear to have

very limited usefulness. However, for certain frequencies and cer-

tain earth conductivities this is not the case. In particular, the skin

depth δ, defined as the depth in the earth by which a downward

propagating wave is attenuated to 1/e or about 37% of its surface

value is given by

$$\delta \approx (\frac{2}{\sigma\mu\omega})^{1/2} \quad \text{if} \quad \sigma \gg \omega\epsilon \tag{1}$$

where

δ = skin depth in meters

σ = electrical conductivity in mhos/m

μ = permeability of the medium in henrys/m

ω = angular frequency of the waves in rad/sec

ϵ = permittivity of the medium in farads/m.

Thus for a given conductivity, virtually any depth of penetra-

tion is possible provided sufficiently low frequencies are studied.

Conversely, a given frequency will penetrate to great depth wherever

conductivities are sufficiently low.

The spatial variations in electrical properties in the earth are

much greater than are the spatial variations in mechanical properties.

While mechanical properties seldom vary by a factor of more than

two or three, contrasts of 10^5 in the electrical conductivity occur

frequently, and contrasts of 10^6 are not unknown.

Since the electrical conductivity of earth material is governed

primarily by its chemical composition and temperature, any earth

probing for conductivity values or conductivity gradients is indirectly

a probing for chemical compositions and temperatures, or chemical and thermal gradients, provided the pertinent relations between conductivity, temperature and chemical composition have been established.

As would be expected, the electrical conductivity of magmas becomes pertinent whenever electromagnetic probing is performed in volcanic regions. Thus, in exploration for or around geothermal anomalies, or in the study of magmatic intrusions or volcanic magma chambers, a knowledge of the electrical conductivity provides a stepping stone to a knowledge of the related magma properties. If electromagnetic measurements are made with a view to observing temperature changes at depth prior to volcanic eruptions, a knowledge of the electrical conductivity of magma will aid in the interpretation of these measurements. Similarly, a knowledge of magma conductivity would improve the interpretation of electromagnetic measurements made with a view to detecting chemical gradations associated with deep magmatic differentiation. In this way, a knowledge of magma conductivity may yield insights into the mechanisms of mineralization or of volcanic evolution. Thus a knowledge of the electrical conductivity of magma is one more link in the chain of inferences that is leading to a more complete understanding of the nature of the earth's interior.

Need for In-Situ Determinations

The electrical properties of various molten lavas have been
studied occasionally in the laboratory (Barus and Iddings, 1892;
Nagata, 1937; Khitarov and Slutskiy, 1965), but the range of values
quoted by the various authors is so wide (from 10 mhos/m to 10^{-4}
mhos/m at 1200°C) it is difficult to make any generalizations about
the conductivity of these samples. Furthermore, these were pri-
marily studies to detect phase transformations or melting, and the
samples studied, whether natural or synthetically compounded, bear
little resemblance to the "pyromagma"[1] of a volcanic conduit, or to
the envisioned character of the "hypomagma" of a magma chamber.

The pyromagma erupting from volcanic fissures or conduits is
highly gas charged, while the lavas studied in the laboratory were

_____

[1]In constrast with common usage where the term "lava" is used
interchangeably to designate either the molten or solid form of vol-
canic rock, and the term "magma" refers only to subterranean mol-
ten rock, the term "pyromagma" as used here follows the more pre-
cise definition of Jagger (1920, p. 163), namely
> "... the foaming, gas-charged, so-called 'liquid' magma of
> lava lakes, lava flows, and lava blowing cones and wells.
> Its bubbles are alive, spherical and expanding. It is the
> 'lake magma' of Hawaii, believed dependent on the heat of
> gas reaction for its mobility, and is not a simple hydrostat-
> ic fluid, but a silicate glass bubbling with rising gases,
> which burn in the air with visible flames. It is the sub-
> stance described by Daly as 'juvenile gases rising from the
> depths in two-phase mixture with liquid lava.' ... Daly's
> 'two-phase' convection, a circulation dependent on efferves-
> cent vesiculation dissipated surficially, is distinctive of
> pyromagma. "

completely outgassed. Thus field measurements of the electrical

conductivity of pyromagma could differ significantly from the meas-

urements made on lava in the laboratory. The gas bubbles present in

a pyromagma could conceivably affect the electrical conductivity in

at least two ways: (1) by acting as non-conducting voids in a conduct-

ing melt or as a second conducting component dispersed throughout

the conducting melt and (2) by lowering the melt viscosity and conse-

quently raising the mobility of ions involved in the conduction mechan-

ism.

Since the presence of gas in pyromagmas could conceivably

have a significant effect on electrical properties, and since producing

gas-charged melts in the laboratory was not possible, and since, after

all, it was the actual pyromagma issuing from the earth whose elec-

trical properties were sought, it was decided to attempt a field meas-

urement, even though the obstacles were known to be great. Although

failures often go unreported, several are known to have occurred.

The only known successful measurement of pyromagma electrical

conductivity is a preliminary measurement by Palmason and

Bjornsson (1966), in the lava stream of Surtsey, Iceland. They re-

port an electrical conductivity of 0.25 mhos/m for the Surtsey pyro-

magma.

Site Criteria and Selection

The eruptive character of volcanoes varies widely, and in a manner controlled by their magma chemistry. As a general rule, the silica-rich, acidic magmas are highly viscous, and release their gases in a violently explosive manner. The magmas crystallize as rhyolites, dacites, or andesites. On the other hand, the silica-poor, basic magmas which crystallize as basalts, trachytes, and trachyandesites tend to be much less viscous, and release their gases relatively quietly. Although all types are capable of violent explosive activity, the silica-rich types are predominantly explosive, and lava flows are few. The silica-poor types, however, show a predominance of flow activity.

Although, as a long term project, it would be desirable to know and understand the electrical conduction characteristics of all the pyromagma types, it was decided that for this investigation, only one type would be studied. Until the measurement techniques were refined, and until experience was gained in the evaluation of volcanic hazards, it was felt essential to limit attention to one of the more basic lavas. It was also felt that instrumentation problems would be sufficiently severe in themselves without having to cope with complex interpretation problems. Therefore every effort was made to locate exposed pyromagma which should have a relatively simple geometry,

rather than studying a subsurface melt involving a more complex geometry. This decision to study exposed pyromagma automatically limited attention to lava lakes or flows.

A few permanent lava lakes do exist, but their very size imposes severe limitations on the experimental techniques which can be used. The radiation from the lake surface is so intense that remote instrumentation becomes essential and large manpower requirements become the order of the day.

Quiet, accessible lava flows are few and infrequent. At the beginning of this study, the only known flow was on Surtsey, Iceland. Plans were laid to study this flow, but activity ceased before all the equipment needed could be obtained. Flows were also reported on Stromboli, near Sicily and a little later reports came of a flow on Mount Etna, Sicily. The Etna reports could not be confirmed, but a representative of Westinghouse Electric Corporation who was in the Malta area verified personally the existence and suitability of the Stromboli lava. Since the possible existence of two flows in the Sicily area increased the chances of success, the decision was made to attempt measurements on one or both of these flows.

The equipment was shipped on the same day that this decision was made, but by the time it had cleared Italian customs, the Stromboli flow had already ceased. However, the Etna flow was located, and found to be both accessible and persistent. Also, since all recent Etna flows have been basaltic, the rather pragmatic choice of Etnean pyromagma proved to be, in the end, a most auspicious one.

EXPERIMENTAL PROCEDURES

Scope of Investigations

Since as complete as possible an understanding of the electrical conductivity was desired, and since it was hoped that the results could be correlated with similar studies in other volcanoes at future times, it was decided to undertake the following specific tasks.

(a) To determine the electrical conductivity of the Etna pryo-magmas by one or more techniques, and to cover as wide a frequency range for as many different conditions of temperature and rock chemistry as were possible on Etna at the time.

(b) To record the chemical parameters and temperature of this particular Etnean pyromagma for future comparison with similar data from other eruptions.

The frequency range chosen was from 1 kHz to 400 kHz. These limits were chosen on the basis that below 1 kHz skin depths would be greater than any conceivable lava flow depth. The upper limit was chosen so as to include all geophysically useful frequencies.

The design of equipment for the expedition posed several problems. There were the usual compromises involved in choosing or building equipment which would be insensitive to shock, gas and heat, but which would be sensitive electrically. There was also the

problem of designing for unknown conditions. No amount of inquiry

was able to secure detailed information on site conditions. Equip-

ment design and selection therefore called for imaginative planning,

and the hope that any unanticipated field conditions could be taken

care of by resourceful improvisation at the site. The results of these

experiments justify the guesses that were made.

Temperature Measurements

Pyromagma temperatures differ considerably from volcano to

volcano, and vary with time at a given volcano. Usually they are in

the neighborhood of 1000° C to 1100° C, (Rittmann, 1963a).

Earliest measurements of the temperature of Mt. Etna pyro-

magmas by Bartoli (1892) indicated values ranging from 970° C to

1060° C. Oddone (1910) reported 1200° C and Platania (1922) meas-

ured values from 940°C to 1,000°C between 1911 and 1918. More recent

measurements by Tazieff (1963) yielded values from 1110° C to

1120° C. Over such a temperature range either optical pyrometers,

platinum resistance thermometers, or platinum-platinum+rhodium

thermocouples should be suitable. However, the literature of vol-

canology is replete with reports of unrealistic or unsatisfactory tem-

perature values.

Optical pyrometry is, in general, unsatisfactory because either

burning surface gases enhance the molten-surface radiation, or the

black crust which forms rapidly on the surface modifies the surface

radiation. Resistance thermometers and thermocouples yield reli-

able temperature values provided they remain intact, but they are

relatively fragile instruments in their usual form, and the breakage

rate during insertion, positioning, or removal from the viscous surg-

ing pyromagma is consistently high. All too frequently, the volcan-

ologist's entry under "magma temperature" reads "instrument lost

in lava. "

With these practical problems in mind it was decided to borrow

from the technology of the steel industry where it is recognized that

the destruction of the temperature transducer is almost inevitable,

and the design approach therefore concentrates on expendability. The

system chosen incorporated the Leeds and Northrup Mark III TEMTIP

expendable thermocouple, and a Leeds and Northrup Model 8718A

permanent, lightweight, orientable, five-foot immersion probe with

a fifteen-foot ruggedized, matched extension cable. EMF's were

measured with a portable Leeds and Northrup potentiometer Model

8696, featuring manually operated reference junction compensation,

20 microvolt resolution, and 66 microvolt accuracy.

As shown in Figure 1a the TEMTIP expendable cartridge in-

corporates an electrically welded platinum-platinum +13% rhodium

thermocouple accurately positioned in a quartz U-tube, mounted in a

low thermal conductivity refractory body, and protected by a copper

Copper protective cap

Cardboard tube
(1/4" walls)

Cylindrical female
ring receptacles

Ceramic support
for thermocouple

Quartz U-tube
housing thermocouple

(a)

90° - 180° adjustable
universal joint

Replaceable stainless-
steel housing for
TEMTIP receptacle

Ruggedized, thermally
compensated cable

(b)
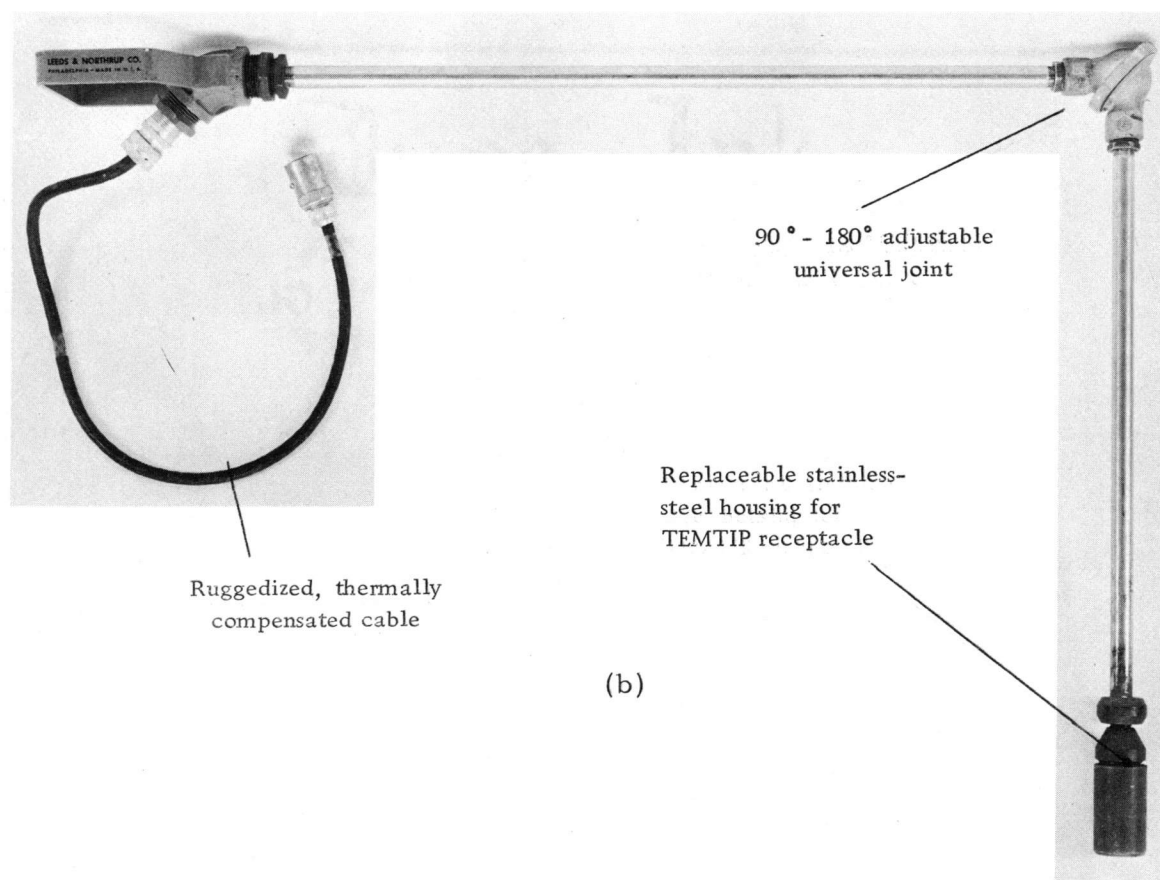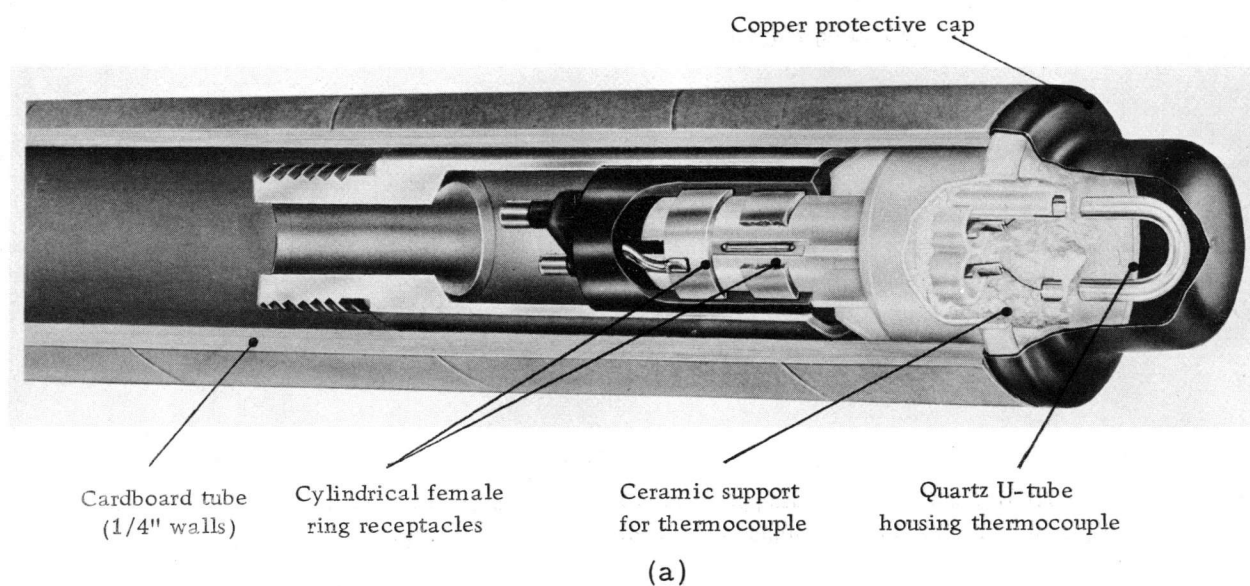
Figure 1.   The expendable-thermocouple temperature probe.
(a) Cutaway view of expendable TEMTIP.
(b) View of permanent probe.

shroud which melts after insertion in the lava. A two foot long heavy cardboard tube with 1/4 inch walls forms a skirt on the rear of the TEMTIP unit and very effectively shields the thermocouple terminals and permanent probe from thermal damage. The tube charring process is sufficiently slow, and the thermal conductivity of the char is so low that even after a full two minute immersion in a 1000° C melt, the receptacle end of the permanent probe is still below 100° C. Response time of the low thermal capacity thermocouple is of the order of one second. Thus observation time is governed solely by the speed of the potentiometer operator. Cost per TEMTIP in October 1967 was a mere 56 cents.

The permanent probe, shown in Figure 1b is of stainless steel construction. An adjustable universal union allows adjustment of the angular position of the TEMTIP in the melt. Terminals are all replaceable in the event of thermal damage. The extension wires are of copper and a special Leeds and Northrup alloy designed to have the same thermoelectric power as the platinum-platinum +13% rhodium thermocouple over the ambient temperature range.

The TEMTIP probe is ideally suited for variable depth measurements. The small volume of the actual transducer, and the good thermal insulation provided by the cardboard tube make it possible to sample a submerged volume without interference from the melt at other levels.

Gas Analysis

The analysis of volcanic gases has long claimed the attention of

volcanologists because of the dominant role which the gases play in

the eruptive process. Major surveys and analyses of Mt. Etna gases

have been made by Silvestri (1869) for the period 1855-1865, by

de Fiore (1922), covering the period from 1865 to 1921 and most re-

cently by Tazieff (1968). Considerable doubt has been cast on most

of the early measurements as a result of the work of Tazieff and

Tonani (1963) on the temporal variation of the gaseous constituents.

Using a newly developed gas chromatographic field kit, they were

able to make rapid simultaneous samplings of several gases in the

mouth of a crater in explosive activity and were able to demonstrate

a rapid temporal and spatial variation in gas concentrations, related

to the explosive activity, but different for different gases. Thus all

previous samplings were concluded to be suspect unless samples were

taken simultaneously, and even then were quite incomplete since they

only showed gas concentrations at a particular moment and point.

For gas measurements on Etna it was decided to use the gas

chromatographic equipment described and tested by Elskens, Tazieff

and Tonani (1964) since they had demonstrated the accuracy and re-

liability of the equipment by intercomparison of the new field method

with the traditional laboratory methods. The equipment,

manufactured by Draeger and Company, Lübeck, Germany is shown in Figure 2a. The calibrated analyzing tubes, each specific for a particular gas and sealed until ready to use, show a quantitative color change when a predetermined volume of gas is drawn through the tube by the calibrated hand pump. Tubes for the analysis of CO, CO_2, CH_4, H_2, H_2S, H_2S+SO_2, HCl, NH_3, and SO_2 were procured for the expedition.

In order to simplify gas collection, a two foot diameter collecting cone was fabricated from 20 gauge stainless steel and a compression type tubing connector was fitted into its apex.

Since the calibration accuracy of the Draeger tubes becomes questionable above 50°C, it was anticipated that provision would have to be made for cooling the gas samples. With this requirement in mind, several eight-foot lengths of 1/4 inch stainless steel tubing and a 32 foot coil of the same tubing (overall dimensions approximately one foot diameter and one foot high) were fitted with compression fittings so that a simple wind cooling system could be improvised once the site requirements became known. The pumping impedance of the maximum tube length was checked before the field party left the United States in order to be sure that the performance of the calibrated pump was not impaired.

The collecting cone and final configuration of the air-cooled radiator as it was used in the field are shown in Figure 2b. All of
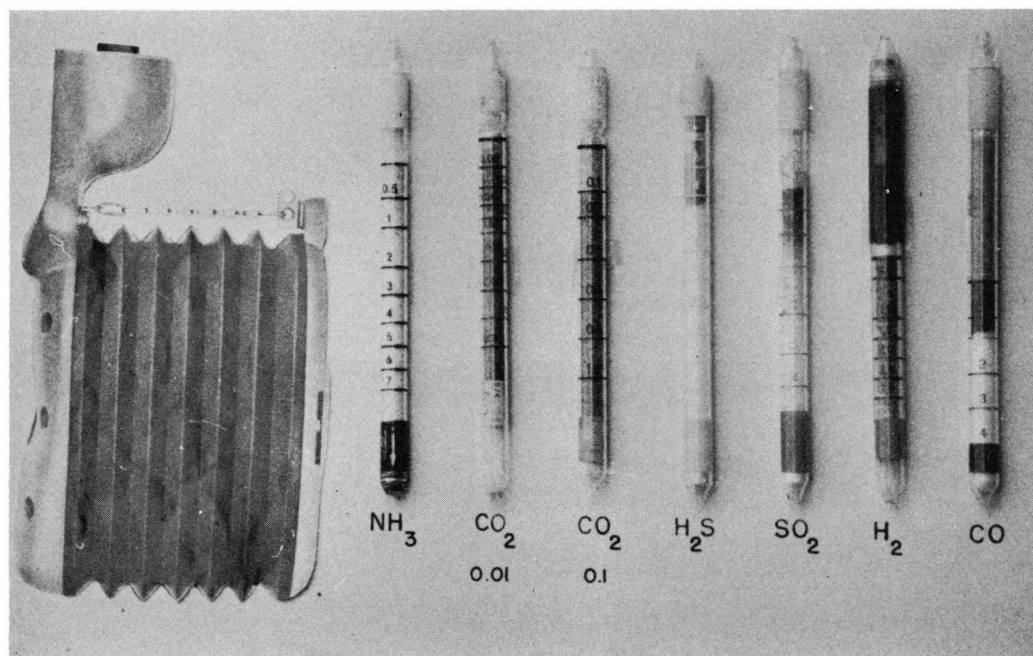
(a)

(b)

Figure 2. Portable gas chromatographic kit.
    (a) Draeger pump and activated tubes.
    (b) Gas collection and cooling assembly.

this cooling assembly was subsequently lost under a sudden lava upsurge, but fortunately not before the last Draeger tube had been used and the gas measurements completed.

Conductivity Measurements

Selection of Methods

A wide variety of methods exists for the measurement of electrical conductivity at audio and radio frequencies. Keller and Frischknecht (1966), Watt, Mathews, and Maxwell (1963), Wait and Conda (1958), and Sunde (1949) have discussed and summarized those which are best applicable to earth materials in situ.

Because of the anticipated extreme danger of the environment in which the measurements were to be made, and because of the expected relative shallowness of any available lava streams, it was felt that only two methods out of the large number normally available gave any hope for success. If the magma were immediately accessible, the so called "four-terminal method" gave promise of fast reliable measurements. If, on the other hand, the magma had roofed itself over and were flowing in a tube, the so called "loop-loop induction method" seemed most feasible. Preparations were therefore made for both four-terminal and loop-loop induction measurements.

Although working lava tubes were found to exist at the site on

Mt. Etna, and although they were usually strong enough to bear a man's weight, the loop-loop induction method had to be discarded because the hot gases escaping through cracks in the tube roof began to damage the equipment in the time required to level the loops on the rough aa surface. Consequently, all measurements were made in the open magma stream using the four-terminal method. (This restriction to open flowing magma automatically restricted the range of magma temperatures available for study.)

The Wenner Four-Terminal Array

In the four-terminal method of electrical conductivity measurement, one pair of electrodes is used to establish a current through the conductor under study, and a second pair of electrodes samples the potential difference established between two other points in the conductor. The electrical conductivity of the medium is proportional to the ratio of the current to this potential difference. Several different electrode configurations have been developed, each designed to reveal a particular type of conductivity contrast to advantage or to facilitate coping with large expanses of terrain. Since the magma stream to be studied here was expected to be fairly narrow and shallow and relatively homogeneous, it was felt that the simplest and most common of all these arrays, the Wenner array (Wenner, 1916) could be used. The Wenner array consists of four collinear, equally

spaced electrodes, with the outer pair establishing the current and the inner pair detecting the desired voltage as shown in Figure 3a.

In order to calculate the potential difference which will appear between the inner two electrodes of a Wenner array, consider first the case of the potential distribution resulting from a current I injected as a point source on the surface of a homogeneous half-space of constant electrical conductivity σ. Referring to Figure 3b, the current source is placed at 0, the origin of a spherical coordinate system. We require that the potential vanish an infinite distance from the source, namely $\lim_{r \to \infty} V(r, \theta, \phi) = 0$. We also require that no current cross the boundary except at the source point, namely $\frac{\partial V}{\partial \theta}(r, \pi/2, \phi) = 0$ for all $r > 0$. The potential within the half-space must be independent of θ and ϕ because of the symmetry of the configuration and the limitation on the surface current. In the volume of the half-space excluding the source point Laplace's equation holds and thus is of the form

$$\frac{\partial}{\partial r}(r^2 \frac{\partial V}{\partial r}) = 0 \tag{2}$$

Hence

$$V = C_1/r + C_2 \tag{3}$$

where C_1 and C_2 are constants.

In order that the potential vanish an infinite distance from the

$10 \, \Omega \; \pm \, 1.0\%$
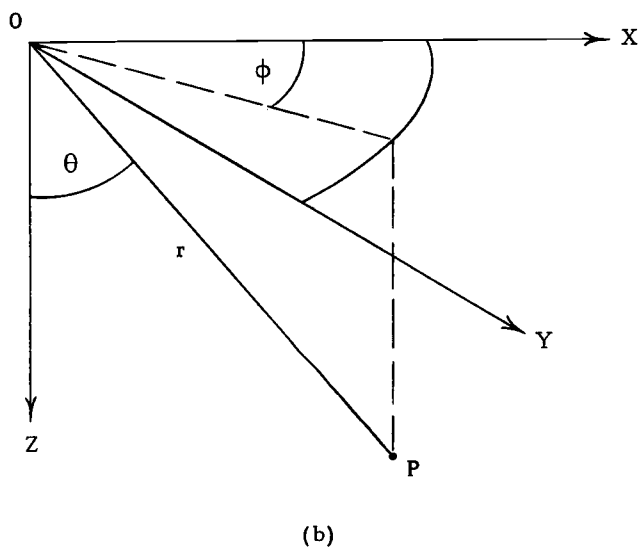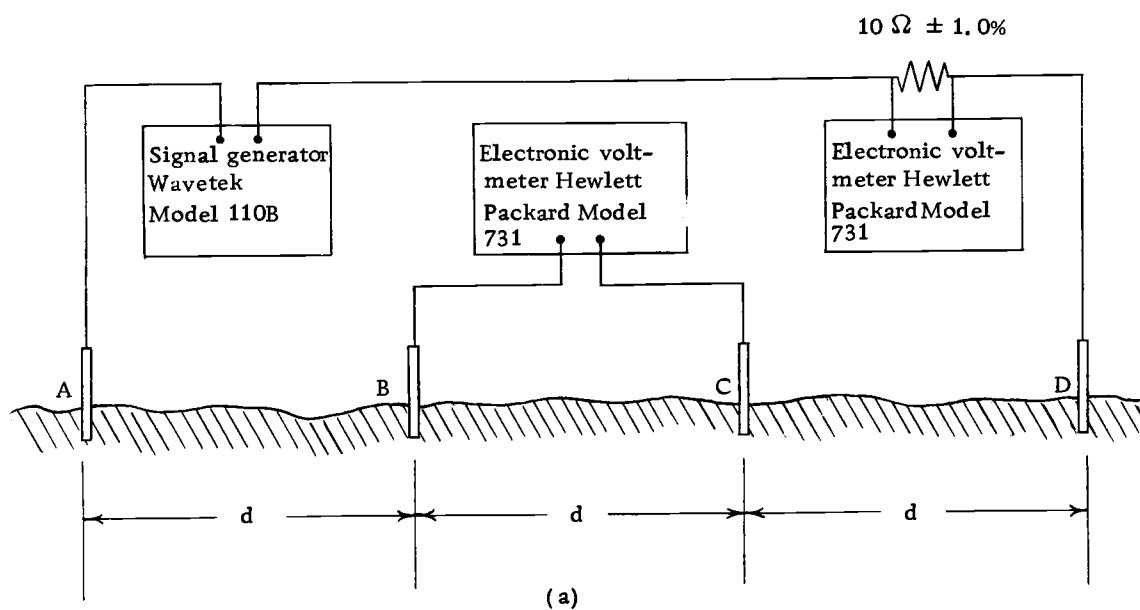
Figure 3. The Wenner four-electrode array.
(a) General configuration
(b) Electrode coordinate system

source point, C_2 is set equal to zero.

In order to evaluate C_1, consider now the potential gradient E about the point 0. If the medium obeys Ohm's Law we have

$$E = j/\sigma \tag{4}$$

where

E = potential gradient, expressed here in Volts/meter

j = current density, in Amperes/meter^2

σ = electrical conductivity, in mhos/meter

Again because of symmetry requirements, the current from the point 0 must be radial, and hence

$$j = I/2\pi r^2 \tag{5}$$

where I = current into the medium, in Amperes.

Hence, substituting Equation (5) into Equation (4) we have

$$E = I/2\pi r^2 \sigma \tag{6}$$

But

$$E = -\partial V/\partial r = C_1/r^2 \tag{7}$$

Hence from Equations (6) and (7) we have

$$C_1 = I/2\pi\sigma \tag{8}$$

Therefore, from Equation (3) we have for the potential about a point, the current I being considered positive when it is into the ground

$$V = I/2\pi\sigma r \qquad (9)$$

Referring now to Figure 3a, the potential at point B due to current source I at point A and current source -I at point D is, applying Equation (9) twice

$$V_B = I/2\pi\sigma d + -I/2\pi\sigma \cdot 2d$$
$$= I/4\pi\sigma d \qquad (10)$$

Similarly, the potential at point C due to these same current sources is

$$V_C = I/2\pi\sigma \cdot 2d + -I/2\pi\sigma d$$
$$= -I/4\pi\sigma d \qquad (11)$$

Finally, the potential difference V_{BC} detected at the voltage dipole BC is

$$V_{BC} = V_B - V_C$$
$$= I/2\pi\sigma d \qquad (12)$$

The electrical conductivity is thus given by the expression

$$\sigma = I/2\pi V_{BC} d \qquad (13)$$

and for a given electrode spacing is thus determined uniquely by the

I to V_{BC} ratio.

If the electrical conductivity of the medium under study is in-homogeneous or non isotropic, the I to V_{BC} ratio can still be used to define an apparent conductivity σ_a such that

$$\sigma_a = I/2\pi V_{BC}d \qquad (14)$$

Thus the apparent conductivity is seen to be that value of conductivity which for the homogeneous, isotropic case gives rise to the same I to V_{BC} ratio as appears in the inhomogeneous, non isotropic case.

For this investigation the current source chosen was a WAVE-TEK Model 110B function generator. This transistorized, portable signal generator develops sine, square, or sawtooth waves from five Hz to five MHz with an adjustable regulated output of up to one Volt peak-to-peak into 600 Ohms. The current was found by monitoring with an electronic voltmeter the voltage across a 10 Ohm ± 1% resistor in the current dipole circuit. The voltage V_{BC} across the inner dipole was monitored with a second electronic voltmeter, and the apparent conductivity σ_a could thus be found as a function of the signal generator frequency. For these two voltage measurements, Hewlett Packard Model 731 electronic voltmeters were chosen. These are lightweight, rechargeable battery powered units, with a maximum full-scale sensitivity of 1.0 milliVolt ± 3% between two Hz

and five MHz.

It should be stressed that the apparent conductivity σ_a thus found is an A. C. conductivity and should therefore properly be denoted as $\overline{\sigma_a}$ since the phase relations between V_{BC} and I are generally not determined in this method.

A further observation of significance is the fact that this method avoids the overvoltage problems inherent in the frequently used two-electrode method where voltage and current electrodes coincide. In the four-electrode method, electrode potentials undoubtedly appear at the current electrodes but have no influence on the conductivity determination since this calculation is based on the actual potential difference V_{BC} and the actual current flowing in the medium, rather than on any current which might have been flowing if electrode potentials had not been present at the current terminals. In the case of the voltage terminals, electrode potentials also no doubt appear. However, they are negligible under the low current conditions inherent in the use of a very high input impedance electronic voltmeter for monitoring V_{BC}.

Electrode Design

Although satisfactory electrode design was essential to the success of the field measurements, the design criteria were so stringent there were doubts that suitable materials could be found.

Imbò (1964) and Walker (1967) had reported lava viscosities of 4×10^4 poises and Oddone (1910) had reported lava temperatures of 1200°C. It was therefore necessary for the electrodes to be of a material which retained good mechanical strength up to at least 1200°C. The gas and petrographic analyses of de Fiore (1922) revealed the chemically active nature of the hot silicate melt. Thus it was necessary to choose electrodes with high corrosion resistance. Furthermore, the electrodes would have to withstand considerable thermal shock during insertion in the melt, since the requirement of personal safety for the operator would preclude any lengthy insertion activity. Finally, of course, the electrodes had to be conductive.

These criteria effectively eliminated most of the usual choices of material. Copper or steel could not be used because they melted or softened well below the lava temperature. Even most of the stainless steels had softening points below 1150°C. The few which retained appreciable strength up to 1200°C were high chromium steels, and thus particularly susceptible to the sulphur in the melt. (As emergency back-up, in case all other electrode choices failed, type 316 stainless steel and type 446 stainless steel electrodes were taken to Etna. These are high molybdenum, high nickel, or high chromium, low carbon stainless steels with good mechanical strength up to 1200°C and superior corrosion resistance. However, the corrosion resistance of even these special stainless steels starts to decrease

above 1000°C. Subsequent experience on Etna confirmed the fears

about corrosion as the electrodes very quickly developed a high stake

impedance and became useless.)

Although zirconium had good high temperature strength it was

rejected because above 800°C it readily oxidizes and forms the hard

insulating film so useful in electrolytic capacitors. Titanium, on the

other hand, has excellent high temperature corrosion resistance but

was rejected because its high temperature strength is not even as

great as that of steel. Graphite was rejected as marginal both in

strength and chemical activity. Refractories such as alumina or

beryllia, even though completely adequate in strength and chemical

inertness were rejected both as stiffeners to weaker conductors or as

insulating supports because of their great weakness to thermal shock.

Silicon carbide and tungsten carbide were rejected for the same rea-

son. Platinum was considered marginal on strength, and was re-

jected because of cost. Tungsten was rejected on the advice of U. S.

Bureau of Mines personnel (Poole, 1967) because of its tendency to

form the carbide and thus become brittle.

The choice finally narrowed to molybdenum because of its su-

perior melt characteristics. Its excellent high temperature strength,

good thermal shock characteristics, and anticipated low chemical

activity in the silicate melt gave molybdenum a decided advantage

over any other material considered. Its only drawback seemed to be

its susceptibility to high temperature oxidation. Since molybdenum oxide has an extremely high vapor pressure, it was certain that any portion of the molybdenum electrode protruding above the melt would rapidly oxidize in the hot atmosphere and sublime away. Thus even molybdenum would not be satisfactory as electrode material unless some way could be found to counter the atmospheric oxidation problem. It was finally decided that the best hope for success lay in shrouding the upper portion of each electrode with graphite. The expendable graphite portion would naturally burn, but in so doing would envelop the molybdenum electrode either in an inert CO_2 atmosphere or in a reducing CO atmosphere. In either case, oxidation of the molybdenum would be inhibited.

The finalized electrode design utilizing this principle is shown in Figure 4. The one inch graphite rod was first drilled and reamed to accommodate the 3/8 inch diameter molybdenum electrode. The graphite was then slit down half its length so that it could be firmly clamped to the molybdenum electrode by means of a thumbscrew operated stainless steel hose clamp. (Field replacement of the burnt graphite sleeves was thus possible without the use of any tools.)

Assembly of the electrodes into a final four-terminal configuration was not possible until the dimensions and accessibility of the lava site had been determined. However, the Westinghouse Electric employee on Malta who was sent to Sicily for this purpose, returned

1/4" x 8" stainless-steel tubing, press-
fitted into molybdenum rod end, to
serve as banana jack

Silver solder
fillet

1" x 12" split graphite
cylindrical sleeve*

3/8" x 30" molybdenum rod
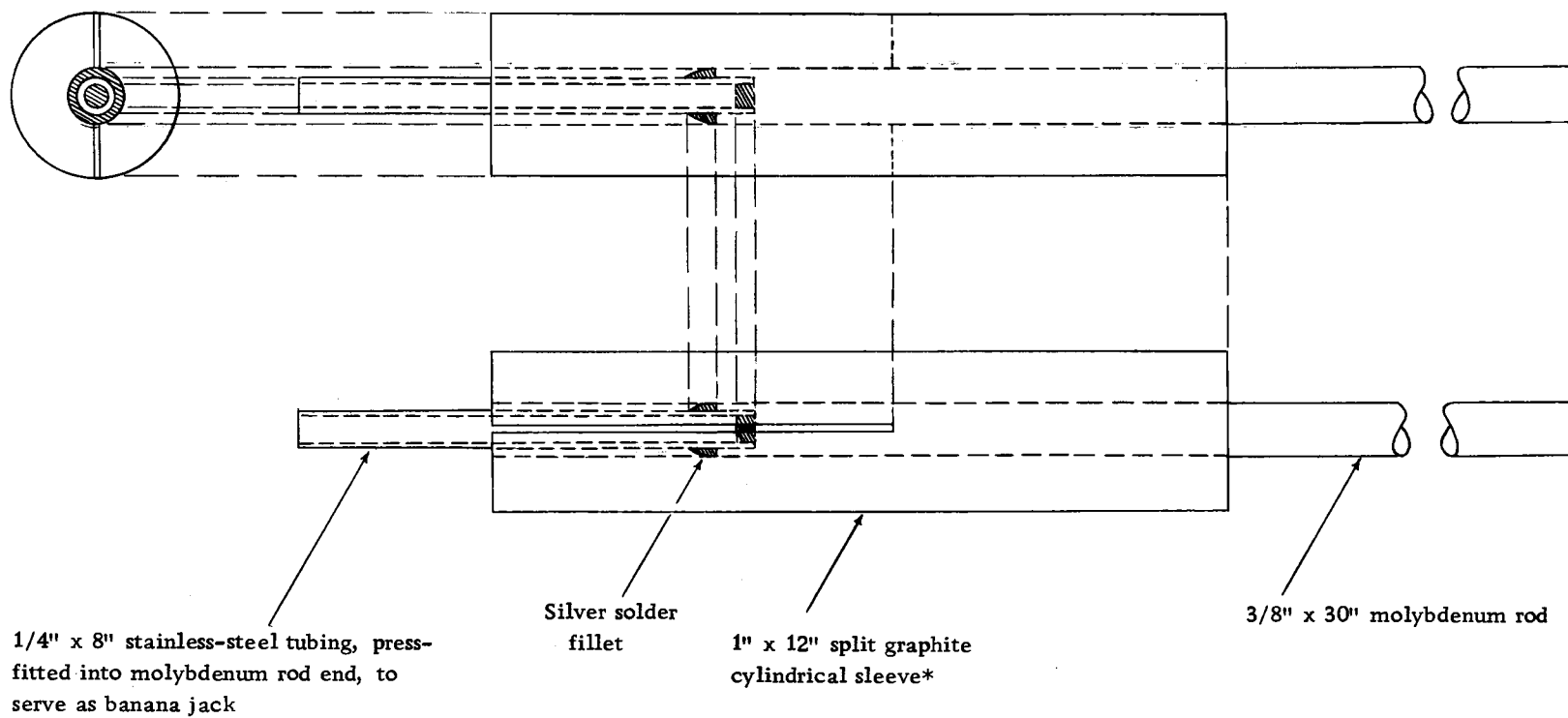
*
  Stainless-steel 1" hose clamp secures graphite sleeve to molybdenum electrode

Figure 4. Electrode detail for Wenner four-electrode array.

after a week without ever having gotten close enough to any flows to obtain the necessary information. Since there was no certainty of the flow continuing it was essential to begin experiments as soon as possible. It was therefore reluctantly decided to ship the electrodes to Sicily, and finalize the probe design after personally reconnoitering the site. This final probe assembly which was constructed near the site is shown in Figure 5a without the radiation reflector, and in Figure 5b in use with the radiation reflector attached. Although crude in appearance, it was reasonably sophisticated in conception, and worked to perfection.

Sonde-Type Four-Terminal Probe

A more sophisticated four-terminal probe was also developed and tried. This was essentially a miniaturized high temperature version of the well-logging resistivity sonde. The well-logging sonde is built with an overall cylindrical symmetry. Four ring-shaped electrodes are mounted concentric with and normal to the axis of a cylindrical support. When used with the cylinder axis vertical, the upper and lower electrodes form the current dipole and the intermediate electrodes form the voltage detecting dipole. For the lava studies, the support cylinder was a six inch length of 1/4 inch thin-walled fused quartz tubing. The electrodes were of platinum. The platinum lead wires were carried internally in the tube and spaced by four-hole
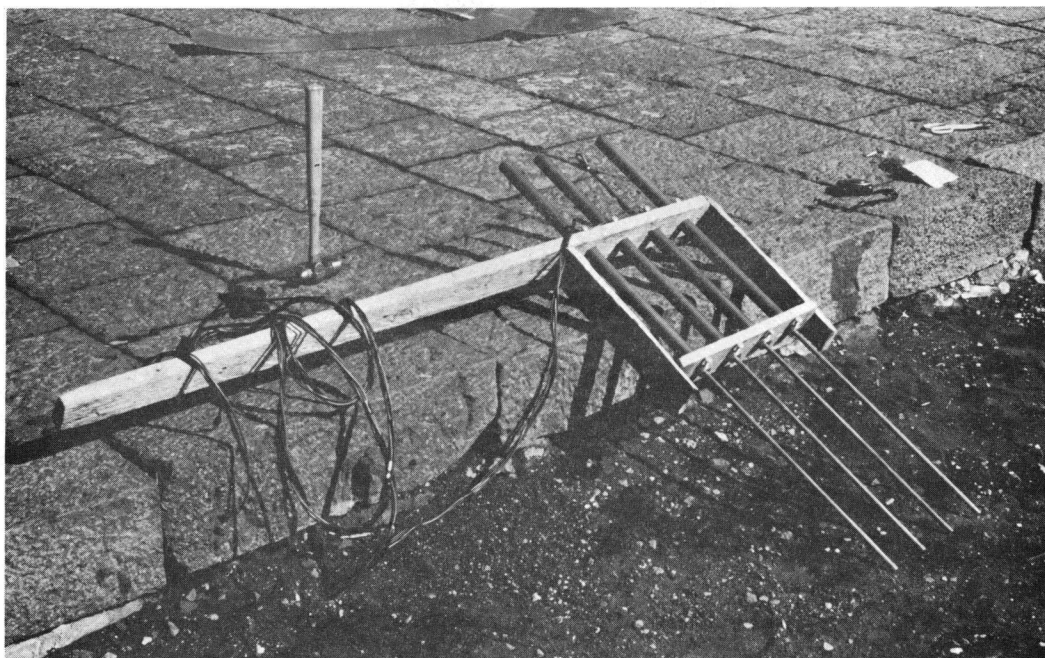
(a)
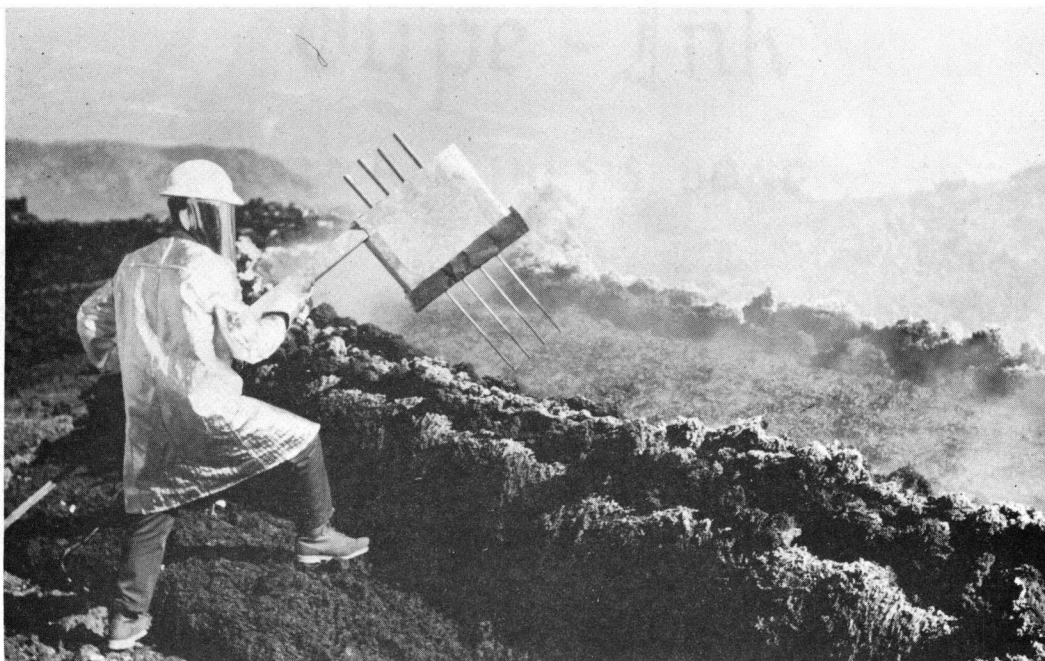
(b)

Figure 5.   The completed Wenner four-electrode probe.
(a) Support assembly, radiation shield removed
(b) In use at field site, radiation shield attached

alumina thermocouple insulators. The whole assembly was attached
with a stainless steel chuck plus refractory cement to a stainless
steel wand through which the four wires were carried internally.
Wire insulation in the wand was fiberglass at the immersion end, and
teflon at the handling end. From the point of view of ease of handling
in the flow, this probe was ideal. Unfortunately, each time one of
these probes was tried, the quartz tube broke with the first immer-
sion. The shattering was probably caused by thermal shock, even
though the expansion coefficient of fused quartz is extremely small.
However, the shearing action between horizontal layers of the turgid
lava cannot be ruled out as a cause of damage. This probe configura-
tion is so very convenient for lava stream use, the design concept
should not be totally rejected. Perhaps a larger tube diameter with
either thicker or thinner walls might prove more rugged.

SIGNIFICANT FEATURES OF THE EXPERIMENT SITE

General Features of Etna

Some insight into the forbidding field conditions encountered may be gained by a brief discussion of the size, form and structure of Etna. The mountain is roughly conical in shape, rising from sea level to a present elevation of almost 3300 meters as shown in Figure 6. Almost the entire mass above sea level appears to be of volcanic origin, and according to Sartorius (1880) consists of some 879 cubic kilometers of erupted material. It is thus one of the highest and largest land volcanic masses on earth. The approximately circular base is over 50 kilometers in diameter, and even at the 2000 meter level where the only access road terminates, the diameter is still considerably more than 10 kilometers. The slopes of the mountain are dotted with over 1000 parasitic cones, several of which are over a kilometer in diameter. From close range, where the grand perspective of the entire mountain is lacking, the flows and cinder cones dominate the landscape. Below the 2000 meter level the harshness of the landscape is muted and softened by vegetation, but above 2000 meters, where nothing grows, only vast black cinder fields, cinder cones, and tumbled scoriaceous aa flows meet the eye. Altogether, a 400 square kilometer area surrounding the summit is without roads. Since the road terminus at the 2000 meter level is on the

Figure 6.   Topographic map of Mt. Etna and its environs.
(Scale 1:264, 000)
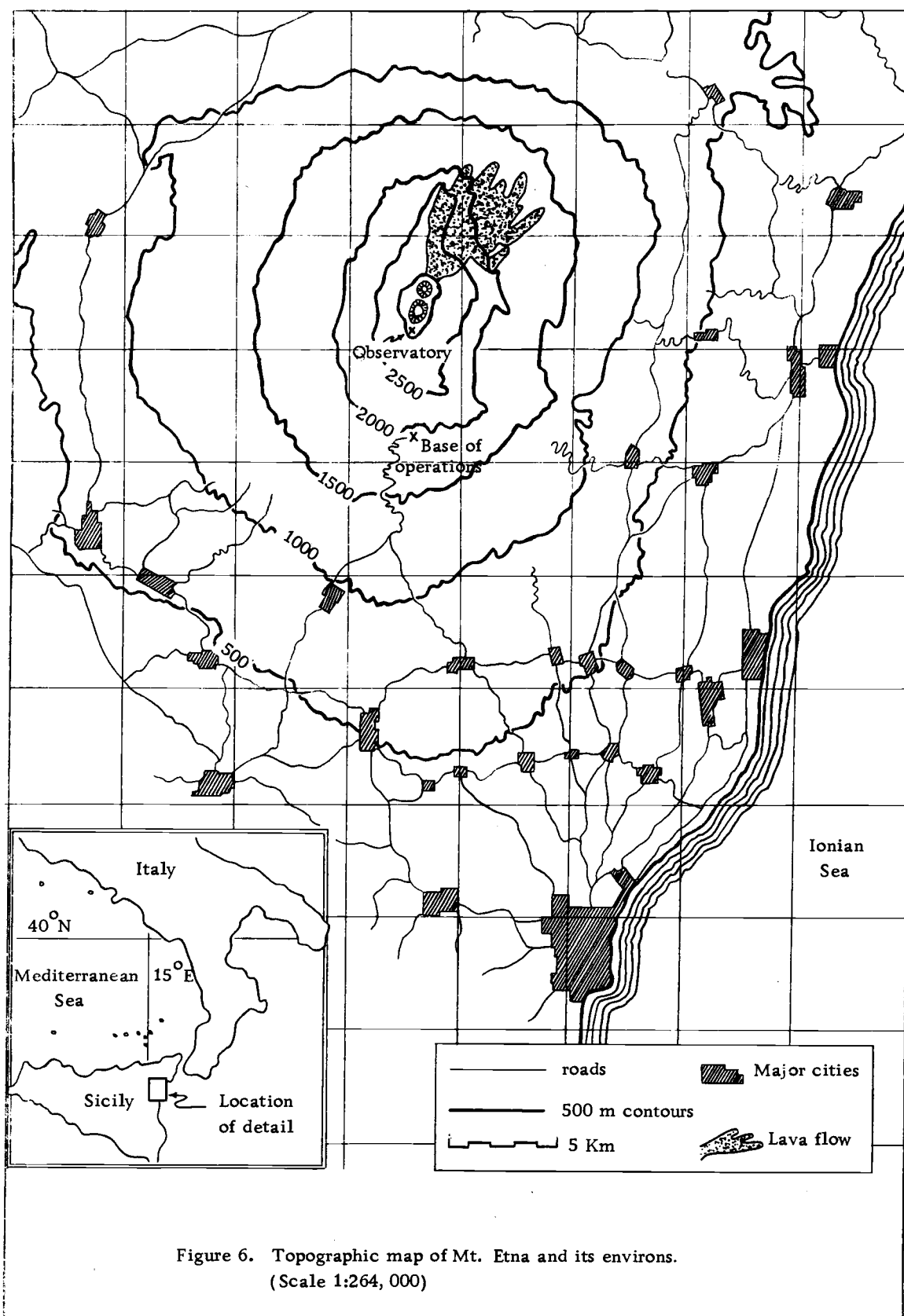
southern flank of the mountain, and since the lava flow under study at the 3100 meter level was on the northeast by north flank, logistics to the field site presented considerable challenge.

Figure 7a shows the form and extent of the mountain in a sea level view from the north east at a distance of 40 kilometers. Figure 7b shows the southern flank, viewed from an elevation of 500 meters. Figures 8a and 8b show the same southern flank from elevations of 1000 meters and 2500 meters respectively.

Eruptive History of Etna

Mt. Etna has an estimated eruptive history of some 50,000 years (Sartorius, 1880), and fragmentary records of major eruptions exist from as early as 1500 B. C. (Imbò, 1965). During its recorded history, eruptions have claimed over 35,000 lives and damaged or destroyed a score of cities and villages. Altogether over 170 distinct eruptions have been recorded, and over 200 eruptive systems have been identified. With such an uninterrupted eruptive history available for study, Imbò (1928) has identified a 50 to 55 year cycle in the activity, each cycle involving from six to nine distinct eruptions before the conduit is thoroughly emptied of lava at the end of the cycle. Also, Perret (1950) has noted a distinct lunisolar influence on the timing of onset of activity within this cycle. (See also Appendix III.)

(a)

(b)

Figure 7.   Views of Etna from near sea level.
(a)   From the northeast
(b)   From the south (note parasitic cones)

(a)

(b)

Figure 8.   Views of Etna - upper elevations.
(a)   From 1000 meter elevation on southern flank
(b)   From 2500 meter elevation on southern flank
(note observatory on distant ridge)

Morphology of Etna

Over the years, the geology and structure of Etna have become
better known as new flows and older buried flows have one by one
been analyzed. Major contributions to this knowledge have been
made by Sartorius (1880), Washington, Aurousseau, and Keyes
(1926), Francaviglia (1961), Rittmann (1963b), and Imbò (1965). This
brief general description of the mountain's development is summar-
ized from these extensive sources. However, knowledge of the Mt.
Etna lavas is still far from complete. Much more is known, for ex-
ample, about other volcanoes with a long documented history, such
as Vesuvius or Kilauea. Consequently, conclusions as to the struc-
ture and development of Etna must still be classified as tentative
although certain general features of its development are fairly well
established.

The sedimentary Eocene to Pleistocene base upon which the
lavas rest shows exposure on all four sides at elevations of a few
meters to a few hundred meters above sea-level. This sedimentary
platform for the superposed strato-volcano dips gently to the south-
east. Rittmann (1963b) has postulated the existence of a northeast
trending sedimentary horst under the superstructure, but evidence in
support of his proposal is scanty.

The lower broad slopes of the mountain are predominantly

lavas. Higher up, the percentage of pyroclastics increases and the slopes steepen. Below 500 meters elevation, slopes are two to five degrees, but above that level they quickly steepen to the 25 or 30 degree slopes that characterize the mountain. At most elevations, a horizontal cross-section of Etna is roughly elliptical with the major axis trending northeast by north. At about 2800 meters elevation, the main cone is truncated by a broad plateau sloping gently upwards towards the north. Much of the evidence for deducing Etna's early activity is found in the vicinity of this plateau, for here are found vestiges of what appear to be at least two large craters antedating a large caldera. The larger of these two craters, the "Elliptical Crater" occupies the northern two-thirds of the plateau. It is almost entirely filled by ash and lava flows. The second crater, the "Piano del Lago", also filled, lies south and slightly west of the Elliptical Crater. Intersecting the eastern rim of the Piano del Lago and the southern and eastern rims of the Elliptical Crater is the Vale del Bove, a huge depression opening generally southeast by eastward to the sea. It has an average diameter of eight kilometers, and vertical walls 100 to 200 meters in height except along the seaward side. Many exposures of a radial dike system along the walls pinpoint an original center of eruptive activity, and give solid evidence that the Vale del Bove is in fact a caldera.

What is generally considered to be the main cone of the modern

Etna has developed near the center of the previously described pla_
teau. Popularly labelled "Gran Cono", it is some three kilometers
in diameter, has a 32 to 33 degree cone typical of the accumulation
of pyroclastic materials, and extends the present elevation of Etna to
some 3300 meters. A hundred years ago, the crater of Gran Cono
was some 500 meters deep, but intracrateral flows and ash eruptions
have reduced this figure to a present-day 200 meters. Recent activity
is mostly in the form of fumaroles, and most interest to_day centers
in the so-called Northeast Crater. This crater had its beginning in
1911 when a fresh lava flow broke out near the base of Gran Cono on
the northeast side. Since that time, some dozen eruptions at this site
have built up a cinder and flow cone which today begins to rival Gran
Cono in size. The Northeast Crater has been in a state of almost
constant explosive activity for the past few years. Ash showers ac_
company the explosions from the crater vent while at the same time
pyromagma in the conduit of the cone, intruding between cinder layers
in what Rittmann (1963b) calls a "mantelsill", breaks out the north_
east flank of the cone at an elevation of some 3100 meters, and main-
tains an almost constant flow in a state known as "subterminal effusive
activity". The violent gas venting from the crater and the quiet pyro-
magma flow from the cone base are contrasted in Figure 9.

(a)
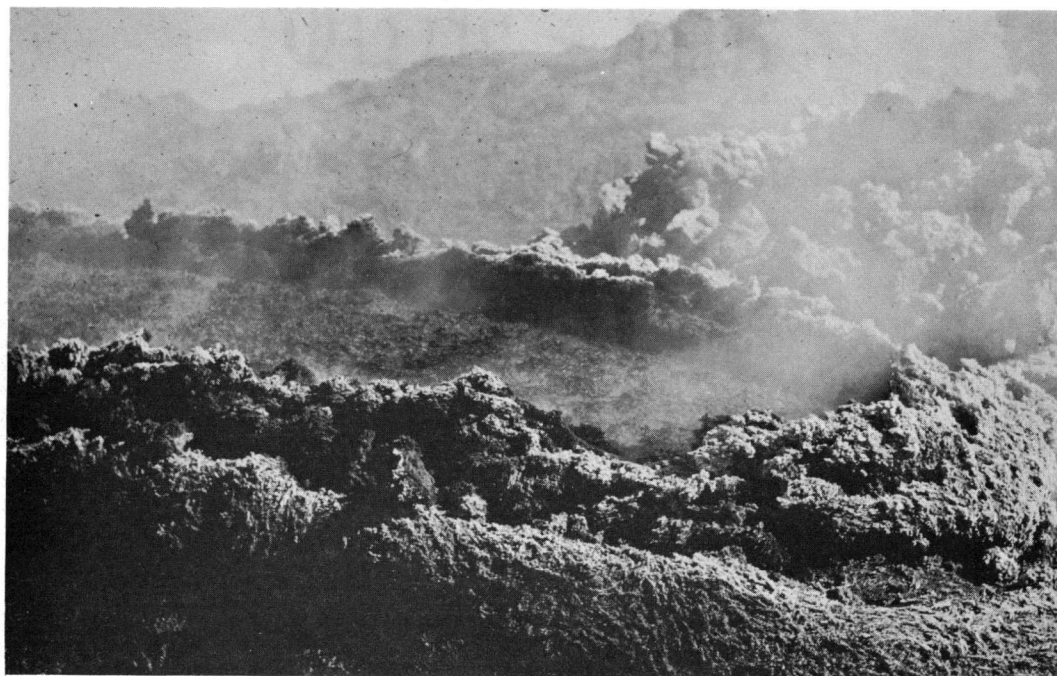
(b)

Figure 9. Gas and pyromagma venting from the Northeast Cone,
October, 1967
   (a) Violent gas explosion venting ash, gases and steam
        from the crater
   (b) Contrasting quiet pyromagma flow from the base of
        the cone

Subterminal Effusive Activity on Etna

This subterminal flow from the northeast flank of the Northeast Crater consists of relatively quiet, relatively low gas content pyromagma. It was this material whose electrical characteristics were measured in the present studies. Figure 10 shows the beginning of the subterminal effusion from the Northeast Crater on May 5, 1958 and a view of the continuing flows four years later from a vantage point six kilometers distant. These flows have persisted more or less continuously until the present, and according to Walker (1967) represent a lava accumulation at the rate of one cubic meter per second, or a volume in the neighborhood of 0.3 cubic kilometers in the last decade. Figure 11 sketches the general character and proportions of the flow emerging from the Northeast Crater as it appeared in 1967 at the time of this study.

The life-cycle of such a typical flow will start with a sudden break-out, often accompanied by brief lava fountains. During the first few hours, and depending greatly on the topography and the prevailing winds, levees form and the lava gradually channels itself into the flume-like formation shown in Figure 11. The flume walls taper upwards and inwards and are reasonably sturdy. Sometimes static pressure of the melt will break out a section of levee and a new branch flume will begin forming. At other times, and beginning

41

Tazieff (IIRV)

(a)

Tazieff (IIRV)

(b)

Figure 10. Subterminal effusive activity, Northeast Cone.
        (a) Beginning of flow on May 5, 1958, looking west
        (b) Extent of the same flow, summer 1962, looking
            southwest by south from a point six kilometers
            from the Northeast Cone (Note vestiges of Elliptical
            Crater on the left and at the far right

(a) Flowing pyromagma
(b) Levees, 10 cm to 50 cm thick
(c) Flood of pahoehoe lava through broken levee
(d) Bocca as shown in Figure 9
(e) Blocks of old lava pushed aside
    during bocca formation
(f) Northeast cone and site of
    1957, 1963 outbreaks
(g) Gran Cono
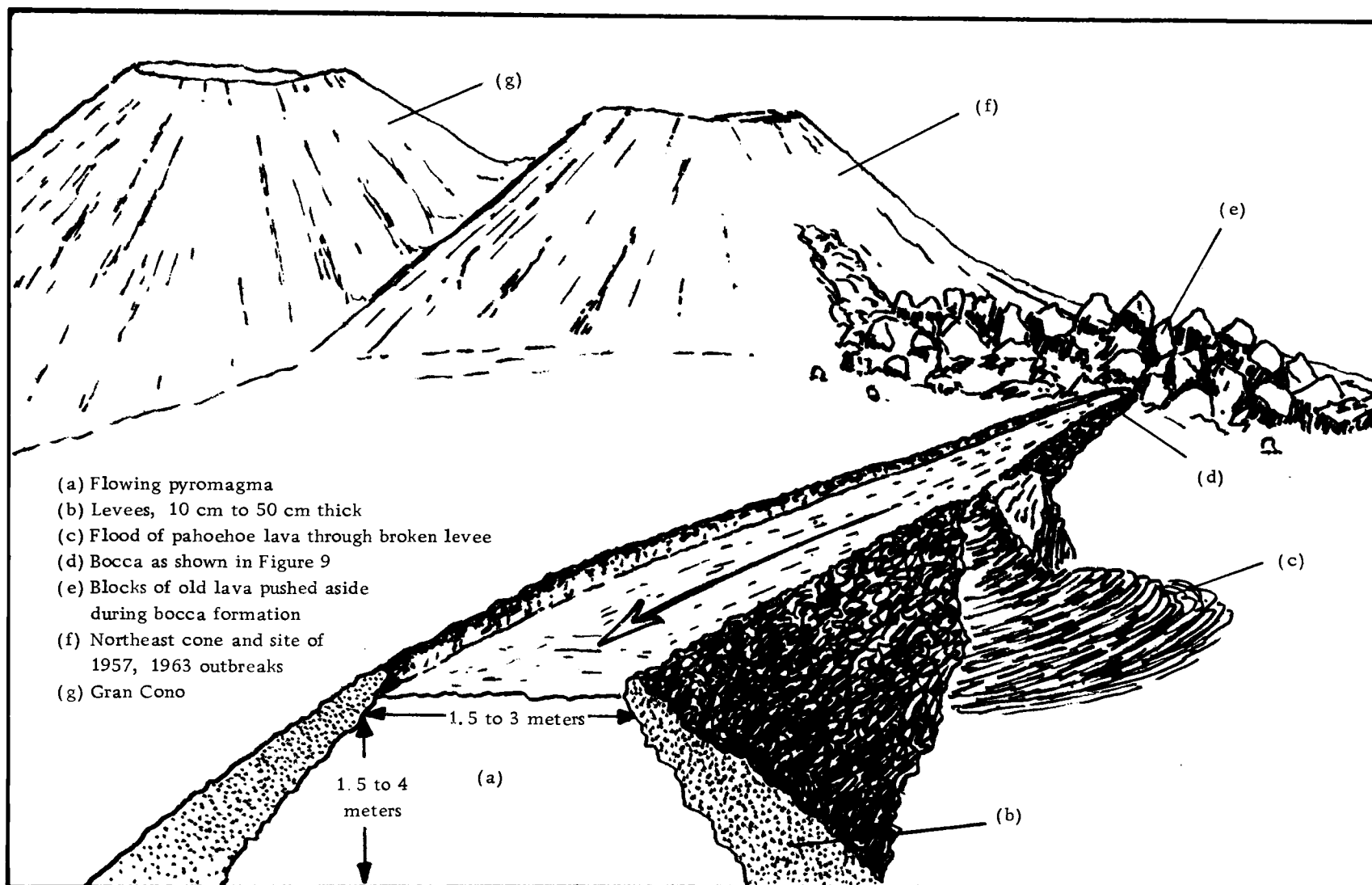
Figure 11. General character and proportions of pyromagma flows.

downstream, the walls will continue to build in height until they meet

and a lava tube will form. As the tube gradually develops uphill to-

wards the source or "bocca", increased drag on the flowing melt re-

sults in an increased pressure head near the bocca. This increased

head will eventually either cause the outbreak of a new bocca else-

where, or result in spillover or wall breakout near the bocca with the

consequent development of a new flume. A given flume may persist

from a few days to several weeks, and at a given time at least one

bocca and frequently several will be active. Figure 12 illustrates the

beginning and ending of a typical flow, and Figure 13 shows stable

and unstable conditions of flow activity. It is entirely possible that,

if the center of eruptive activity continues to shift towards the north-

east, these tubes and flumes covered by some future cinder cone

could form the conduits or zones of weakness leading to future sub-

terminal eruptions.

Regional Tectonics of Sicily

Little is known about the deep structure of Etna. In contrast to

Vesuvius, where considerable evidence points to the existence of a

large and reasonably well delineated magma chamber, such evidence

is missing on Etna. Rittmann (1963b) has made a statistical study of

the distribution and chemical compositions of eruptive centers on

Etna and infers the existence of two axes of activity. The earlier,

(a)

(b)

Figure 12.   Typical flow activity (beginning and end).
(a)   First few moments in the formation of a bocca
(b)   A choked-off flow with flume full of congealed magma

(a)

(b)

Figure 13. Typical flow activity (stable and unstable).
    (a) Stable flow. Lava is very hot and fluid. Maximum width of flow = 3.5 meters.
    (b) Typical surge at bocca before spilling over the levees. Height of surge ≈ 1 meter.

trending northwest consists of olivene andesites associated with Trifoglietto, the ancient volcano which culminated in the Val del Bove caldera. The recent axis, trending northeast by north shows basalts and andesitic basalts representative of the modern Etnean activity. Rittmann associates these two axes with an intersecting fault system consistent with the regional tectonics of Eastern Sicily, and postulates no magma chamber as such, but rather envisions magma rising along fissures of the intersecting fault system and originating directly in the low velocity region of the mantle.

A still broader view of the regional tectonics is of interest. Although not related directly to the primary object of these investigations, it nevertheless would be pertinent whenever attempts were made to correlate sub-surface structure with the results of electrical conductivity depth-profiling. A glance at Figure 14 shows that not only the Etnean activity, but also the volcanic and earthquake centers of the entire region, and even the major landform lineations are relatable to three major directions. Although this observation has not been reported previously for the entire Sicilian region, almost identical observations have been reported by Tjia (1968) for the Indonesian Island Arcs, by Sonder (1936) for Central America, by Melton (1931) for the south west portion of North America, and by Friedlander (1918) for the Hawaiian, Lipari, Galapagos and Japanese Islands, and the lesser Antilles. Tjia, in particular, uses these volcanic lineations to infer major regional crustal stress patterns which are consistent with the observed regional structural trends.

Italy

+
.Stromboli
oPanarea
o Lipari
Vulcano

Sicily

Pantellaria

o Linosa   Malta

o
Lampedusa

Directions of
major lineation
or faulting

+ Major earthquake epicenter or
   submarine eruption

—.— Major faults in Sicily

_____ _____ Direction of lineation
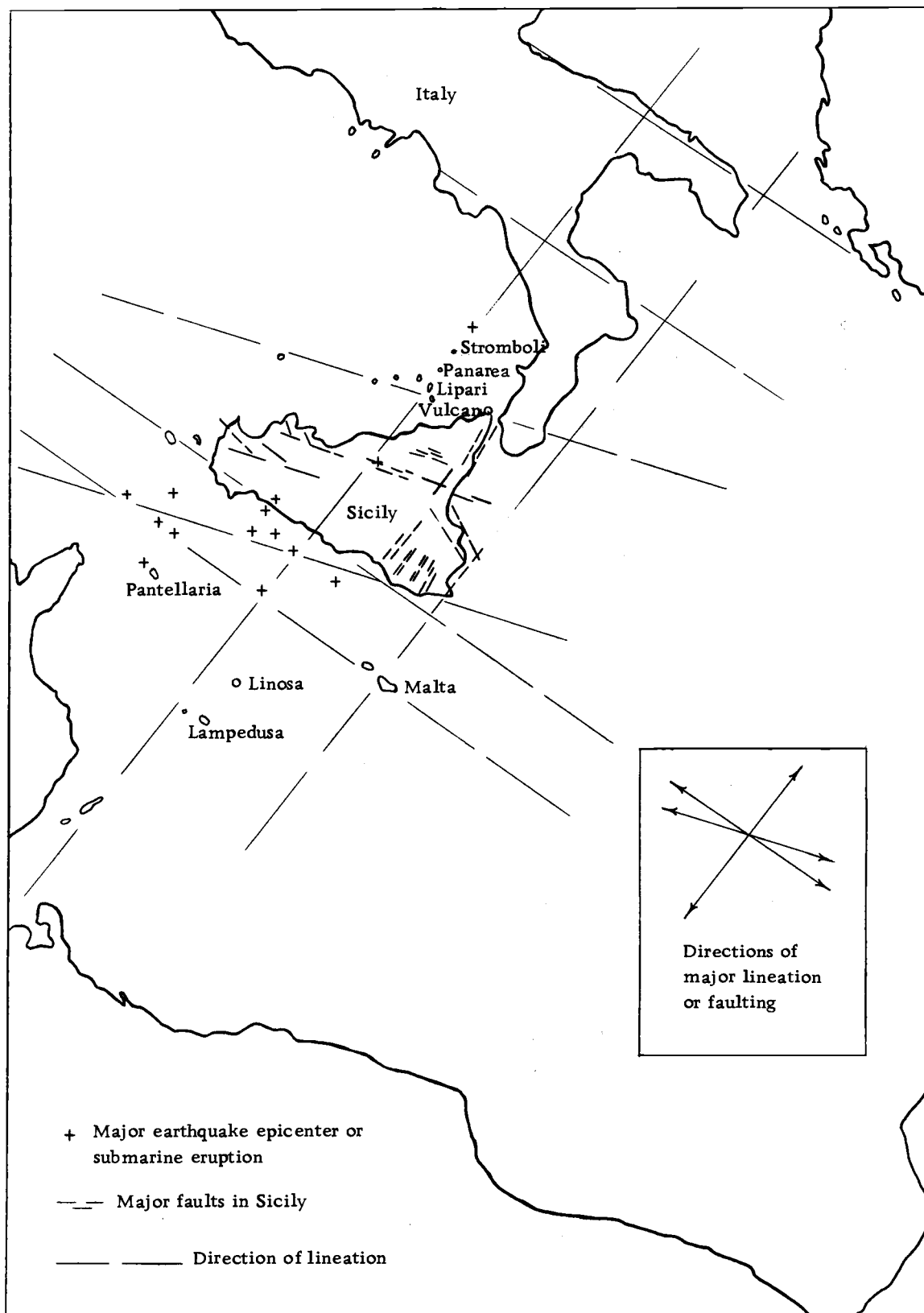
Figure 14.   Tentative regional tectonics of Sicily.

EXPERIMENTAL RESULTS

Purpose of Temperature and Chemistry Determinations

The detail recorded here on the temperature and chemical composition of the gas and melt will primarily benefit future experiments by providing a unique identification of the chemical character of the Etnean pyromagma whose electrical characteristics were measured. In the interests of thorough understanding of the behavior of pyromagma it is desired to understand the effect of temperature, gas content, and rock chemistry on the electrical conductivity, but it will not be possible to observe the functional relationships between temperature, chemical composition, and conductivity over any appreciable range of the variables until future eruptions occur on Etna and elsewhere and the procedures of this investigation are repeated. Thus in the larger sense, the thermal and chemical data recorded here will have their greatest usefulness at some future date.

Chemical Sampling

Gas Analysis

The Draeger tube method of chromatographic gas analysis proved admirably suited to the difficult field conditions on Etna. In particular, the speed of operation was the most valuable feature of the system since the operators were completely at the mercy of the

shifting winds, and frequently had to make a hasty withdrawal in order

to avoid the swirling poisonous gas cloud. The pyromagma issuing

from the bocca is technically classified as outgassed, but the term is

relative. Although certainly less gas-charged than the violently ex-

plosive pyromagma of the central conduit, the pyromagma at the

bocca still contains gas under pressure. It is almost as effervescent

as a violently shaken freshly opened container of carbonated beverage.

The gas clouds at the bocca are thick and choking. SO_2 and HCl

vapor abound, and the operators have no choice but to keep to wind-

ward of the bocca.

Although the operators' tasks would have been considerably

simplified if sampling had been carried out downstream where the

gases were more dispersed, it was considered essential to confine

gas sampling operations to the bocca in order to hold atmospheric

dilution or contamination to a minimum. In order to secure a sample,

the collecting cone was positioned in the lee of the largest lava block

to windward of the bocca. The cone was balanced on any available

lava projections at the edge of the bocca, and cleared the lava sur-

face by two or three centimeters. Before any sampling tube was

opened, the collector system was first pumped free of any accumu-

lated air, and the outlet temperature was checked with a thermome-

ter. The cooling coil proved entirely adequate as a radiator, and

excessive gas temperature was never a problem during the

measurements. Initially, difficulties were encountered with water vapor condensation in the cooling coil, and it was therefore necessary to maintain the cooling coil axis in a rather awkward vertical position while taking samples. Gases were sampled at least twice on each of two different days, and the results are summarized in Table 1. Unfortunately, it was not possible to measure the rate of evolution of the gases.

Table 1. Proportions of gases in the pyromagma, in percent.

Gas	Tube No(s).	Day 11	Day 14
CO	CH 249	21. 6	none
CO_2	CH 235, CH 308	20. 2	50. 9
CH_4	CH 200	none	none
H_2	CH 309	9. 35	6. 79
H_2S	CH 282, CH 291	0. 67	0. 14
SO_2	CH 242, CH 282	46. 7	40. 0
HCl	CH 295	1. 48	1. 83
NH_3	CH 255	none	0. 34

The two days chosen for gas sampling represent, in many ways, extremes of the lava conditions encountered on Etna. On day 11, the lava was hot (T = 1042° C), turgid, depleted of gas, and tending to form pahoehoe type solids whenever spillover of the flume occurred. On day 14, the lava was cool (T = 988° C), fluid, heavily gas charged, and formed aa type lava in the spillovers. It is interesting

to observe that, judging by the CO/CO_2 ratios, the cooler melt of day 14 is apparently considerably less reducing or more oxidizing than the hotter flow of day 11.

Rock Analysis

Three samples were drawn from the melt at approximately fifteen minute intervals on each of two successive days (days 12 and 13) in order to evaluate any daily chemical variation. Portions of each of the three specimens for a given day were finely ground and mixed in equal proportions by weight in order to provide a single averaged daily specimen for standard silicate analysis. The most coherent portions of each day's melt sample were prepared in thin-section and examined microscopically. These are shown in Figures 15 and 16.

In order to detect if there were any gravitational differentiation of phenocrysts submerged in the melt, three samples were taken from the interior bottom of the levee walls after the flow had ceased. Again a single powdered sample was prepared for silicate analysis and thin sections were prepared from the larger coherent fragments. These sections are shown in Figure 17.

The results of the silicate analysis, (done by Charles O. Parker and Company, assayers, Denver, Colorado) are presented in Table 2 in conjunction with analyses of lavas from other recent eruptions of Etna as reported by Washington et al. (1926), Cumin (1954), or Imbò

Section 1

(a)

(b)

Olivene

Plagioclase

Magnetite

Pyroxene

Void

(a)

Section 2

(b)
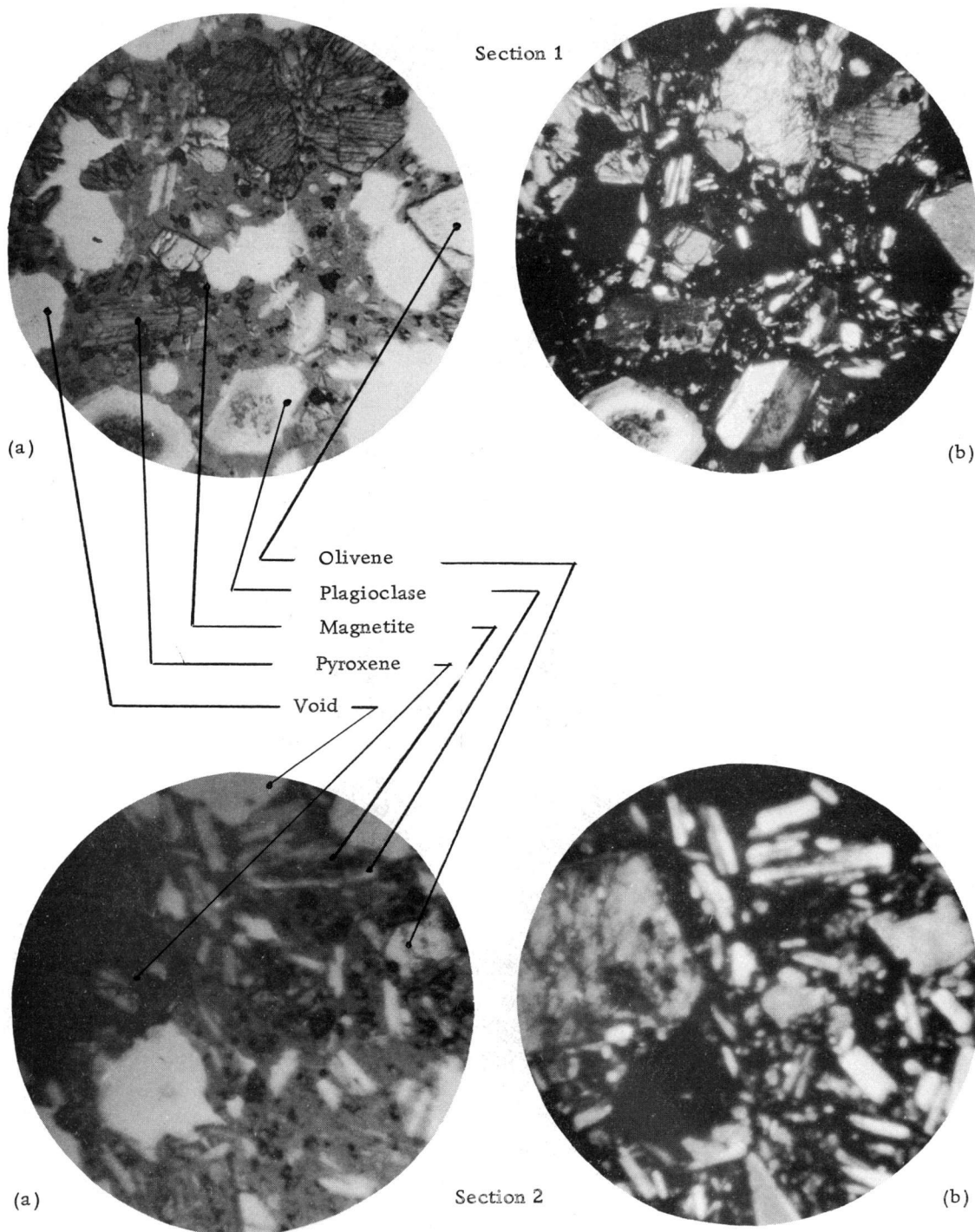
Figure 15. Microphotographs (x15) of thin-sections 1 and 2 of lava taken
from the top of the flow, day 12.
(a) Under ordinary light
(b) Between crossed Nicols
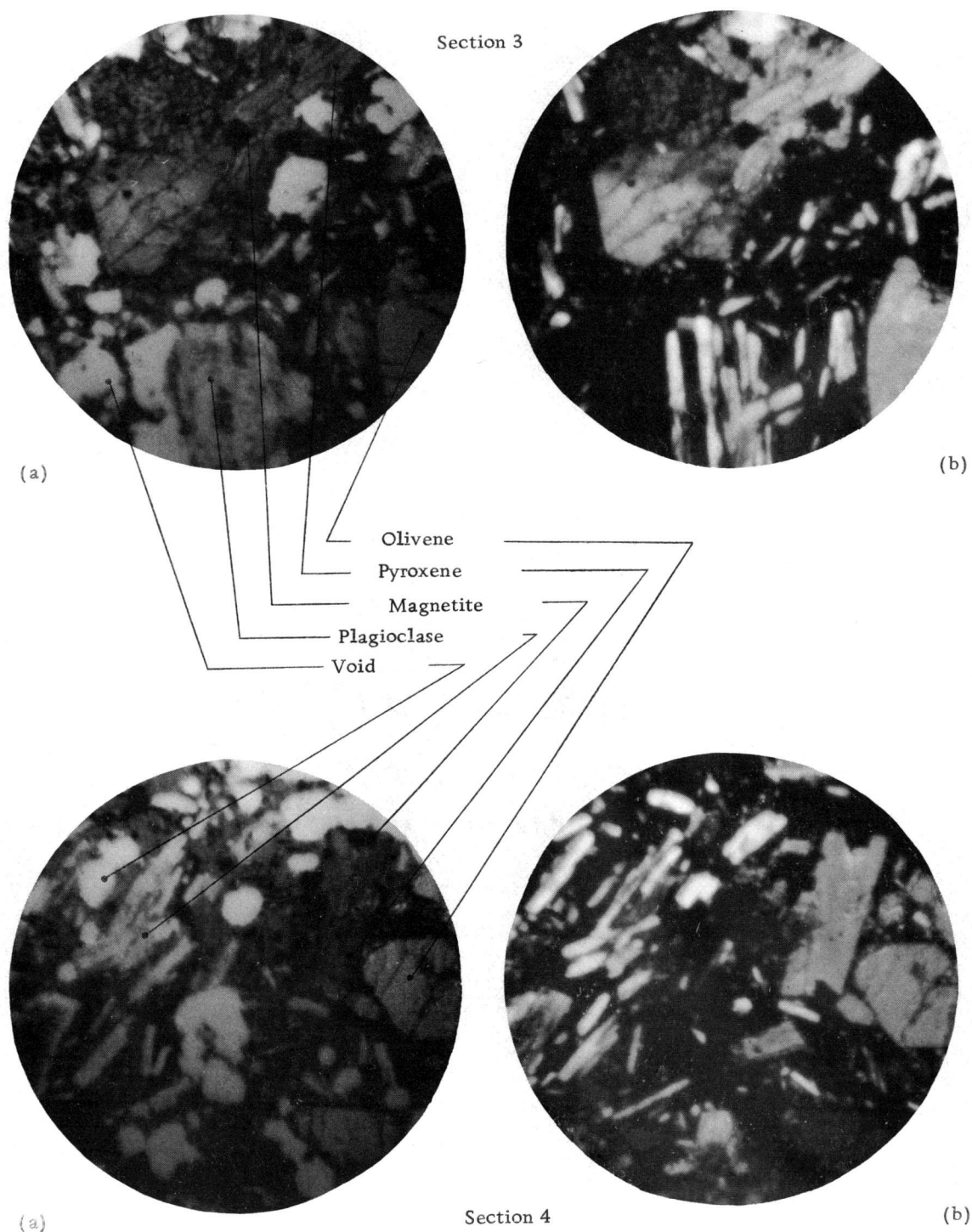
Figure 16. Microphotographs (x15) of thin-sections 3 and 4 of lava taken from the top of the flow, day 13.
(a) Under ordinary light
(b) Between crossed Nicols

Section 5

(a)

(b)

Olivene

Void

Magnetite

Plagioclase

Pyroxene

(a)

Section 6

(b)
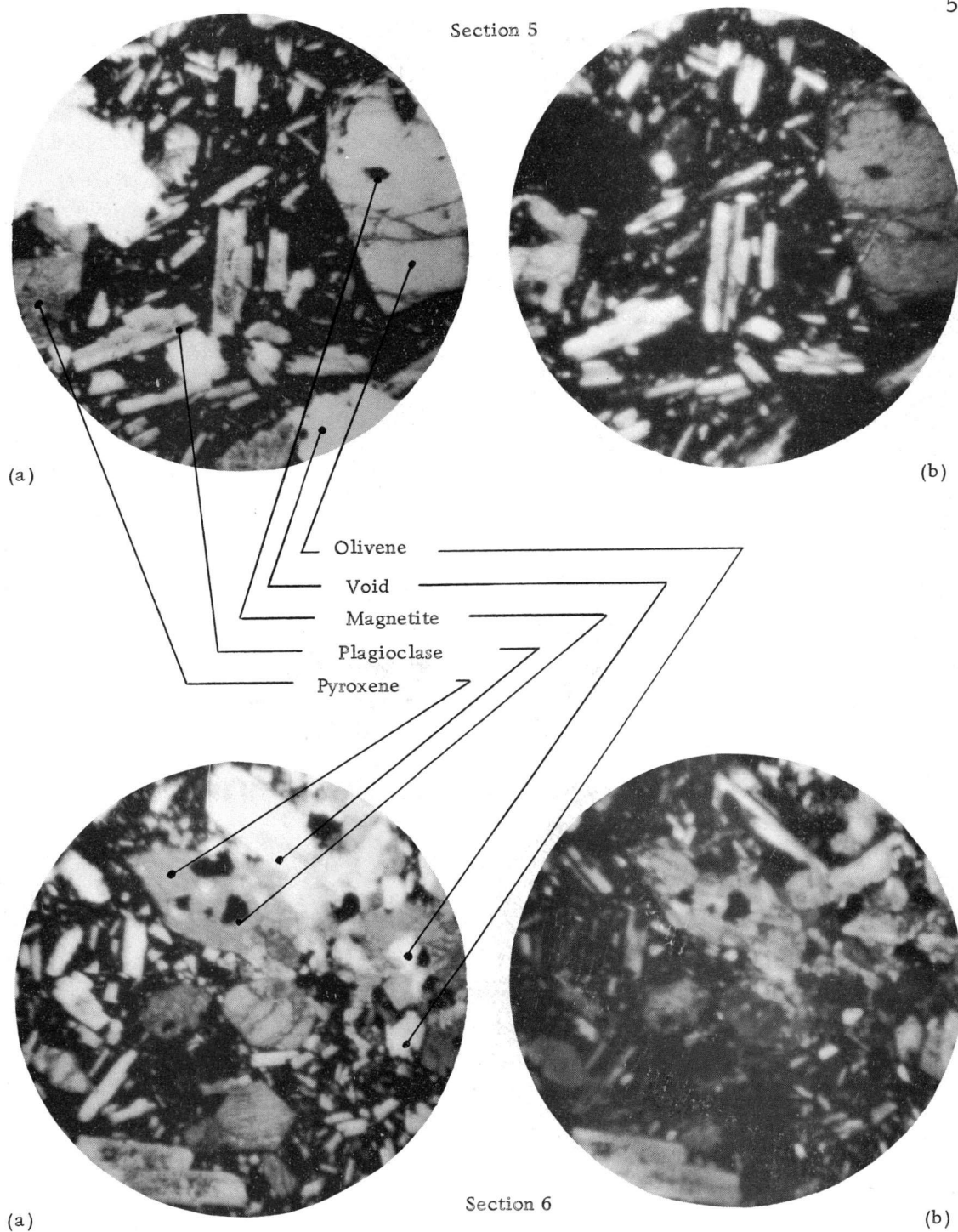
Figure 17. Microphotographs (x15) of thin-sections 5 and 6 of lava taken from the bottom of the inner flume walls.

(a) Under ordinary light

(b) Between crossed Nicols

Table 2. Silicate analysis of "recent" Etnean lavas (in weight percent).

Oxide	Year of flow 1669 (a)	1792 (b)	1883 (a)	1886 (a)	1892 (a)	1908 (a)(b)	1910 (b)(c)	[+]1911 (a)	1928 (a)	1950 (c)	1956 (a)	[#]1967 subterminal effusion day 12	day 13	levee
K_2O	1.15	1.62	1.36	1.41	1.22	1.87	1.47	1.99	1.51	1.51	1.76	1.26	2.32	1.73
Na_2O	4.13	4.45	4.41	4.52	4.91	4.93	4.75	3.75	4.85	4.66	4.45	4.19	5.17	5.80
CaO	10.07	9.99	10.26	9.89	9.72	9.71	10.26	9.66	10.22	10.57	11.54	11.10	9.60	9.65
Al_2O_3	17.18	17.94	15.95	16.03	18.08	18.51	17.85	19.82	17.80	16.76	16.45	19.10	19.62	20.07
MgO	5.89	4.23	4.93	5.10	3.90	3.44	4.03	3.73	5.03	5.24	4.58	4.20	4.35	3.70
FeO	6.94	6.89	9.54	9.31	6.04	5.40	6.80	2.91	5.84	6.36	6.31	8.63	9.27	8.78
SiO_2	49.21	48.53	47.11	46.86	49.17	49.29	49.01	50.30	47.67	46.69	46.67	46.60	46.20	45.84
Fe_2O_3	3.15	2.82	5.44	5.34	4.32	4.17	2.66	5.46	4.56	6.10	6.15	2.71	2.28	2.96
TiO_2	1.74	2.27	1.26	1.17	1.91	2.32	1.97	1.99	1.81	1.82	1.75	0.60	0.75	0.68
H_2O	0.09	0.12	0.16	0.16	0.08	0.32	0.07	0.12	0.12	0.03	0.05	1.25	0.06	0.48
MnO	0.08	0.11	0.12	0.12	---	trace	0.18	0.12	0.12	0.15	0.13	0.10	0.12	0.10
BaO	---	trace	---	---	trace	---	0.09	---	trace	0.16	trace	0.17	0.13	0.15

(a) in Imbò (1965).

(b) in Washington et al. (1926).

(c) in Cumin (1954).

[+] Sample taken from ash deposits.

[#] Data tabulated in Appendix I.

(1965). Most of the analyses tabulated are analyses of a single sample. Only the 1908, 1910, 1911 and 1967 data represent averages of several samplings. Even though the lavas of Etna are considered to be remarkably uniform in character (Washington et al., 1926), a glance at the 1967 tabulation is sufficient to indicate that the day to day variations and the top to bottom variations are considerable. Whether these are true daily and depth variations, or whether they are statistical variations related to the normal or lognormal distribution of the minerals making up the melt cannot be known without undertaking an extensive program to determine the actual distributions.

Even though there is a spread in the analyses, valid generalizations concerning the lava can still be drawn provided they do not necessitate a detailed scrutiny of the chemical composition. Thus the observations of Cumin (1954) concerning the long-term change in silica content can be updated as shown in Figure 18. The continued quiet effusive activity and lack of extreme explosive activity on Etna is consistent with the lowered viscosity present in these melts of lowered silica content.

Mineral norms and modes can also be calculated and a broad classification of the lava can be made. The norms for the three 1967 samples were calculated using the CIPW classification system summarized by Johannsen (1931) and are shown in detail in Tables 3, 4 and 5. Normal and modal analyses are summarized in Tables 6 and 7
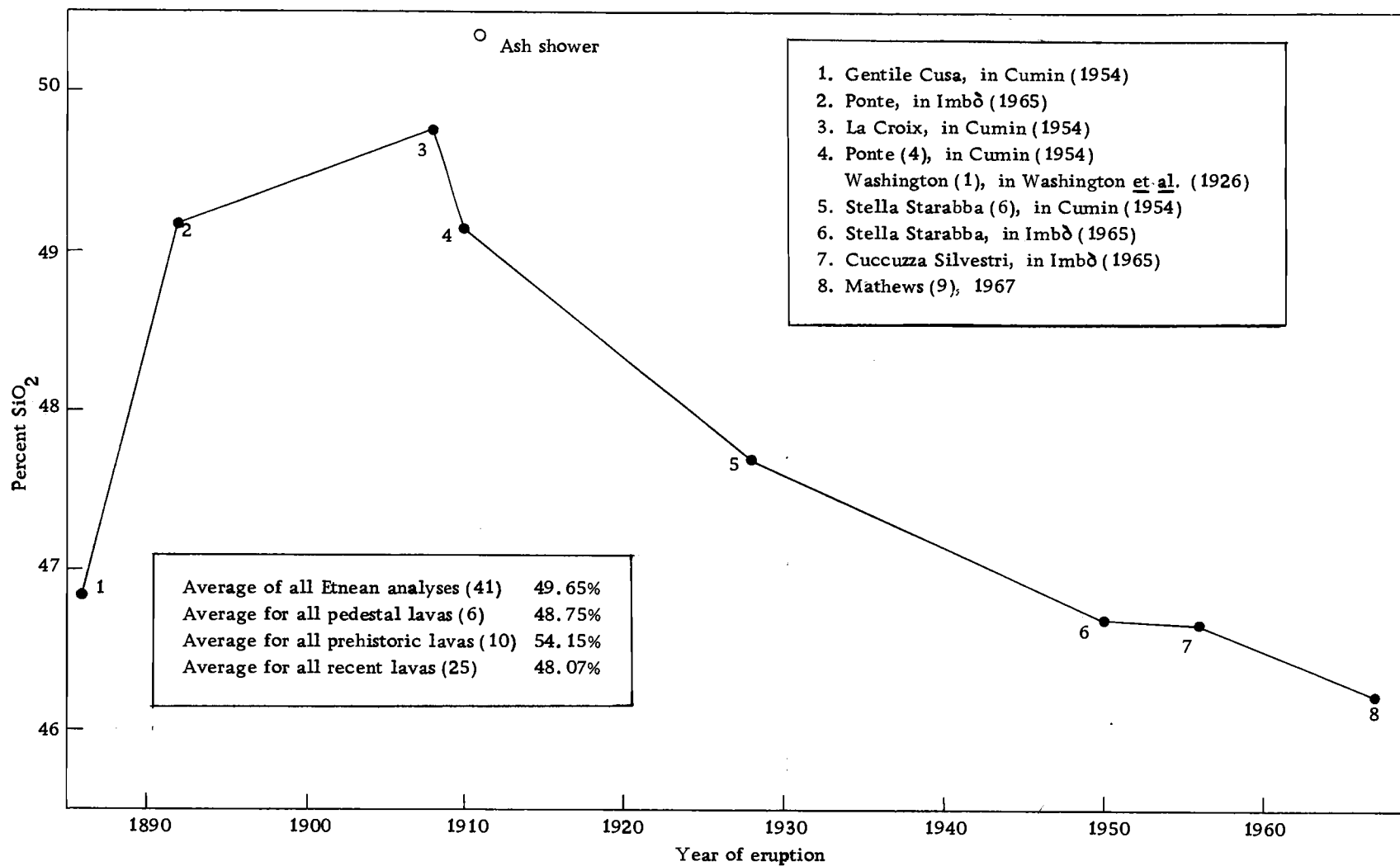
Figure 18. Eighty-year trend in SiO_2 content of Etnean lavas.

The chart contains the following:

O Ash shower

1. Gentile Cusa, in Cumin (1954)
2. Ponte, in Imbò (1965)
3. La Croix, in Cumin (1954)
4. Ponte (4), in Cumin (1954)
   Washington (1), in Washington et al. (1926)
5. Stella Starabba (6), in Cumin (1954)
6. Stella Starabba, in Imbò (1965)
7. Cuccuzza Silvestri, in Imbò (1965)
8. Mathews (9), 1967

Average of all Etnean analyses (41)	49.65%
Average for all pedestal lavas (6)	48.75%
Average for all prehistoric lavas (10)	54.15%
Average for all recent lavas (25)	48.07%

Table 3. Distribution of normative minerals in day 12 samples (all figures in moles per 100g of sample).

Normative minerals consistent with chemical analysis of sample	Oxides reported in sample analysis									Moles of normative mineral per 100g of sample
	K_2O	Na_2O	CaO	Al_2O_3	MgO	FeO	SiO_2	Fe_2O_3	TiO_2	
	.0131	.0676	.1933	.1872	.1050	.1218	.7768	.0169	.0075	
Orthoclase $K_2O \cdot Al_2O_3 \cdot 6SiO_2$	.0131			.0131			.0786			.0131
Albite $Na_2O \cdot Al_2O_3 \cdot 6SiO_2$		.0274		.0274			.1644			.0274
Nephelite $Na_2O \cdot Al_2O_3 \cdot 2SiO_2$		.0402		.0402			.0804			.0402
Anorthite $CaO \cdot Al_2O_3 \cdot 2SiO_2$			.1065	.1065			.2130			.1065
Diopside $CaO \cdot (Mg, Fe)O \cdot 2SiO_2$			.0928		.0481	.0447	.1856			.0928
Olivene $2(Mg, Fe)O \cdot SiO_2$					.0569	.0527	.0548			.0548
Magnetite $FeO \cdot Fe_2O_3$						.0169		.0169		.0169
Ilmenite $FeO \cdot TiO_2$						.0075			.0075	.0075

Table 4. Distribution of normative minerals in day 13 samples (all figures in moles per 100g of sample).

Normative minerals consistent with chemical analysis of sample	Oxides reported in sample analysis									Moles of normative mineral per 100g of sample
	K_2O .0242	Na_2O .0833	CaO .1715	Al_2O_3 .1923	MgO .1087	FeO .1311	SiO_2 .7699	Fe_2O_3 .0143	TiO_2 .0094	
Orthoclase $K_2O \cdot Al_2O_3 \cdot 6SiO_2$	.0242			.0242			.1452			.0242
Albite $Na_2O \cdot Al_2O_3 \cdot 6SiO_2$		.0126		.0126			.0756			.0126
Nephelite $Na_2O \cdot Al_2O_3 \cdot 2SiO_2$		.0707		.0707			.1414			.0707
Anorthite $CaO \cdot Al_2O_3 \cdot 2SiO_2$			.0848	.0848			.1696			.0848
Diopside $CaO \cdot (Mg, Fe)O \cdot 2SiO_2$			.0867		.0436	.0431	.1734			.0867
Olivene $2(Mg, Fe)O \cdot SiO_2$					.0651	.0643	.0647			.0647
Magnetite $FeO \cdot Fe_2O_3$						.0143		.0143		.0143
Ilmenite $FeO \cdot TiO_2$						.0094			.0094	.0094

Table 5. Distribution of normative minerals in levee samples (all figures in moles per 100g of sample).

Normative minerals consistent with chemical analysis of sample	Oxides reported in sample analysis									Moles of normative mineral per 100g of sample
	K_2O .0183	Na_2O .0940	CaO .1720	Al_2O_3 .1967	MgO .0925	FeO .1237	SiO_2 .7640	Fe_2O_3 .0186	TiO_2 .0088	
Orthoclase $K_2O \cdot Al_2O_3 \cdot 6SiO_2$	.0183			.0183			.1098			.0183
Albite $Na_2O \cdot Al_2O_3 \cdot 6SiO_2$		.0179		.0179			.1074			.0179
Nephelite $Na_2O \cdot Al_2O_3 \cdot 2SiO_2$		.0761		.0761			.1522			.0761
Anorthite $CaO \cdot Al_2O_3 \cdot 2SiO_2$			.0844	.0844			.1688			.0844
Diopside $CaO \cdot (Mg,Fe)O \cdot 2SiO_2$			.0876		.0429	.0447	.1752			.0876
Olivene $2(Mg, Fe)O \cdot SiO_2$					.0496	.0516	.0506			.0506
Magnetite $FeO \cdot Fe_2O_3$						.0186		.0186		.0186
Ilmenite $FeO \cdot TiO_2$						.0088			.0088	.0088

61

Table 6. Norms of Etnean 1967 lavas.

Mineral	Weight percent in sample		
	Day 12	Day 13	Levee
Orthoclase	7.4	13.5	10.2
Albite	14.0	6.6	9.4
Nephelite	11.6	20.1	21.6
Anorthite	30.1	23.6	23.5
Diopside	21.1	20.1	20.4
Olivene	9.5	11.1	8.7
Magnetite	3.9	3.3	4.3
Ilmenite	1.1	1.4	1.3

Table 7. Modes of Etnean 1967 lavas.

Mineral	Day 12		Day 13		Levee	
	point count	percent	point count	percent	point count	percent
Plagioclase	772	33.7	759	33.4	1062	34.3
Pyroxene	312	13.6	276	12.2	405	13.1
Olivene	102	4.4	90	3.9	92	3.0
Magnetite	87	3.8	46	2.0	1064*	34.3
Glass	736	32.1	720	31.8		
Voids	283	12.4	377	16.6	469	15.2
TOTAL	2292		2268		3092	

*Magnetite and glass indistinguishable in levee sample.

respectively. On the basis of these values, and using the classification scheme proposed by Rittmann (1952) the lava is identified as nepheline tephrite and nepheline basanite.

The σ-index is also used in the determination of rock suites. As defined by Rittmann (1963a) the σ-index is given by

$$\sigma = \frac{(Alk)^2}{Si-43} \qquad (15)$$

where

$\quad$ Alk = weight percent of K_2O and Na_2O

$\quad$ Si = weight percent of SiO_2

The average σ-index for the 1967 specimens is 14.4. This clearly identifies the Etnean lavas as belonging to the alkaline series or Atlantic suite of volcanics.

Temperature Measurements

Temperature determinations in the pyromagma were made with ease and yielded values mostly in the neighborhood of 1040° C. A detailed listing of the individual values, and the depth at which they were taken is given in Table 8 in association with the related conductivity values.

The actual measurement conditions which were encountered at the site had been well anticipated and the TEMTIP thermocouple

Table 8. Electrical conductivity data.

Pyromagma temperature °C	Depth in pyromagma cm	Electrical conductivity σ, in mhos/m						
		1.0 kHz	10 kHz	20 kHz	40 kHz	100 kHz	200 kHz	400 kHz
1032	2.5	0.31	0.33	0.33	0.31	0.32	0.33	0.32
1040	5.0							
1053	17							
1042	2.5	+0.28	0.35	0.39	0.39	0.37	0.39	0.36
1071	2.5	0.44	0.48	0.48	0.47	0.49	0.48	0.47
1043	*2.0							
1066	*20							
980	#5							
988	#8							

+ Gas content considerably higher than normal; more magma frothing; larger, more frequent crater explosions.

* More highly viscous than usual, forming pahoehoe, surface very uneven.

Pyromagma extremely fluid, forms very light grey rock, rock sampling not possible.

probe proved ideal for the type of measurement involved. Two operators were able to obtain four or five temperature determinations per minute with ease. This compares very favorably with temperature measurements made on lava lakes where eight operators require up to 30 minutes to make a single temperature determination using resistance thermometers.

Lava stream velocities varied between 0.1 and 0.4 meters per second, and the lava viscosity was sufficiently high that the thermocouple probe was forcibly carried along in the stream. The measurement procedure therefore consisted in inserting the probe at arms' length upstream from the probe operator, allowing it to be carried downstream at a predetermined depth and withdrawing it when it reached the arms' length position downstream. This procedure allowed more than sufficient time for the second operator to null the potentiometer and verify that the EMF had become constant. The TEMTIPS proved to be so rugged that four to six immersions were usually possible before the protective tube became dangerously charred or the thermocouple element ruptured.

By using Leeds and Northrup Company specifications on the TEMTIPS and potentiometer, and National Bureau of Standards standard thermocouple tables (Shenker, 1955), the absolute accuracy of the temperature measurements is determined as follows:

Potentiometer resolution (based upon galvanometer sensitivity and minimum detectable deflection)	± 20 μV
Potentiometer accuracy (allowing for thermal drift of standard cell and slide-wire non-linearities)	± 66 μV
Cold junction error (allowing for a ± 3°C error in cold junction compensating setting near 20°C)	± 22 μV
TOTAL	± 108 μV

At a typical pyromagma temperature of 1040°C this uncertainty of ± 108 μV in the EMF is equivalent to a temperature uncertainty of ± 8°C. This estimate is considered a conservative one since the precision thermometer used for determining cold junction compensation could be read with ease to the nearest degree, and agreed within one degree of both ice and steam points when calibrated.

To this uncertainty of ± 8°C must be added a correction for possible departure of thermoelectric power of the thermocouple material from the standard values for platinum-platinum+13% rhodium thermocouples listed by Shenker in National Bureau of Standards Circular 561. Leeds and Northrup Company certifies its grade A platinum-platinum+13% rhodium thermocouples to have thermoelectric powers of sufficient accuracy to yield temperatures to within ± 0.25% of the actual value over the temperature range 540°C to 1480°C. For temperatures in the neighborhood of 1040°C this amounts to an additional uncertainty of ± 2.6°C. Thus the total uncertainty in the temperature readings listed in Table 8 is of the order of ± 10.6°C.

Relative accuracy over small temperature ranges is much more difficult to assess. To do so would require a detailed knowledge of the way the various inaccuracies vary with potentiometer dial setting. However, it is certain that the relative accuracy will be much greater than the absolute accuracy. The only major contribution to the uncertainty in relative readings will come from the $\pm$ 20 μV resolution uncertainty. This is equivalent to a relative temperature uncertainty of $\pm$ 1.4° C.

Average thermal gradients near the surface were determined over two different depth intervals. Observations were taken between eight and ten meters from the bocca. Thus for magma velocities of from 0.1 to 0.4 meters per second the magma had radiated and cooled for a minimum of 20 seconds and a maximum of 100 seconds after leaving the bocca. For this short a time interval the bottom layers of the flow are unaffected by the surface radiation, and the heat loss through the levee walls is negligible. Hence for purposes of heat flow analysis, the midstream portions of the flow may be treated as portions of a semi infinite medium.

In order to analyze the heat flow relationships in the magma, consider a right handed rectangular coordinate system with the positive x-axis downstream and the positive z-axis vertically downward. If the melt flows with velocity u_x, then the expression for the heat flux across an arbitrary y-z plane will include a convective

component $\rho c T u_x$ where

ρ = pyromagma density

c = pyromagma specific heat

T = pyromagma temperature

Thus the heat flux vector f_x across the y-z plane will be of the form

$$f_x = -k \partial T / \partial x + \rho c T u_x \qquad (16)$$

where k = thermal conductivity of the pyromagma.

In addition,

$$f_y = -k \partial T / \partial y \qquad (17)$$

$$f_z = -k \partial T / \partial z \qquad (18)$$

In considering the heat balance for an arbitrary element of volume we have

$$\rho c \partial T / \partial t + \partial f_x / \partial x + \partial f_y / \partial y + \partial f_z / \partial z = 0 \qquad (19)$$

Substituting Equations (16), (17) and (18) into Equation (19) we have

$$\partial T / \partial t + u_x \partial T / \partial x - \frac{k}{\rho c} \nabla^2 T = 0 \qquad (20)$$

This is the Eulerian form of the heat flow equation for a moving

medium. In its Lagrangian form, and provided u_x is constant, this becomes

$$\frac{DT}{Dt} - a\nabla^2 T = 0 \tag{21}$$

where $a = k/\rho c$ = thermal diffusivity.

Thus, viewed from the moving medium, the heat flow is describable in terms of the usual stationary case. Therefore, since the mid-stream upper layers of the pyromagma may be treated as portions of an infinite half-space, we seek solutions to the one-dimensional heat flow problem

$$\frac{\partial}{\partial t} T(z, t) - a\nabla^2 T(z, t) = 0 \tag{22}$$

subject to the boundary conditions

$$T(z, 0) = T_0 \tag{23}$$

$$k\frac{\partial}{\partial z} T(0, t) = \epsilon\sigma(T(0, t)^4 - T_s^4) \tag{24}$$

where

T_0 = original magma temperature

ϵ = emissivity of the surface

σ = Stefan Boltzmann constant

T_s = effective sky temperature

This is the case of a linear differential equation with a non-linear

boundary condition for which the existence of solutions has not yet been demonstrated.

Carslaw and Jaeger (1959) have developed an approximate solution for the case $T_a = 0$, for small values of time. This solution involves an approximation of the second boundary condition, Equation (24), to a less accurate representation of the energy balance at the surface, namely

$$k\frac{\partial T}{\partial z} = \epsilon\sigma[T_0^4 - 4T_0^3(T_0 - T)] \qquad (25)$$

The solution to this lesser problem has the form

$$T(z, t) = .25T_0[3 + \mathrm{erf}\frac{z}{2\sqrt{at}} + e^{hz+h^2at}\,\mathrm{erfc}\{\frac{z}{2\sqrt{at}} + h\sqrt{at}\}] \qquad (26)$$

where

$$h = \frac{4\epsilon\sigma T_0^3}{k}$$

This solution was evaluated for $T_0 = 1300°K$ for the upper and lower time limits $t = 100$ seconds and $t = 25$ seconds, using the following estimates for the necessary constants

$\epsilon = 0.5$ based on the behavior of steels and molten slags at
   elevated temperatures

$\rho = 3.0$ g/cm^3 for basalt

$c = 1.4$ Joules/g/°C, McConnell et al. (1967)

$k = 1.0$ Watts/cm/°C, Lee and Kingery (1960)

The results are shown in Figure 19. Within the limits of observa-
tional uncertainty, the observed gradients are consistent with the the-
oretically calculated curves. The large value of thermal conductivity
used here reflects the fact that at elevated temperatures the thermal
conductivity k can be expressed as

$$k = k_p + k_r, \quad k_r \gg k_p \quad \text{for} \quad T > 1000° \text{ C}$$

where

k_p = the phonon contribution to the thermal conductivity which

  decreases as $1/T$ at high temperatures

k_r = the photon or radiation conductivity involving the emission

  and reabsorption of photons and varying as T^3.
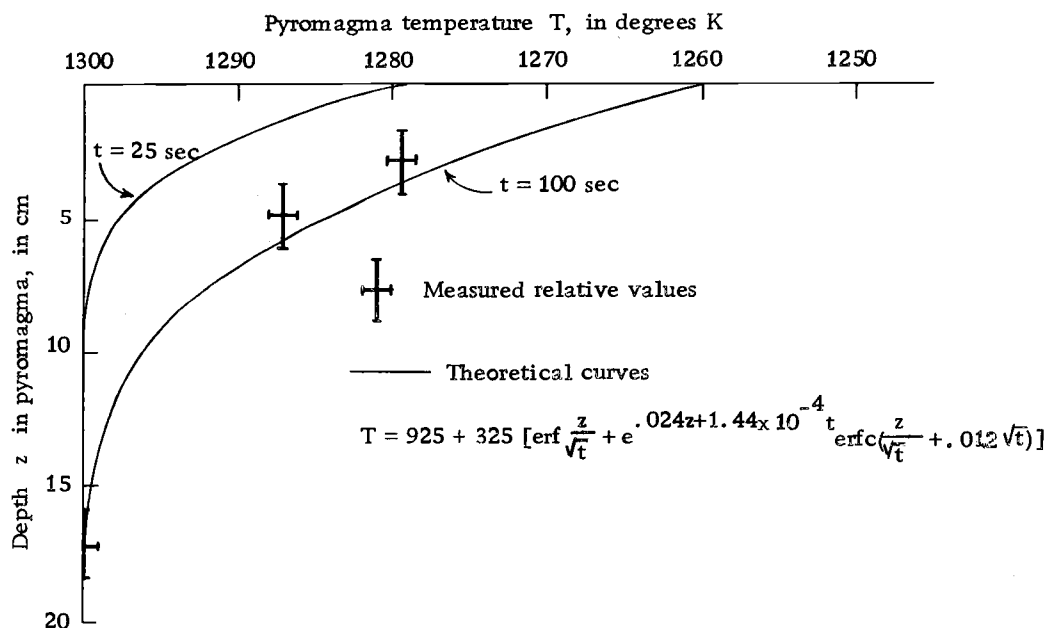
Figure 19. Calculated temperature gradients in the surface layers
of a semi-infinite pyromagma flow.

Jaeger (1950) has developed an exact, series solution for the non-linear problem for the surface z = 0.   Comparison of the surface temperatures from the exact solution with those shown in Figure 19 indicates that for the first 100 seconds, the discrepancies are less than one percent.

Conductivity Measurements

Wenner Probe Performance

In initial measurements with the four-electrode probe at the site, electrical noise of an unknown origin almost masked any usable signal. Efforts were therefore directed towards isolating and removing this interference. Once melt generated noise and signal generator radiation had been eliminated as possible sources of the interference, it was felt that the problem had to be in the circuitry of the probe itself. The difficulties were finally traced to the existence of distributed capacitive coupling between the voltage dipole leads and the current dipole leads. This problem is common in four-terminal arrays and has been treated in some detail by Wait (1959). As would be expected, the problem was most severe at the upper end of the frequency spectrum under study. The problem was more apparent than real, since under the high impedance conditions existing in the voltage dipole when the probe was out of the conductive melt, the

signal coupled into the voltage dipole was appreciable. However, once the voltage dipole was loaded with a dummy resistance approximating the melt resistance, the coupled signal dropped. The stray voltage was still appreciable, however, and careful twisting of the current pair and the voltage pair was called for. Actual measurements were never taken until the coupled signal had been minimized by judicious separation of the two pairs of leads and trial reversals of the connections. With these precautions the coupled signal was always kept at least 30 db below the signal expected from the current in the melt.

The behavior of the Wenner array under actual operating conditions appeared at first to be anomalous, and electrochemical reactions at the electrodes were suspected. Although ordinarily one would not expect the Wenner array to be affected by unexpected electrode potentials, it was felt essential to understand the nature of the anomalous behavior before overvoltage effects could be removed entirely from suspicion. The probe behavior was as follows: when the probe was first inserted in the pyromagma, the current in the melt was very low and the signal at the voltage dipole was large. The probe was dipped into the melt in a manner similar to that used with the thermocouple probes. Several consecutive dips were necessary before the current into the melt would increase appreciably. As the current built up to a final steady value there was a corresponding

drop in the voltage detected at the voltage dipole, rather than the ex-
pected rise. These trends are illustrated in Figure 20a. Readings
were taken only after continual dipping confirmed that the current had
indeed reached a definite maximum and the voltage a definite mini-
mum.

Insight into this behavior can best be gained by referring to the
equivalent circuit diagram of Figure 20b. In particular, the relative
impedances presented by the melt resistance R_m, the stray capaci-
tance C, and the stake impedance Z_s need to be considered.

Melt Resistance

An approximate melt resistance can easily be determined from
the value of apparent conductivity eventually determined. Using the
Wenner relationship, Equation 12

$$V_{BC}/I = 1/2\pi\sigma a$$

The expression V_{BC}/I gives a value for the apparent resistance
seen by the voltage dipole under current conditions established by the
current dipole. For a magma apparent conductivity of 0.3 mhos/m
and an electrode spacing of 8 cm the apparent resistance is approxi-
mately 7 ohms. This resistance estimate is perfectly adequate for
the order-of-magnitude estimates needed to analyze the probe behav-
ior.
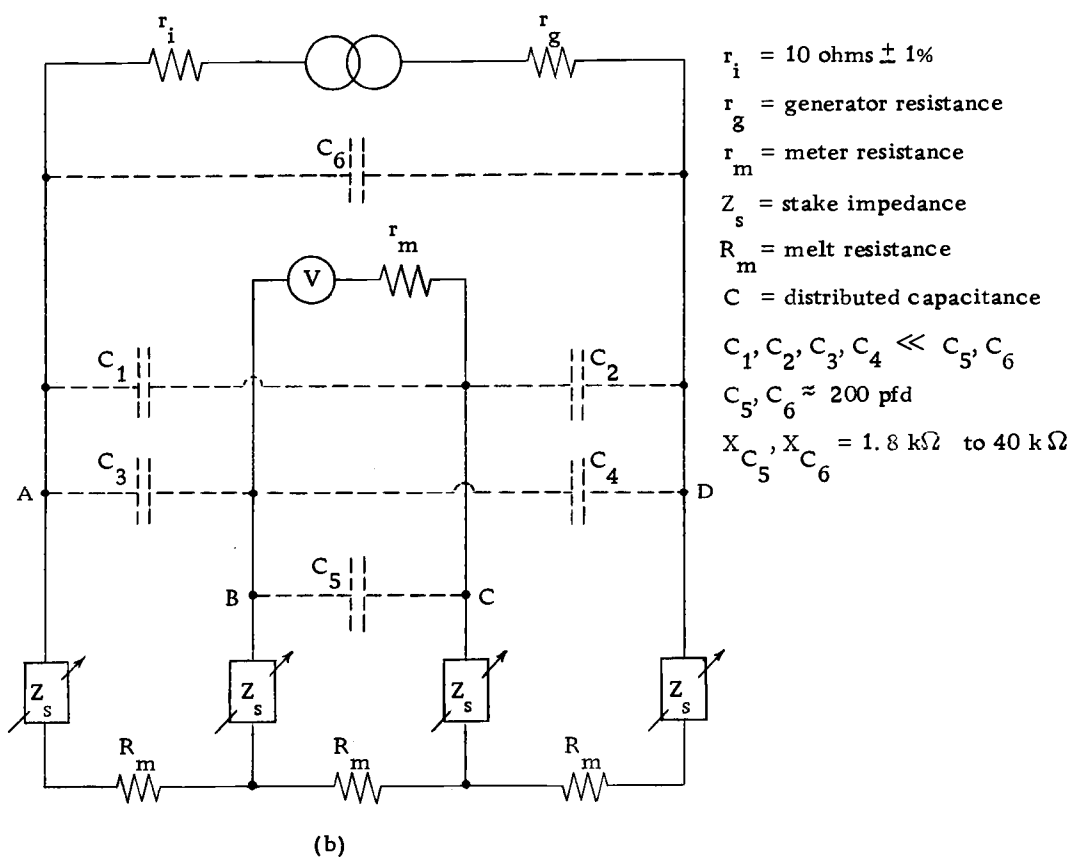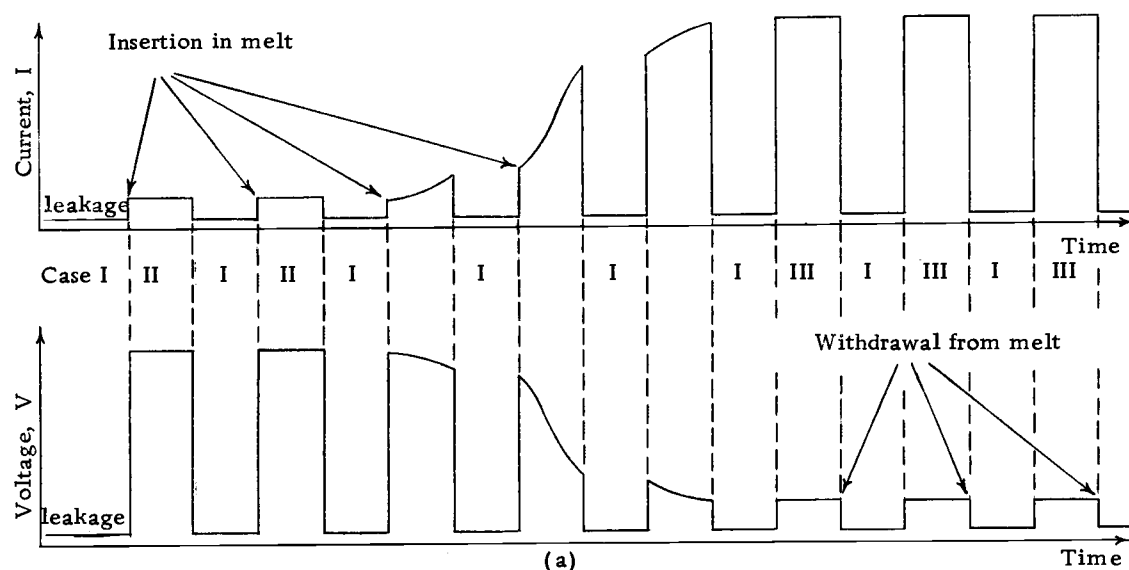
Figure 20. Analysis of performance of four-terminal Wenner probe.
(a) Temporal volt-ampere relationships in Wenner array
(b) Wenner array equivalent electrical circuit

Stray Capacitance

Unavoidable distributed capacitance existed between each of the four wires forming the current and voltage dipoles, and each of the other three in turn. These stray capacitances are represented by C_1, C_2, C_3, C_4, C_5 and C_6 in the equivalent circuit shown in Figure 20b. An estimate of the magnitude of these stray capacitances was obtained by shorting electrode A to electrode B, and shorting electrode C to electrode D. This composite dipole was then fed from the signal generator, and the current and voltage developed were noted over the frequency range 20 kHz to 400 kHz while the probe was out of the melt. The logarithm of the resultant impedance was then plotted as a function of the logarithm of the frequency. The resultant straight line plot of slope -1 confirmed that the impedance out of the melt was purely capacitive, and from plot intercepts the distributed capacitance between the two leads of the composite dipole was determined to be 420 pfd, representing a reactance of 920 ohms at 400 kHz and 20,600 ohms at 20 kHz. This would appear to be a reasonable value for the distributed capacitance of the voltage dipole leads in parallel with the current dipole leads in view of the fact that the capacitance between the voltage electrodes alone is approximately one pfd. This is most easily demonstrated by using the relationship (Watt, 1967)

$$C = \frac{0.1208\, \ell}{\log\left[\frac{D+(D^2-d^2)^{1/2}}{d}\right]} \tag{27}$$

where

C = capacitance between two parallel rods, in pfd

ℓ = rod length, in cm (30 cm)

D = rod separation, in cm (8 cm)

d = rod diameter, in cm (0.95 cm)

The distributed capacitance between the current dipole elements should be comparable to that for the voltage dipole elements since both pairs were equally tightly twisted and were of comparable length. Thus since the shorting arrangement used connected them essentially in parallel, each pair would appear to have a distributed capacitance in the order of 200 pfd and a capacitive reactance varying from 1,800 ohms at 400 kHz to 40,000 ohms at 20 kHz.

The capacitance between a voltage element and a current element should be considerably less than 200 pfd, and not at all constant, since current and voltage pairs were separated over a large portion of their length and were continually being repositioned.

Stake Impedance

Three factors generally contribute to the resistance of an electrode immersed in a conductor, namely

(a)   The resistance of the actual electrode.

(b)   The contact resistance or reactance between the electrode

and the surface of the conductor.

(c)   The resistance of the conductor immediately surrounding

the electrode.

In the case of molybdenum, the high temperature conductivity is of

the order of 2.5×10^6 mhos/m. Thus for a 3/8 inch diameter, 30

inch rod the resistance is a fraction of a milliohm, and consequently

is negligible.

The contact impedance is an unknown quantity depending on the

chemical reactions in the melt. It is not known what molybdenum

compounds form from the melt at the interface. Since certain moly-

bdenum compounds such as $MoSi_2$ are excellent high temperature

conductors, while others such as MoS are not, it is apparent that a

wide range of surface resistances should be considered.

The resistance of the conductor in the immediate neighborhood

of the electrode can be calculated for simple geometrical shapes.

The case of a short cylindrical electrode is not particularly simple,

but limits can easily be set on the value by considering the value for

a hemisphere as one extreme, and the value for a long narrow semi-

ellipsoid of revolution as the other.

For a hemispherical electrode where the current will be radial,

consider a concentric hemispherical shell in the surrounding

conductor of conductivity σ. If r is the radius of the hemispherical shell measured from the center of the hemispherical electrode, and dr is the infinitesimal thickness of the shell, then the shell will present a resistance dR to the outgoing current where

$$dR = \frac{dr}{\sigma \cdot 2\pi r^2} \tag{28}$$

Since all such spherical shells surrounding the electrode are in series, we have, for the total resistance to the current flowing from the electrode

$$R = \frac{1}{2\pi\sigma} \int_{r_0}^{\infty} \frac{dr}{r^2} \tag{29}$$

where

$$r_0 = \text{radius of the hemisphere}$$

Thus

$$R = \frac{1}{2\pi\sigma r_0} \tag{30}$$

In the case of a hemisphere of 3/8 inch diameter $(r_0 = 4.75 \times 10^{-3} \text{ m})$ immersed in a melt of conductivity 0.3 mhos/m, this reduces to a volume resistance of 112 ohms.

The second limiting case of a half ellipsoid of revolution has been treated by Tagg (1964) who shows that

$$R = \frac{1}{2\pi\sigma\ell} \ln (2\ell/a) \tag{31}$$

where

ℓ = length of immersed electrode

a = radius of electrode

Therefore, in the case of a rod of 3/8 inch diameter

$(a = 4.75 \times 10^{-3} m)$ immersed $3 \times 10^{-2} m$ into a melt of conductivity

0.3 mhos/m we have

$$R = 45 \text{ ohms}$$

This figure can by no means be considered exact since an ellipsoid of

eccentricity six is a rather poor approximation to a cylinder. How-

ever, when taken in conjunction with the estimate for a hemisphere,

it indicates that the volume resistance should be somewhere in the

neighborhood of 50 to 100 ohms.

Thus the total stake impedance is expected to be 50 to 100 ohms

plus whatever contact impedance may develop at the electrode sur-

faces. This is represented by the variable impedance Z_s in Fig-

ure 20b.

Circuit Analysis

By referring now to Figure 20b with these approximate values

of melt resistance R_m, coupling reactance X_c, and stake im-

pedance Z_s in mind, the behavior of the molybdenum Wenner ar-

ray can be readily understood. There are essentially three

configurations of current flow possible in the array depending on the

relative magnitudes of the changing resistances and the fixed capaci-

tive reactances.

Case I. With the probe out of the melt and R_m essentially

infinite, a small AC current still flows from the generator through

the various distributed capacitances shown. The potential difference

V_{BC} across capacitor C_5 is determined by the potential dividers

formed by capacitances C_1, C_2 and C_3, C_4 respectively. Since

these distributed capacitances are all different because of the differ-

ent lengths and configurations of the leads, the potential difference

across C_5 can become an appreciable fraction of the input voltage

from the signal generator. This is the "noise" voltage previously

examined and minimized. The AC current in the distributed capaci-

tances constitutes the "noise" or "leakage" current.

Case II. After the probe insertion in the melt, R_m, which

depends now only on the melt characteristics, immediately drops to

its final low value of around 7 ohms. Since the current is observed to

rise only slightly from its "noise" value it is concluded that the cur-

rent path Z_s, R_m, R_m, R_m, Z_s through the melt is a high imped-

ance path, and consequently Z_s must include an appreciable sur-

face impedance term. Since the melt current is still minimal while

the detected voltage is a maximum it would appear that the voltage in-

crease cannot be attributed to fields in the melt, but must occur

because of changes in the balance of the bridge circuit formed by

C_1, C_2, C_3 and C_4. The changes observed are consistent with the

existence of a large capacitive reactance term in Z_s such that C_2

and C_3 are shunted with resultant bridge imbalance, but such that

the melt is still fed through a high impedance path.

Case III. Z_s drops to its final low value and the voltmeter re-

cords the signal of the low impedance melt rather than the signal of

the high impedance distributed capacitance bridge.

It would thus appear that the anomalous behavior of the array

is consistent with the interpretation that some unknown chemical re-

action is occurring at the electrodes in the melt and creating a high

surface impedance which only burns off at high temperatures after

several immersions in the melt.

Confirmation of this interpretation was obtained by parallelling

the voltage and current dipoles and making a two-terminal determina-

tion of resistance in the melt. When the current had again stabilized

at a highest value and the voltage at a lowest value, the total circuit

impedance equal to $Z_s + R_m + Z_s$ was found to be 149 ohms, in

reasonably good agreement with the earlier minimum estimate of

$(45 + 7 + 45) = 97$ ohms and maximum estimate of

$(112 + 7 + 112) = 231$ ohms. Thus no suspicion of overvoltage effects

remained even at the lowest frequencies, and the meter indications

were believed to be true indications of the melt conductance.

Experimental Results

   In the earlier development of Wenner four-electrode theory it
was assumed that the conductor involved obeyed Ohm's Law.   As a
first procedure therefore, it was necessary to establish whether this
were true for pyromagma.   Conductivity determinations were there-
fore made using a variety of drive voltages from the signal generator.
The range of voltages available from the portable unit was somewhat
limited, but over the decade range available the conductivity did in
fact appear unchanged.   This is shown in Figure 21.
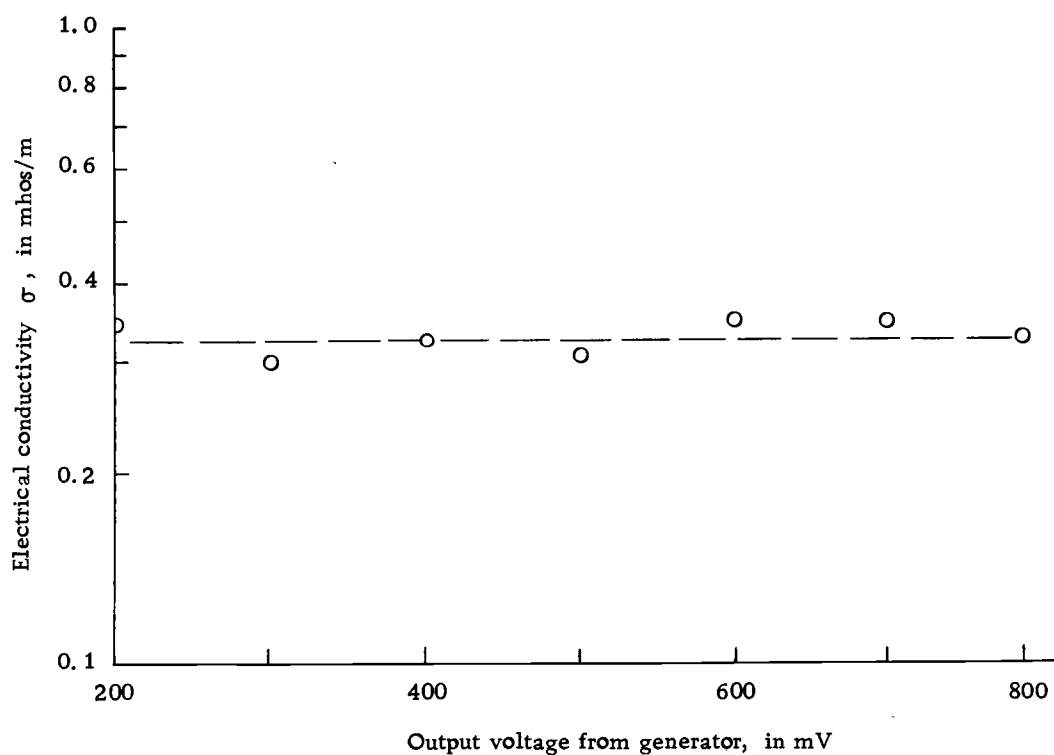
Figure 21.   Verification of Ohm's Law for Etnean pyromagma.

A summary of all conductivity measurements made appears in Table 8. These values have a probable error of $\pm$ 6% based on the following facts and assumptions.

(a) The precision current monitoring resistor was 10 ohms $\pm$ 1%.

(b) The voltage and current monitoring meters had machine engraved, individually calibrated mirror scales, and were certified to $\pm$ 3%.

(c) The probe spacing was within one millimeter of the desired eight centimeters spacing. Periodic checks were made for rod warpage, but none appeared. Although molybdenum has great rigidity, the rods could be sprung slightly by hand. Consequently, to allow for any springing due to turbulence in the crusting melt, the estimate of the uncertainty in the spacing is placed at $\pm$ 2%.

(d) Scatter in the observations for a given current or voltage data point had a standard deviation of less than 8% of the mean value.

(e) It was not possible to assess the uncertainties due to magma inhomogeneity or surface irregularity. In view of the magnitude of the surface temperature gradient the apparent conductivity σ_a could differ appreciably from the conductivity in the vicinity of the electrodes.

The electrical conductivity as a function of frequency and temperature is shown in Figure 22.

Any dispersion occurring is very small. Since the uncertainty in the absolute value of the measurements is $\pm$ 6%, only those data for T = 1042° C (showing a departure of 20% from the mean value) can be taken as indicative of dispersion. However, even this case cannot be interpreted unambiguously as dispersive since the abnormally high gas content associated with these data could easily have resulted in a lowering of the apparent conductivity. This absence of appreciable dispersion is not surprising in view of the work of Keller and Frischknecht (1966) who report a marked decrease in the dispersion of the electrical conductivity as most minerals are heated. Their work shows that in many minerals, dispersive effects had almost entirely disappeared by the time their maximum temperature of 900° C had been reached.

The temperature dependence of the electrical conductivity of rocks, minerals, molten glasses and slags is known to follow a law of the form

$$\sigma = \sigma_0 e^{-\Delta E/kT}$$

where

ΔE is in the nature of an activation energy

k = Boltzmann's constant

T = Absolute temperature

For the three temperatures recorded in Etnean pyromagma, the temperature dependence of the electrical conductivity is found to be consistent with an activation energy $\Delta E = 1.5 \pm 0.5$ eV.
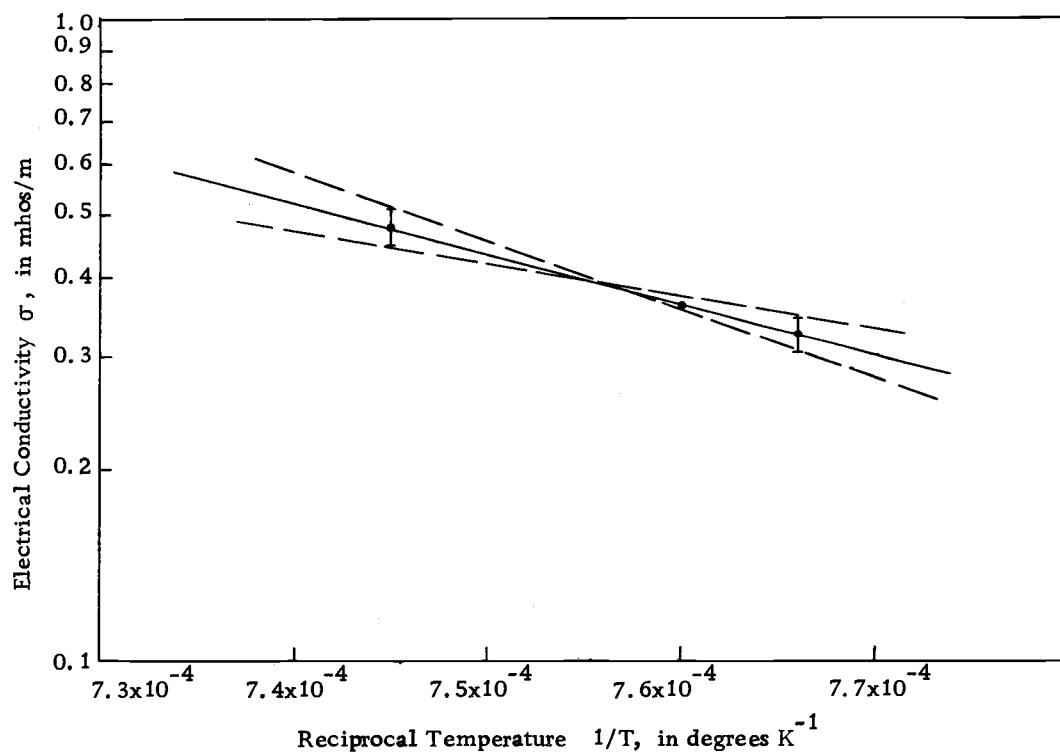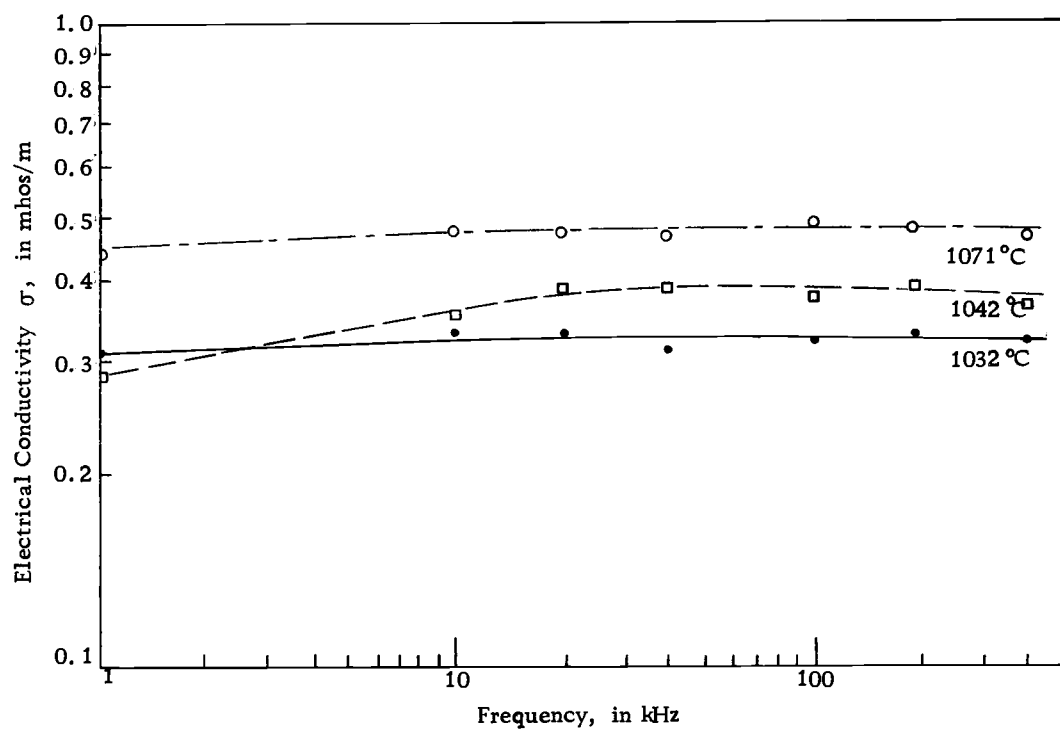
Figure 22. Frequency and temperature dependence of the electrical
conductivity of Etnean pyromagma.

THE CHARACTER OF ELECTRICAL CONDUCTION
IN PYROMAGMA

Conducting Phases Present in Pyromagma

The thin-sections whose microphotographs are shown in Figures 15 and 16 reveal the conditions existing in the melt itself. The sections were cut from specimens pulled from the upper part of the melt. Since these melt samples cooled and solidified very rapidly there was no opportunity for any crystal growth to occur after the sample was taken. Any crystals present in the thin-sections must have been present in the melt itself. That portion of the pyromagma which was molten when the sample was taken would form a glassy matrix upon cooling. Thus it is apparent that the pyromagma is an extremely heterogeneous mixture of solid crystals and gas bubbles of varied sizes in a matrix of molten glass. More specifically, the phenocrysts are mainly plagioclase (sodic and calcic feldspars), pyroxenes, olivene and magnetite; the gas bubbles contain mostly CO_2, CO, and SO_2 at a pressure slightly greater than one atmosphere; and the glassy melt contains all the elements listed in the silicate analysis shown in Table 2 but in different proportions because the silicate analysis of the phenocrysts will be different from that of the ground-up samples.

At the present stage of knowledge of the nature of conduction in

such a mixture, any discussion of the character of the conduction
must of necessity be general in nature. However, conduction mechan-
isms and glass structure are sufficiently well understood to give in-
sight into the relative importance of these three phases, and to enable
a plausible explanation to be made for the value of the conductivity
actually observed.

Phenocryst Conduction

The temperature dependence of the electrical conductivity of
most of the phenocryst minerals present has been measured frequent-
ly in the laboratory (Noritomi, 1955; Veltri, 1963; Keller and
Frischknecht, 1966). Figure 23 shows representative curves for
feldspars, pyroxenes and olivene. It is apparent that at 1050°C, with
the possible exception of magnetite, the electrical conductivity of all
the minerals present as phenocrysts in the pyromagma is from one
to two orders of magnitude smaller than that of the net conductivity
of the pyromagma as measured in this study (Figure 22 and Table 8).
No high-temperature conductivity data are available for magnetite,
but even though it were highly conducting, it would have no appreci-
able effect on the bulk conductivity because its concentration is so
small.
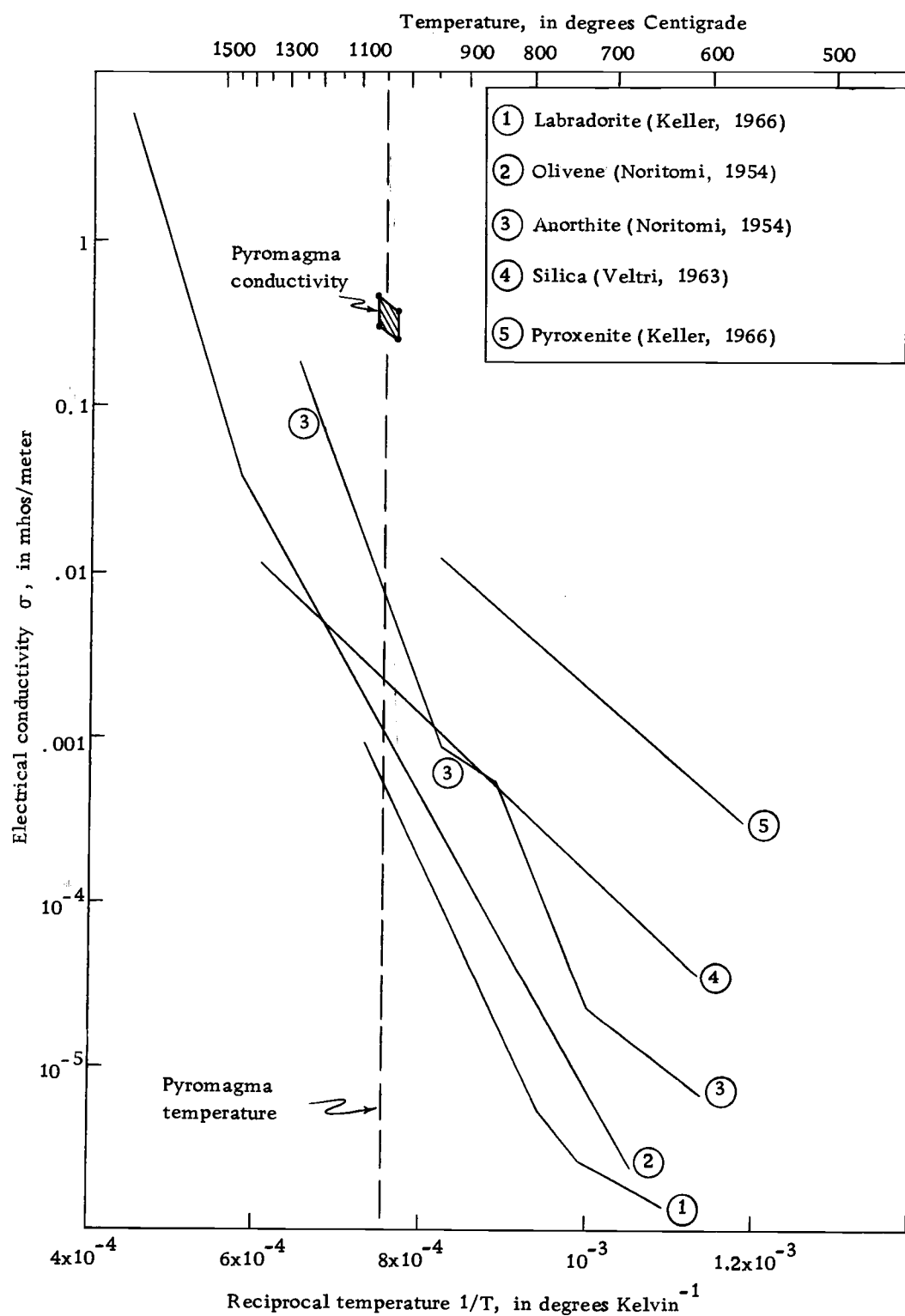
Figure 23. Electrical conductivity as a function of reciprocal absolute temperature for common rock-forming minerals.

Effects of the Gas Phase

Some limits can be placed on the magnitude of anticipated con-
duction effects in the gas bubbles. In general, the thermal ionization
of molecules in a gas as a function of the gas temperature and pres-
sure is expressible by one of the forms of the Saha equation. In its
simplest form, where equilibrium between thermionic emission and
recapture of electrons in a single constituent gas is the only process
considered, the ionization can be readily calculated as a function of
temperature and pressure. However in more complex real situations,
involving multi-component systems with an appreciable probability of
molecular dissociation, the relationship becomes much more com-
plex because a number of competing equilibria have to be considered
simultaneously. Thus in practice the conductivity of a given gas
mixture at a given temperature and pressure is usually determined
experimentally. In connection with MHD generator design studies,
Moore (1963) has made measurements which indicate an electrical
conductivity of 10^{-3} to 10^{-4} mhos/m for a one atmosphere mixture of
the usual atmospheric gases plus water vapor and hydrogen at 1050°C.
The bulk of the contribution comes from the water molecules which
have a permanent dipole moment, and almost all the remainder
comes from the CO_2 molecules which are polarizable. Since, with the
exception of SO_2 which is also polarizable, the gas mixture reported

on by Moore (1963) and the pyromagma gas studied here have the

same critical components, it is expected that the two mixtures would

have electrical conductivities of the same order of magnitude, namely

10^{-3} to 10^{-4} mhos/m.

This low value of conductivity would seem to indicate that the

gas bubbles make an insignificant contribution to the bulk conductivity

of the pyromagma. However Brogan (1963) and Moore (1963) have

both reported on the "seeding effect" of adding elements of low ioniza-

tion potential such as the alkali metals to the gas of an MHD genera-

tor. In particular, the presence of Na, K, or Ba in concentrations

of as little as 0.1% by weight raised the conductivity by factors of at

least 100. Since all of these elements migrate as charge carriers in

the melt, and since electron conduction in the melt has not yet been

ruled out as a conduction mechanism, the participation of these

charge carriers in the conduction mechanism of the gas phase cannot

be ruled out with any certainty.

Some of the uncertainty as to the relative magnitude of the elec-

trical conductivity of the gas and melt phases of the pyromagma can

be removed by a consideration of the frequency dependence of the

pyromagma conductivity. If the gas bubbles were to have an electri-

cal conductivity appreciably greater than that of the melt phase, in-

terfacial polarization of the Maxwell-Wagner-Sillars type would most

certainly occur and reveal itself as a dispersion in the AC electrical

conductivity of the pyromagma. Its total absence in the Etnean pyro-
magma indicates a gas conductivity no larger than that of the melt.

Thus, with reasonable certainty, the conductivity of the gas phase is

in the range 10^{-4} to 3×10^{-1} mhos/m with the lower figure pertaining

unless melt alkali ions or melt electrons are proven to enhance the

gas conductivity.

Conduction in the Glassy Melt

The remaining phase to be considered, the glassy melt, is the

only continuously connected phase in the pyromagma, and its conduc-

tion is thus of paramount significance. The electrochemistry of sili-

cate melts is a subject still largely unexplored. Although extensive

conduction measurements have been made on solid silicates at ele-

vated temperatures, the work in general stops short of the melting

point of these silicates. In the few cases where studies have been

made on the molten phase they have been of an ad hoc character,

usually concerned with specific technological problems relating to

glasses or to steel slags. Thus Bockris et al. (1952), Abe (1952),

Eitel (1954), Taylor (1959), Urnes (1959), Owen (1961), Endell and

Helbrugge (1967) and Tickle (1967) have made significant contributions

to a survey of electrical conduction in binary glass systems of the

form M_2O-SiO_2, MO-SiO_2, or M_2O_3-SiO_2 (where M is a univalent,

divalent or trivalent metal), and in ternary melts of glasses in the

$CaO-B_2O_3-Al_2O_3$, $Li_2O-Na_2O-SiO_2$, $Na_2O-K_2O-SiO_2$ and $Li_2O-K_2O-SiO_2$ systems.

Several ternary slags have also been studied. Wejnarth (1934) measured the electrical conductivity of the $CaO-FeO-SiO_2$ system. Martin and Derge (1943) repeated the procedure for $CaO-Al_2O_3-SiO_2$ slags and Toropov and Bryantsev (1965) have made extensive measurements on the $MgO-FeO-SiO_2$ system. Elliot, Gleiser and Ramakrishna (1963) have reported some work on a four component $CaO-MgO-Al_2O_3-SiO_2$ melt. While it is at once apparent that none of these melts approaches in complexity the fluid phase of the Etnean pyromagma, they nevertheless provide valuable insights into the conduction mechanisms present in silicate melts in general, and also provide indications of the effects to be expected as the number of metal oxides present in the pyromagma is proliferated.

From these studies, a reasonably clear picture of the structure and the atomic behavior of silicate melts has begun to emerge. Based on the pioneering work of Zachariasen (1932) it is believed that silicate melts possess a structure demonstrating short-range order. Of all the atoms present in the melt, silicon dominates the structural behavior because of its particular characteristics. The silicon ion is much smaller than most of the other ions of the melt, and in addition has a larger charge than any of the other cations present. Since these properties enable the silicon ion to attract oxygen much more

strongly than can other cations, the silicate tetrahedron consisting of four nearly close-packed oxygen atoms surrounding a much smaller silicon atom becomes the fundamental and stable building block of all silicates.

These tetrahedral silicate ions, $(SiO_4)^{-4}$ form larger groups by sharing corners through a common oxygen ion. Thus chains, rings, sheets and three dimensional networks can form, depending on the number of corners of the silicate tetrahedra involved in the linkages. When all four corners of all tetrahedra are involved in such linkages as illustrated in Figure 24a the result is silica with the formula SiO_2 since each oxygen ion is shared by two tetrahedra. It should be noted that as the degree of tetrahedral corner sharing increases, the oxygen/silicon ratio decreases continuously from four to two.

When silica is fused, the result is as represented schematically in Figure 24b. Corner linkages break with difficulty, long chains and rings and a tenuous three-dimensional structure still exist and the melt is extremely viscous. If, however, basic metal oxides are added to the melt, the increased oxygen abundance makes the sharing of oxygen between two tetrahedra less necessary. This results in less corner linkages, a much more open unconnected structure, a dramatic decrease in melt viscosity and a dramatic increase in electrical conductivity. The cation portion of the metal oxide is localized in the structure near the site of the oxygen utilization, and it may or

Silicon
Tetrahedron

Oxygen

Silicon

(a)

(b)

Metal
● cation

(c)
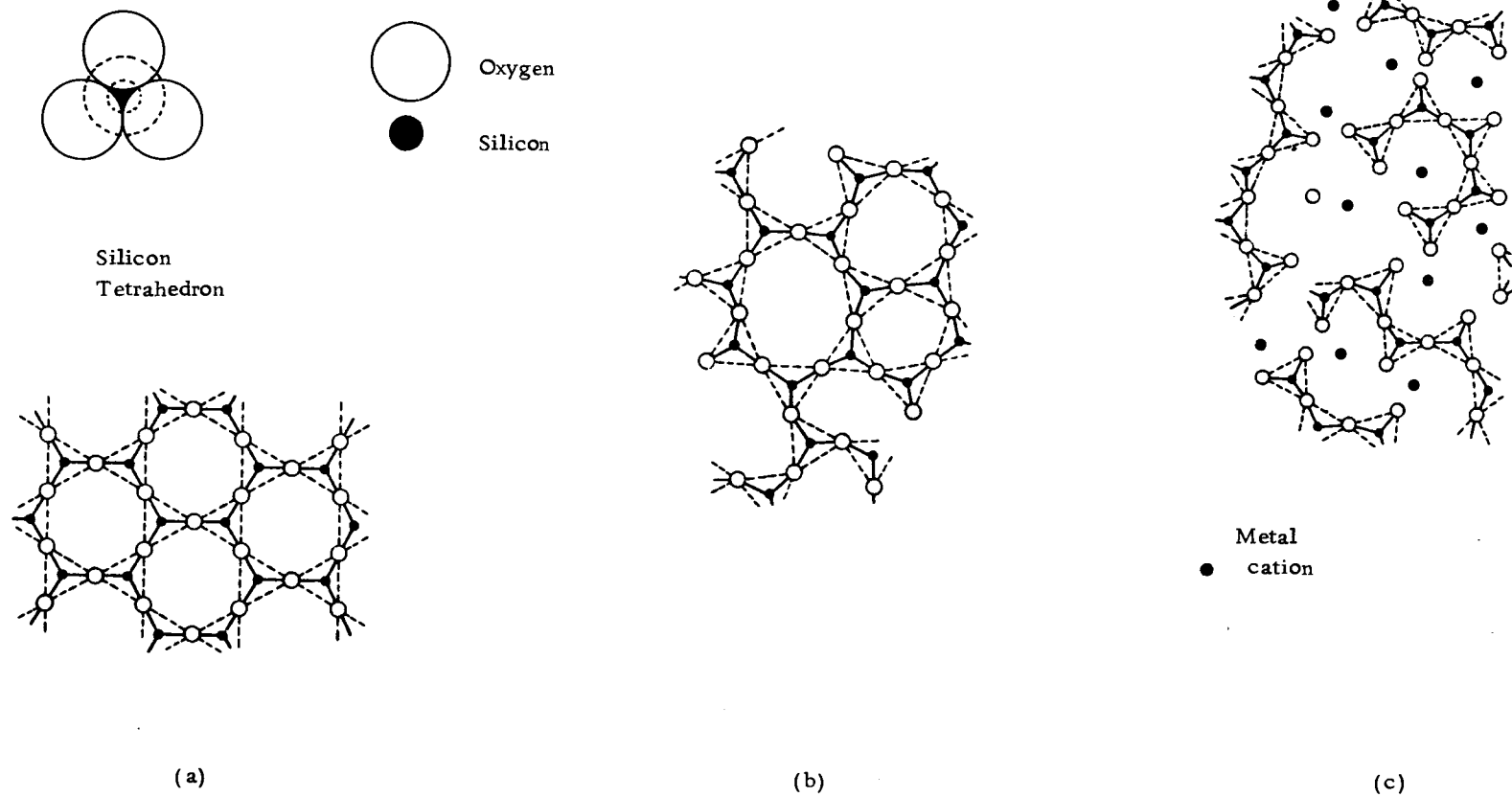
Figure 24. Idealized structure of silicates.
   (a) Silicon tetrahedron and silica
   (b) Fused silica
   (c) Silicate melt with metal oxides added

may not be available for conduction. This is illustrated in Figure 24c.

Electrolysis experiments have shown that all the metal ions occurring normally in silicate melts, including even relatively large metal ions such as iron and calcium, can participate as charge carriers (Dickson and Dismukes, 1962). Even oxygen ions sometimes serve as charge carriers in very basic melts (oxygen/silicon ratio of four or higher) and electronic conduction and p-type semiconduction are suspected to exist in certain very basic melts and high iron content melts.

Much of the remaining insight into conduction mechanisms in silicate melts is of an empirical nature. It is largely a qualitative and geometrical approach and considers the effect of ionic size and charge on the ability of metal cations to migrate through structural breaks. For example, the mobilities of Ca^{++}, K^+, and Na^+ are generally in the ratio of about 1: 10: 100. These ratios can vary drastically however, since the presence of positive ions in the melt appears to polarize the oxygen bonds. Addition of a particular metal oxide to a melt may either enhance conductivity due to the increased charge carrier concentration, or else reduce conductivity because of a rearrangement of the melt structure. Thus few generalizations are possible on the effects of changing the proportions of the various metal oxides in a silicate melt.

Figure 25 shows the complexity present in the few known ternary systems. It is immediately apparent that little can be inferred from these specialized systems as to the particular conductivity of the Etnean melt. The only reasonable inference that can be drawn is that since the concentrations giving rise to conductivity maxima have only a very narrow range of values, the probability is low that the particular concentrations found in Etnean pyromagma fall in one of these ranges. Since the oxygen/silicon ratio of the pyromagma (3.5) is similar to that of the basic slags of Figure 25, the charge carrier concentrations involved must also be similar. Since the viscosity of the Etnean pyromagma (4×10^4 poise, Imbò, 1964) is very close to that of the basic slags described in Figure 25 (from 5×10^3 to 10^4 poise, Toropov and Bryantsev, 1965) the degree of "openness" of the melt structures must also be similar. Hence it would appear reasonable to conclude that the electrical conductivity of the molten glass phase of the Etnean pyromagma is about the same or slightly lower than that of the slags of non-optimum proportions. A reasonable estimate for this conductivity would be somewhere in the range, one to ten mhos/m.

Effects of Voids on Electrical Conductivity

The modal analysis recorded in Table 7 indicates that almost 60% of the volume of the pyromagma is composed of voids and
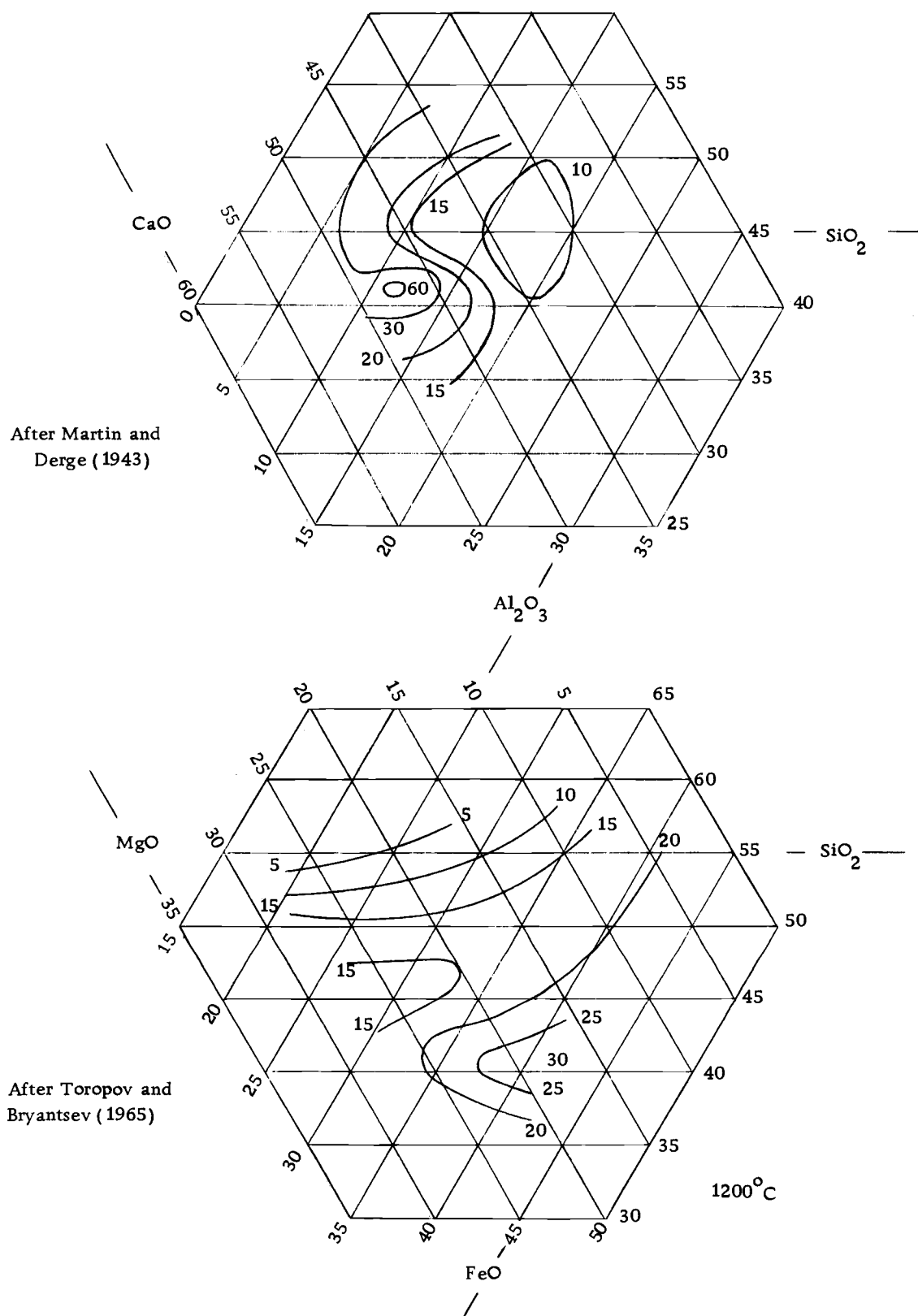
Figure 25. Electrical conductivity of ternary slags, in mhos/m.

phenocrysts. Since these phases have a conductivity which is probably 100 times smaller than that of the glassy phase, it becomes important to consider the effect of the poorly conducting phase on the bulk conductivity of the pyromagma.

Meredith (1959) has assembled a detailed summary of the score of approaches that have been made to the analysis of the effects on the conductivity when a poorly conducting discontinuous phase is dispersed throughout a continuous, more highly conducting phase. For these analyses it is convenient to define contrast parameters K_d and K_m such that

$$K_d = \sigma_d / \sigma_c$$

$$K_m = \sigma_m / \sigma_c$$

where

σ_d = conductivity of the dispersed phase

σ_c = conductivity of the continuous phase

σ_m = conductivity of the mixture.

Almost all of the relationships developed over the years can be shown to be reducible to forms developed either by Maxwell (1881) or by Bruggeman (1935). Maxwell's relation treats the case of a dispersion of spheres sufficiently dilute that field distortion introduced by one sphere does not influence neighboring spheres. For this case

$$K_m = \frac{K_d + 2 - 2f(1 - K_d)}{K_d + 2 + f(1 - K_d)} \qquad (32)$$

where f = the volume fraction of the dispersed phase.

Bruggeman's work allows for a distribution of sphere sizes and considers concentration effects. K_m is not expressed in explicit form except for the case when K_d approaches zero.   For this case ($K_d \rightarrow 0$)

$$K_m = (1 - f)^{3/2} \qquad (33)$$

According to Meredith, the Maxwell equation and the Bruggeman equation appear as upper and lower bounds between which almost all the reported experimental data lie.

The Bruggeman equation considers only a distribution of spheres since it was based on Maxwell's earlier work.   Meredith has taken the outline of the Bruggeman analysis, but in addition has incorporated the effect of the shape of the dispersed volumes.   Among others, he has considered the case of the combination of the sphere and the prolate spheroid of axial ratio two in equilibrium concentrations.   This represents the case of a concentrated dispersion where inelastic collisions of spheres result in shapes approaching that of the prolate spheroid of axial ratio two, and is particularly suitable for application to pyromagma analysis.

(In the course of preparing the modal analysis of Table 7 over 9,000 points throughout the thin sections were examined microscopically. In this process every void in the thin-sections came under scrutiny even if it did not fall on the spot being point counted. Almost without exception the voids showed an approximately circular or elliptical outline, those of elliptical form undoubtedly indicative of spherical bubbles only recently coalesced and not yet reformed to a new, larger spherical contour.)

For the case of an equilibrium distribution of spherical and spheroidal volumes, Meredith has developed the following relation

$$K_m = \frac{1-2(f'\,Y'+f''Y'')}{1+(f'\,Y'+f''Y'')} \tag{34}$$

where single and double primes refer to sphere and spheroid respectively.

$$f'' = 4(f')^2$$

Y' and Y'' are "form factors" which vary with the K_d value chosen.

The Y' and Y'' values of interest in analyzing the Etnean pyromagma are listed in Table 9.

Table 9. Form factors for Meredith's doublet model (Meredith, 1959).

K_d	Y'	Y''
0	0.500	0.515
0.01	0.493	0.507
0.1	0.429	0.438
1.0	0	0

Meredith has also developed a "distribution model" in which he incorporates the concept that "the effective conductivity of the continuous medium in the neighborhood of a particle is better represented by the conductivity of the surrounding mixture than by the conductivity of the continuous medium alone." For this model

$$K_m = (\frac{2+(WK_d-1)f}{2+(W-1)f})(\frac{2(1-f)+WK_df}{2(1-f)+Wf}) \tag{35}$$

where

$$W = \frac{3}{K_d+2}$$

In order to evaluate the degree to which the gas bubbles and phenocrysts decrease the effective conductivity of the Etnean pyromagma, the K_m values for a realistic range of conductivity contrasts K_d are calculated for the two Meredith models and the Bruggeman and Maxwell models and shown in Table 10.

Table 10. K_m values pertinent to Etnean pyromagma.

Model	K_m		
	$K_d = 0$	$K_d = 0.01$	$K_d = 0.1$
Maxwell	0.308	0.315	0.386
Bruggeman	0.251	---	---
Meredith doublet	0.298	0.308	0.381
Meredith dispersion	0.286	0.293	0.351

*The differences between the various models are not of great concern since the variations related to phenocryst shapes and non-uniformity of conductivity of the dispersed phase preclude any great accuracy in the analysis. However, these figures do indicate that the conductivity of a non-gassy melt should be higher than that of the pyromagma by a factor of three to four. They thus help to explain most of the disparity between the conductivity of Etnean pyromagma and the reported conductivity values of the few molten basalts that have been measured in the laboratory.

Figure 26 summarizes all the available data on electrical conductivity of basalts. The laboratory figures are all for gas-free melts. Thus there is substantial agreement with the Nagata data and with the Khitarov and Slutskiy data. Those of Nagata are possibly somewhat high in view of the previously discussed slag data and the apparent pressure coefficient of the Khitarov and Slutskiy data. Those of Barus and Iddings are most probably in error even though they are still being used and quoted in the current literature (England
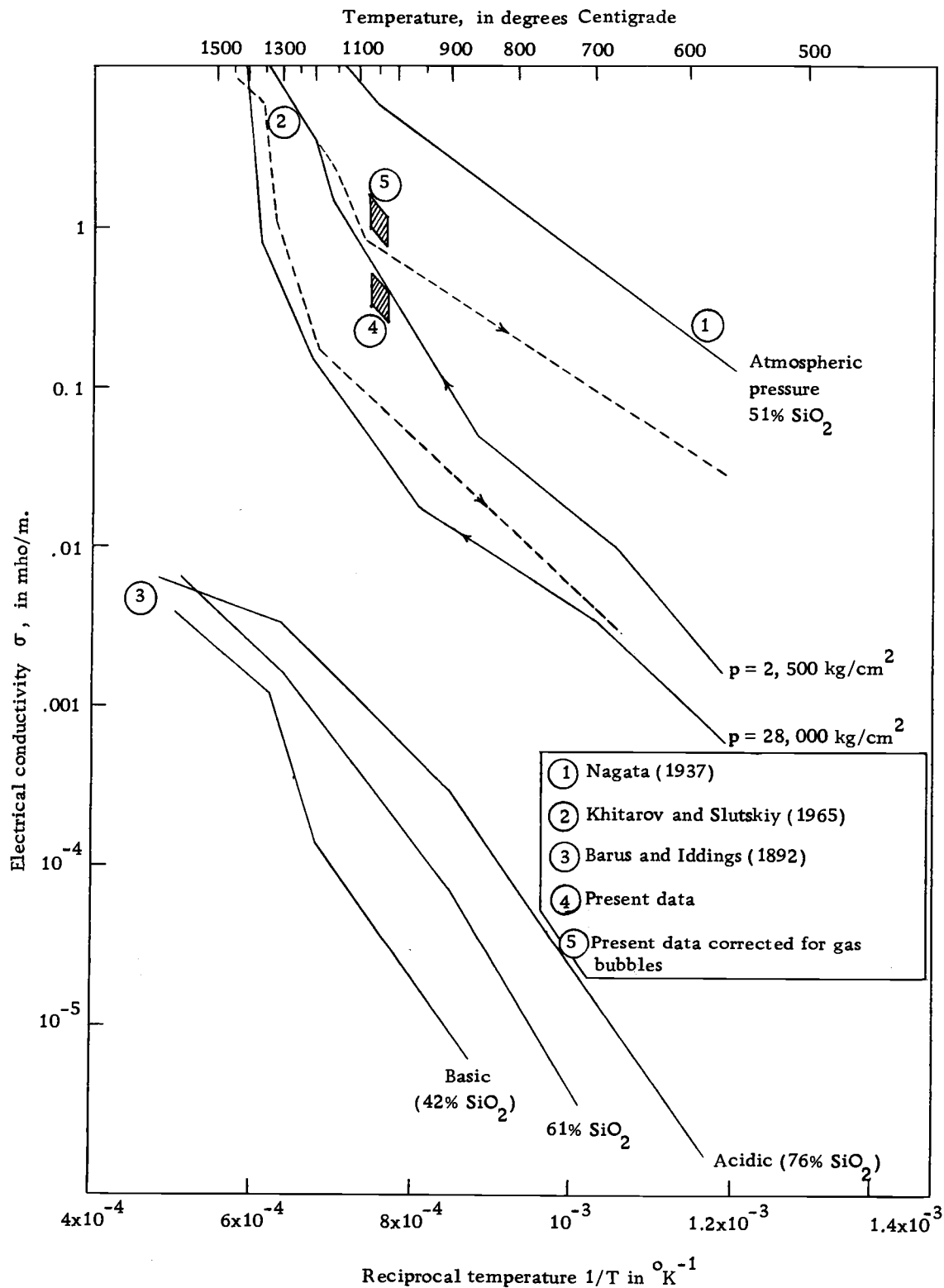
Figure 26. Laboratory measurement of electrical conductivity of lavas as a function of reciprocal temperature.

et al., 1968).

Pyromagma Conductivity Variations with Depth

This analysis of the electrical behavior of pyromagma would not be complete without a brief discussion of the variation of conductivity with depth in the volcanic conduit. A freely flowing conduit is assumed so that the pressure in the pyromagma is essentially hydrostatic. The temperature gradient in the conduit is not expected to be large. As temperature and pressure variations exist down through the volcanic conduit, the three phases of the pyromagma will be affected differently.

The gas phase will be modified in three ways. At depth, before much bubble coalescence has occurred, bubbles will be smaller and more uniformly dispersed. Gas bubbles will also be smaller by virtue of the vastly increased hydrostatic pressure. Lastly, the increased pressure will greatly enhance the electrical conductivity of the gases. Below a critical depth, the so-called "bubble point" where the hydrostatic pressure of the melt equals the vapor pressure of the gas, the gaseous phase will disappear entirely.

Verhoogen (1951) has produced the definitive analysis of gas bubble dimensions in volcanic conduits. Rittmann (1962) has analyzed the rates of gas evolution with depth for the Etnean conduit during the present phase of slow sub-terminal effusion. Ryabinin (1957) has

reported on conductivity enhancement in pressurized gases due main-ly to reductions in ionization potentials. Laboratory experiments indicate that at a pressure of 9,000 kg/cm^2, (corresponding roughly to a depth of 30 km in the earth) conductivity of typical industrial and atmospheric gases increased by factors of from 100 to 1,000,000. Thus it is expected that the pyromagma bubbles will shrink in size, and become more numerous and more conducting at depth. Whether their conductivity exceeds the melt conductivity when they first form at some particular depth is not known.

Both the phenocrysts and the glassy melt have a conductivity-temperature relationship of the form

$$\sigma(T) = \sigma_0 e^{-W/kT} \qquad (36)$$

where

W is an energy related to an electronic or ionic activation po-
tential

k = Boltzmann's constant

T = absolute temperature of phenocryst or melt

σ_0 and W are, of course, different for the melt and each of the different phenocryst types.

The pressure effect on electrical conductivity of molten basalts and basalt minerals has been considered only infrequently. Rikitake

(1952) has made a theoretical analysis of the problem. A few good sets of experimental data are available. The curves of Khitarov and Slutskiy shown in Figure 26 indicate a conductivity decrease in basaltic melts of an order of magnitude over a depth interval of about 100 km. This change is due to pressure effects on the melt structure itself, and is distinct from the pressure effects on the gas bubbles. Hughes (1955) has observed the pressure effect on the conductivity of minerals such as olivene. The decrease in the solid crystal is less than the decrease in basaltic melts, amounting only to a factor of three or four over a 100 kilometer depth interval.

Any decrease in melt and phenocryst conductivity due to pressure increase with depth will very probably be overridden by the increase associated with temperature increases. While the temperature increase with depth is probably not large, the exponential factor controlling the conductivity is such a strong function that it could easily dominate the net result. Thus the melt and phenocryst phases of the pyromagma can show no more than a small increase with depth, certainly less than a decade over the first 100 km. Near the surface, the conductivity of the gas phase will increase rapidly with depth, but the volume of the gas phase will decrease. The net result will be an increase in the pyromagma conductivity by a factor of $1/K_m \approx 3$ over the shallow interval between the surface and the level of the bubble point. Below the bubble point, the conductivity

of the conduit walls will increase at a much greater rate by virtue of the much larger vertical temperature gradients in the rock surrounding the conduit. Since, in electromagnetic probing at depth, the conductivity contrast between the magma column and the conduit walls is the significant factor, it is of interest to know whether this contrast will vanish before magma chamber depths are reached. Reference to Figures 23 and 26 shows that the conductivity contrast is still greater than ten for conduit walls and pyromagma both at the same temperature, since the curves of Figure 26 reflect the depression due to pressure increase with depth, while those of Figure 23 do not. On the basis of geomagnetic variation measurements, other workers such as Lahiri and Price (1939) have concluded that the bulk conductivity of deep crustal and upper mantle rock is of the order of 10^{-3} mho/m down to a depth of several hundred kilometers. Since, typically, magma chambers occur at depths of a few tens of kilometers, the electrical contrast between the country rock and the associated conduit or magma chamber should therefore always remain large.

SUMMARY AND CONCLUSIONS

The electrical conductivity of Etnean pyromagma has been determined over the temperature range 1032°C to 1071°C and over the frequency range 1 kHz to 400 kHz with an absolute accuracy of better than 6%.

The values measured are the second ever to be secured in actual pyromagma, the first to cover such a wide range of frequencies, the most accurate presently available and the first to be carefully identified with the chemical composition and temperature of the pyromagma. The electrical conductivity of Etnean nepheline basanite and nephelene tephrite varies between 0. 32 ± .02 mhos/m and 0. 48 ± . 03 mhos/m over the temperature interval 1032°C to 1071°C. This change with temperature corresponds to an activation energy of 1. 5 ± 0. 5 eV.

On the basis of a qualitative assessment of the variation of electrical properties down through the volcanic conduit, it is concluded that even down to the depth of the magma chamber the electrical conductivity of the magma will still be greater than that of the surrounding country rock by at least an order of magnitude.

The design of semi-expendable graphite-molybdenum electrodes and the selection of TEMTIP thermoprobes contributed to the success of these measurements.

Their use is recommended for any future electrical and thermal measurements whenever the nature of the flow permits close approach to the pyromagma.

BIBLIOGRAPHY

Abe, T. 1952. Borosilicate glasses. Journal of the American Ceramic Society 35:284-299.

Bartoli, Adolphus G. 1892. Sulla temperatura delle lave dell'attuali eruzione dell'Etna. Rivista di Mineralogia e Cristallografia Italiana 12:61-63.

Barus, C. and J.P. Iddings. 1892. Note on the change of electric conductivity observed in rock magmas of different composition in passing from liquid to solid. American Journal of Science 144:242-249.

Bockris, J. O'M., J.A. Kitchener, S. Ignatowicz and J.W. Tomlinson. 1952. Electric conductance in liquid silicates. Transactions of the Faraday Society 48:75-91.

Brogan, T.R. 1963. Electrical properties of seeded combustion gases. In: Progress in astronautics and aeronautics, Vol. 12. Ionization in high-temperature gases, ed. by Kurt E. Shuler, New York, Academic. p. 319-345.

Bruggeman, D.A.G. 1935. Berechnung verschiedener physikalischer Konstante von heterogenen Substanzen. Annalen der Physik 24:636-679.

Carslaw, H.S. and J.C. Jaeger. 1959. Conduction of heat in solids. 2d ed. Oxford, Clarendon. 386 p.

Chapman, Sidney. 1968. Distinguished Visiting Professor of Astro-Geophysics, High Altitude Observatory, University of Colorado. Private communication. Boulder, January.

Cumin, G. 1954. L'eruzione laterale etnea del novembre 1950-dicembre 1951. Bulletin Volcanologique, ser. 2, 15:1-70.

de Fiore, O. 1922. Studi sull'esalazione vulcanica. Acireale, Coi Tipi Cozzolino. 393 p.

Dickson, W.R. and E.B. Dismukes. 1962. Electrolysis of FeO-CaO-SiO$_2$ melts. Transactions of the American Institute of Mining and Metallurgical Engineers 224:505-512.

Eitel, Wilhelm. 1954. The physical chemistry of the silicates. Chicago, University of Chicago. 1592 p.

Elliot, John F., Molly Gleiser and V. Ramakrishna. 1963. Thermochemistry for steelmaking, Vol. 2. Reading, Addison Wesley. 846 p.

Elskens, I., H. Tazieff and F. Tonani. 1964. A new method for volcanic gas analysis in the field. Bulletin Volcanologique, ser. 2, 27:1-4.

Endell, K. and H. Helbrügge. 1967. The electrical conductance of molten alkali silicates. Physics and Chemistry of Glasses 8:101-111.

England, A. W., Gene Simmons and D. Strangway. 1968. Electrical conductivity of the moon. Journal of Geophysical Research 73:3219-3226.

Francaviglia, Antonino. 1961. L'imbasimenti sedimentario dell'Etna e il golfo pre-etneo. Bolletino del Servizio Geologico d'Italia 81:593-684.

Friedlander, I. 1918. Regelmassigkeit der abstande vulkanischer Eruptionszentren. Zeitschrift für Vulkanologie 4:15-32.

Hughes, H. 1955. The pressure effect on the electrical conductivity of peridot. Journal of Geophysical Research 60:187-191.

Imbò, G. 1928. Variazione cicliche nella successione dei periodi di riposo etnea. Bulletin Volcanologique 5(15-18):80-88.

_____ 1964. Sulla viscosità magmatica. Stromboli, Rivista di Vulcanologia 10:35-47.

_____ 1965. Catalogue of the active volcanoes of the world: Part XVIII, Italy. Rome, International Association of Volcanology. 71 p.

Jaeger, J. C. 1950. Conduction of heat in a solid with a power law of heat transfer at the surface. Proceedings of the Cambridge Philosophical Society, ser. A, 46:634-642.

Jagger, T. A. 1920. Seismometric investigations of the Hawaiian lava column. Bulletin of the Seismological Society of America 10:155-275.

_____ 1931. Volcanic cycles and sunspots. The Volcano Letter, no. 326, p. 1-3.

Johannson, Albert. 1931. A descriptive petrography of the igneous rocks. Chicago, University of Chicago. 4 vols.

Johnston-Lavis, H. J., G. Platania, C. Sambon, P. Zezi and A. Johnston-Lavis. 1891. The South Italian volcanoes. Naples, F. Furchheim. 342 p. (Cited in: de Margerie, Emmanuel. 1896. Catalog des Bibliographies Geologiques. Paris, Gauthier-Villars et Fils. 733 p.)

Keller, George V. and Frank C. Frischknecht. 1966. Electrical methods in geophysical prospecting. New York, Pergamon. 519 p.

Khitarov, N. I. and A. B. Slutskiy. 1965. The effect of pressure on the melting temperatures of albite and basalt (based on electro-conductivity measurements). Geochemistry 12:1395-1403 (translated from Geokhimiya)

Lahiri, B. N. and A. T. Price. 1939. Electromagnetic induction in non-uniform conductors and the determination of the conductivity of the earth from terrestrial magnetic variations. Philosophical Transactions of the Royal Society, London, ser. A, 237:509-540.

Lee, D. W. and W. D. Kingery. 1960. Radiation energy transfer and thermal conductivity of ceramic oxides. Journal of the American Ceramic Society 43:594-607.

Martin, A. E. and Gerhard Derge. 1943. The electrical conductivity of molten blast-furnace slags. Metals Technology August 1943:1-11. (American Institute of Mining and Metallurgical Engineers Technical Publication no. 1569)

Maxwell, J. C. 1881. A treatise on electricity and magnetism. 2d ed. Oxford, Clarendon. 435 p.

McConnell, R. K., L. A. McClaine, D. W. Lee, J. R. Aronson and R. V. Allen. 1967. A model for planetary igneous differentiation. Reviews of Geophysics 5:121-172.

Melton, F. A. 1931. Joint structures in the south west and their bearing on tectonic history. Bulletin of the Geological Society of America 42:231-248.

Meredith, Robert Eugene. 1959. Studies on the conductivities of dispersions. Doctoral dissertation. Berkeley, University of California. 133 numb. leaves.

Moore. G. E. 1963. Experimental studies of some electrical properties of seeded flame gases. In: Progress in astronautics and aeronautics, Vol. 12. Ionization in high-temperature gases, ed. by Kurt E. Shuler, New York, Academic. p. 347-377.

Nagata, Takesi. 1937. Some physical properties of the lava of volcanoes Asama and Mihara. I. Electrical conductivity and its temperature coefficient. Bulletin of the Earthquake Research Institute, University of Tokyo 15:663-672.

Narbone, A. 1850-1855. Bibliografia Sicola sistematica o apparato metodico alla storia letteraria delle Sicilie. Palermo, G. Pedona. 4 vols. (Cited in: de Margerie, Emmanuel. 1896. Catalog des Bibliographies Geologiques. Paris, Gauthier-Villars et Fils. 733 p.)

Noritome, Kazuo. 1955. Studies on the change of electrical conductivity with temperature of a few silicate minerals. Science Reports of Tohoku University, ser. 5, 6:119-125.

Oddone E. 1910. L'eruzione etnea del marzo-aprile 1910. Bolletino della Società Sismologica Italiana 14:6-14.

Owen, A. E. 1961. Properties of glasses in the system CaO-B_2O_3-Al_2O_3. Physics and Chemistry of Glasses 2:152-162.

Palmason, G. and S. Bjornsson. 1966. Geothermal Department, State Electricity Authority. Private communication. Reykjavik.

Perret, F. A. 1950. Volcanological observations. Washington, Carnegie Institution of Washington. 162 p.

Platania, Giovanni. 1922. Temperatura di lave fluenti dell'Etna. Rendiconti e Memorie delle R. Academie di Scienze, Lettera ed Arti degli Zelanti (Acireale), ser. 3, 10:23-25.

Poole, H. Gordon. 1967. Research Director, U. S. Bureau of Mines. Private communication. Albany, August.

Rikitake, Tsuneji. 1952. Electrical conductivity and temperature in the earth. Bulletin of the Earthquake Research Institute, University of Tokyo 30:13-24.

Rittmann, A. 1962. On the mechanism of persistent volcanic activity. Bulletin Volcanologique, ser. 2, 24:301-313.

_____ 1963a. Les volcans et leur activité, tr. by Haroun Tazieff. Paris, Masson et Fils. 461 p.

_____ 1963b. Vulkanismus und Tektonik des Ätna. Geologischen Rundschau 53:788-800.

Ryabinin, Y. N. 1959. Gases at high densities and temperatures, tr. by H. K. Zienkiewicz. New York, Pergamon, 1961. 52 p.

Sartorius, F. v. Waltershausen, Wolfgang. 1880. Der Aetna. Leipzig, W. Engelmann. 2 vols.

Shenker, Henry. 1955. Reference tables for thermocouples. Washinton, D. C. 84 p. (National Bureau of Standards Circular 561)

Silvestri, Orazio. 1869. Der Ätna in dem Jahren 1863-1866. Stuttgart, Schweizerbart. 57 p.

Sonder, R. A. 1936. Grosstektonische Probleme des mittel amerikanischen Raumes. Zeitschrift für Vulkanologie 17:1-34.

Stramondo, Antonino. 1962. Sicilia. Bibliografia Geologica D'Italia 8:1-324.

Sunde, Erling Ditlef. 1949. Earth conduction effects in transmission systems. New York, Van Nostrand. 373 p.

Tagg, G. F. 1964. Earth resistances. New York, Pitman. 258 p.

Taylor, H. E. 1959. Electrical conductivity in soda-lime-silica glasses. Journal of the Society of Glass Technology 43:124-128.

Tazieff, Haroun (ed.). 1963. Les volcans at leur activité. Paris, Masson et Fils. 461 p. (translated from Rittman, A. 1959. Die Vulkane und ihre Tätigkeit)

_____ 1968. Secrétariat, Institut International de Recherches Volcanologiques, Catania. Private communication. Paris, June 13.

Tazieff, Haroun and F. Tonani. 1963. Fluctuations rapides et importantes de la phase gazeuse éruptive. Comptes Rendus de l'Academie de Science (Paris) 257:3985-3987.

Tickle, R. E. 1967. The electrical conductivity of molten alkali silicates: Theoretical discussion. Physics and Chemistry of Glasses 8:112-124.

Toropov, N. A. and B. A. Bryantsev. 1965. The physicochemical properties and crystallization of melts in the system magnesium oxide-ferrous oxide-silica. In: The structure of glass, Vol. 5. Structural transformations in glasses at high temperatures, ed. by N. A. Toropov and E. A. Porai-Koshits, tr. by E. B. Uvarov, New York, Consultants Bureau. p. 178-200.

Tjia, H. D. 1968. Volcanic lineaments in the Indonesian island arcs. Bulletin Volcanologique, ser. 2, 31:85-96.

Urnes, S. 1959. Conduction mechanisms in Li_2O-SiO_2 melts. Glass Industry 237:105-116.

Veltri, R. D. 1963. The electrical resistivity of solid and molten fused silica. Physics and Chemistry of Glasses 4:221-228.

Verhoogen, J. 1951. The mechanics of ash formation. American Journal of Science 249:729-739.

Wait, James R. 1959. Overvoltage research and geophysical applications. New York, Pergamon. 158 p.

Wait, James R. and A. M. Conda. 1958. On the measurement of ground conductivity at VLF. Institute of Radio Engineers, Transactions on Antennas and Propagation AP-6:273-277.

Walker, G. P. L. 1967. Thickness and viscosity of Etnean lavas. Nature 213:484-485.

Washington, H. S., M. Arousseau and Mary G. Keyes. 1926. The lavas of Etna. American Journal of Science, ser. 5, 12:371-408.

Watt, A. D. 1967. VLF radio engineering. New York, Pergamon. 701 p.

Watt, A. D., F. S. Mathews and E. L. Maxwell. 1963. Some electrical characteristics of the earth's crust. Proceedings of the Institute of Electrical and Electronic Engineers 51:897-910.

Weynarth, Axel. 1934a. The current conducting properties of slags in electric furnaces. Part I. Transactions of the Electrochemical Society 65:177-187.

_____ 1934b. The current conducting properties of slags in electric furnaces. Part II. Transactions of the Electrochemical Society 66:329-343.

Wenner, Frank. 1916. A method of measuring earth resistivity. Bulletin of the Bureau of Standards 12:469-478. (U. S. Bureau of Standards. Scientific Paper no. 258)

Wood, H. O. 1917. On cyclical variations in eruption at Kilauea. Cambridge, Massachusetts Institute of Technology. 59 p. (Hawaiian Volcano Observatory. Second [Special] Report)

Zachariasen, W. H. 1932. The atomic arrangement in glass. Journal of the American Chemical Society 54:3841-3851.

APPENDICES

APPENDIX I

| 2114 CURTIS STREET | | | | | | | TELEPHONE 623-1652 |

CHARLES O. PARKER & CO.

CHEMISTS • ASSAYERS • ENGINEERS
DENVER, COLORADO 80205

Folio   9193

Date July 29, 1968.

Frank Mathews,
c/o Oceanography Department (Geophysics)
Oregon State University,
Corvallis, Oregon. 97330

We hereby Certify, that the samples assayed for you gave the following results:

DESCRIPTION	GOLD OUNCES PER TON	SILVER OUNCES PER TON	COPPER PER CENT (WET)	LEAD PER CENT (WET)	ZINC PER CENT	IRON PER CENT	INSOLUBLE PER CENT	VALUE PER TON
			Basalt 1 piece:		Thursday 12th sample:		Friday 13th sample:	
Loss on ignition - - - - - - -			0.48%		1.25%		0.06%	
Silica (SiO2)- - - - - - - -			45.84%		46.60%		46.20%	
Alumina (Al2O3) - - - - - - -			20.07%		19.10%		19.62%	
Iron as Fe2O3 - - - - - - - -			2.96%		2.71%		2.28%	
Iron as FeO - - - - - - - - -			8.78%		8.63%		9.27%	
Lime (caO) - - - - - - - - -			9.65%		11.10%		9.60%	
Magnesia (MgO) - - - - - - -			3.70%		4.20%		4.35%	
Soda (Na2O) - - - - - - - -			5.80%		4.19%		5.17%	
Potash (K2O) - - - - - - - -			1.73%		1.26%		2.32%	
also shows:								
Copper (Cu) - - - - - - - - -			0.034%		0.020%		0.025%	
Zinc (Zn) - - - - - - - - -			0.020%		0.017%		0.023%	
Lead (Pb) - - - - - - - - -			0.016%		0.021%		0.038%	
Nickel (Ni) - - - - - - - - -			0.008%		0.004%		0.009%	
Titanium as TiO2 - - - - - -			0.685%		0.601%		0.751%	
Manganese (Mn) - - - - - -			0.10%		0.10%		0.12%	
Barium as BaO - - - - - - -			0.146%		0.166%		0.135%	
Phosphorus - - - - - - - - -			TRACE		TRACE		TRACE	

Gold at_____per ounce   Copper at_____per unit

Silver at_____per ounce   Zinc at_____per unit

Lead at_____ per unit   _____

Charge $ 75.00
paid

CHARLES O. PARKER & CO.
CHEMISTS, ASSAYERS and ENGINEERS

CaO, Fe_2O_3, FeO, MgO, Na_2O, K_2O, SiO_2, Al_2O_3, TiO_2, BaO

APPENDIX II

Ancillary Bibliography

In the future it is quite possible that investigators may attempt to improve eruption prediction techniques for Mt. Etna by making electrical conductivity soundings on the pyromagma in the conduit. If magma level, temperature, or gas content are to be inferred from these soundings, interpretation accuracy would be enhanced by any knowledge of details of the geologic structure of Etna. With this application in view, a list of pertinent publications giving details of previous eruptions would be highly desirable.

Prior to 1891 the literature on Etna was summarized in the excellent and extensive bibliographies by Johnston-Lavis et al. (1891) and Narbone (1850) cited by de Margerie (1896). Since that time, however, no bibliography relating specifically to Etna has been produced, although the extensive bibliography by Stramondo (1962) on the geology of Sicily does list many of the more recent publications on Etna. However, it suffers from many omissions and inaccuracies. A more carefully scrutinized list is therefore presented here which includes: (a) references prior to 1891 which are still used frequently, (b) references since 1891 but missing from Stramondo's bibliography, (c) references cited erroneously by Stramondo, and included here in corrected form. Although quite naturally, the bulk of these

publications is in Italian journals, they are all available in libraries

in this country with the exception of those few marked by an aster-

isk (*).

Alessi, G. 1835. Storia critica delle eruzioni dell'Etna. Atti della
    Accademia Gioenia di Scienze Naturali (Catania), ser. 1,
    9:121-206.

Amore, A. 1906. Sull'Etna. Catania, Gianotta. 200 p.

Arcidiacono, S. 1899. L'esplosione centrale dell'Etna del 19
    luglio 1899. Bollettino della Società Sismologica Italiana 5:12.

_____ 1910. L'eruzione etnea del 1910. Parte prima:
    L'Etna dal 1 gennaio 1893 al 31 maggio 1906, sotto il punto di
    vista geodinamico-eruttivo. Atti della Accademia Gioenia di
    Scienze Naturali (Catania), ser. 5, 4(17):65.

Castiglione, M. 1958a. Il carattere seriale delle lave etnee.
    Stromboli, Rivista di Vulcanologia, no. 6, p. 30-32.

_____ 1958b. Sulla natura delle volcaniti della zona etnea.
    Bollettino delle Sedute dell'Accademia Gioenia di Scienze
    Naturali in Catania, ser. 4, 4(6):325-342.

Cucuzza Silvestri, S. 1948. Stato del cratere centrale dell'Etna nel
    gennaio 1948. Bollettino delle Sedute dell'Accademia Gioenia
    di Scienze Naturali in Catania, ser. 4, 1:74-77.

_____ 1949. L'eruzione dell'Etna del 1947. Parte I:
    Fenomeni eruttivi. Bulletin Volcanologique, ser. 2, 9:81-111.

_____ 1957a. L'attività eruttiva dell'Etna nei primi mesi
    del 1957 (gennaio-maggio). Bollettino delle Sedute dell'
    Accademia Gioenia di Scienze Naturali in Catania, ser. 4, 4:3-
    31.

_____ 1957b. L'Etna nel 1956. Atti della Accademia
    Gioenia di Scienze Naturali (Catania), ser. 6, 11:29-98.

_____ 1960. Attività esplosiva dell'Etna nel 1960.
    L'Universo 40(5):957-964.

Cumin, G. 1943. Appunti sull'eruzione laterale etnea del 30 giugno 1942. Bollettino della Società Geografica Italiana (Roma), ser. 7, 8:10.

_____ 1950. L'eruzione etnea del dicembre 1949. Bollettino della Società Geografica Italiana (Roma), ser. 8, 84(3): 323-334.

_____ 1953. L'eruzione laterale etnea del dicembre 1949. Bollettino delle Sedute dell'Accademia Gioenia di Scienze Naturali in Catania, ser. 4, 2:301-307.

_____ 1955. Su l'attività eruttiva terminale dell'Etna, iniziatasi il 25 giugno 1955. Stromboli, Rivista di Vulcanologia, no. 4, p. 3-9.

D'Arrigo, A. 1951. La recente eruzione dell'Etna. L'Universo 31(2):157-168.

de Fiore, O. 1911a. Il periodo Hawaiano dell'Etna nel 1910-1911. Rivista Geografica Italiana 18(4):8.

_____ 1911b. L'eruzione etnea del 1910. Parte quarta: visite al teatro eruttivo. Atti della Accademia Gioenia di Scienze Naturali (Catania), ser. 5, 4:47-51.

* _____ 1912. Il periodo di riposo dell'Etna (1893-1907). Rendiconti e Memorie della R. Accademia di Scienze, Lettere ed Arti degli Zelanti (Acireale), ser. 3, 6:57-128.

_____ 1920. L'eruzione radiale dell'Etna del novembre 1918. Bollettino delle Sedute dell'Accademia Gioenia di Scienze Naturali in Catania, ser. 2, 48:52-56.

_____ 1925. I fenomeni eruttivi e sismici avvenuti all' Etna dal 1919 al 1923. Annali del R. Osservatorio Vesuviano (Napoli), ser. 3, 2:59-103.

_____ 1928. Sistemi eruttivi etnei. Bulletin Volcanologique, nos. 15-18, p. 89-119.

di Franco, S. 1928. The recent eruption of Etna. Nature 122:926-928.

_____ 1930. Ricerche petrografiche sulle lave dell'Etna. Atti della Accademia Gioenia di Scienze Naturali (Catania), ser. 5, 17:120.

*di Lorenzo, Giuseppe. 1907. L'Etna. Bergamo, Istituto Italiano d'Arti Grafiche. 154 p.

Ferrare, F. 1818. Descrizioni dell'Etna con la storia dell eruzioni ed il catalogo dei prodotti. Palermo, L. Dato. 256 p.

Franzina, U. 1953. Ricognizioni ed osservazioni effetuati in occasione della eruzione dell'Etna del 2-12-1949 versante sudovest. Stromboli, Rivista di Vulcanologia, no. 2, p. 26-29.

Friedlander, I. 1923. Der Aetnaausbruch 1923. Zeitschrift für Vulkanologie 7:188-192.

_____ 1929. Der Ätna-ausbruch 1928. Zeitschrift für Vulkanologie 12:33-46.

Gentile-Cusa, B. 1886. Relazione sulla eruzione dell'Etna di maggio-giugno 1886. Catania, Martinez. 216 p.

Gurich, G. 1929. Der Ätna-ausbruch im November 1928. Mitteilungen der Geographischen Gesellschaft 4:166-180.

Guzzanti, C. 1929. L'eruzione dell'Etna ed i fenomeni sismici. Bollettino delle Sedute dell'Accademia Gioenia di Scienze Naturali in Catania, ser. 2, 59:29-30.

Haeni, Curt. 1930. Das Eruptionstheater im hohen Teil des Valle del Leone vom 1. Ausbruchstag der November-eruption des Etna 1928. Zeitschrift für Vulkanologie 13(1):54-55.

_____ 1931. Tätigkeit und Veränderungen am Etna seit dem Ausbruch von 1928 bis Ende 1930. Zeitschrift für Vulkanologie 13(4):245-248.

_____ 1932. Nachtrichtendienst über vulkanische Ereignisse. Zeitschrift für Vulkanologie 14(3):244-245.

_____ 1934. Der Zustand des Ätna im Frühjahr 1934. Zeitschrift für Vulkanologie 16(1):51-54.

_____ 1938. Neues vom Ätna. Zeitschrift für Vulkanologie 17(4):280-283.

Hamilton, William. 1773. Observations on Mt. Vesuvius, Mt. Etna, and other volcanoes. London, T. Cadell. 179 p.

Hantke, G. 1959. Übersicht über die vulkanische Tätigkeit 1954-1956. Bulletin Volcanologique 20:1-33.

Imbò, G. 1928a. Sistemi eruttivi etnei. Bulletin Volcanologique 5(15-18):1-31.

_____ 1928b. Osservazioni e ricerche in relazione all' eruzione etnea 2-20 novembre 1928. Bulletin Volcanologique 5(15-18):31-59.

_____ 1928c. Terremoti della regione orientale etnea. Bulletin Volcanologique 5(15-18):221-238.

_____ 1934. L'attività eruttiva e sismica dell'Etna dal novembre 1928 a tutto il 1933. Annali del R. Osservatorio Vesuviano (Napoli), ser. 4, 2:279-283.

* _____ 1935. I terremoti etnei. Pubblicazioni. Commissione Italiana per lo Studio e la Prevenzione delle Grandi Calamità, (Accademia dei Lincei) (Roma) 5(1):93.

_____ 1947. Considerazioni a proposito delle recenti eruzioni etnee. Bollettino della Società di Naturalisti in Napoli 56:16.

_____ 1948. A proposito di un analisi termica relativa a lava etnea del 1947. Rendiconti della Accademia delle Scienze, Fisiche, e Matematiche (Napoli), ser. 4, 15:6.

_____ 1951. Temperature d'irrigidimento di attuali lavi etnee. Rendiconti della Accademia delle Scienze, Fisiche, e Matematiche (Napoli), ser. 4, 18:4.

_____ 1955. Nécrologie: Francesco Stella Starabba. Bulletin Volcanologique, ser. 2, 16:251-268.

_____ 1959a. Quelques considerations sur le tension magmatique, et sur le temperature d'irrigidimente. Bulletin Volcanologique, ser. 2, 22:125-133.

_____ 1959b. Considerazioni sui fenomeni sismici e vulcanici. Annali del R. Osservatorio Vesuviano, (Napoli), ser. 6, 3:27-54.

Imbò, G. and G. Luongo. 1964. Coefficienti di viscosità del magma etneo. Annali del R. Osservatorio Vesuviano, (Napoli), ser. 6, 6:14.

Johnston-Lavis, Henry James and A. Johnston-Lavis. 1918. Bibliography of the geology and eruptive phenomena of the more important volcanoes of southern Italy. 2d ed. London, University of London. 375 p.

Klerx, J. 1962. Le volcanism ancien de l'Etna. Annales de la Société Géologique de Belgique (Liege) 85(5):175-180.

Maier, W. 1929. Beitrag zur Morphologie des Ätna. Zeitschrift für Geomorphologie 4(5):241-254.

_____ 1931. Beitrag zur Morphologie des Ätna. II Beit. Zeitschrift der Deutschen Geologischen Gesellschaft 83:215-223.

_____ 1937. Beitrag zur Morphologie des Ätna. III Beit. Zeitschrift der Deutschen Geologischen Gesellschaft 88:326-338.

Maranca, F. 1944. Il rilievo fotogrammetrico delle zona etnea. L'Universo 14(11):837-847.

Mercalli, Giuseppe. 1883. Vulcani e fenomeni vulcanici in Italia. Geologia d'Italia, Parte Terza. Milano, F. Vallardi. 374 p.

Pieruccini, R. 1955. Una visita ai crateri di Vulcano, dello Stromboli e dell'Etna. Stromboli, Rivista di Vulcanologia, no. 4, p. 10-18.

Platania, G. 1916. Sul periodo sismico maggio 1914 nella regione orientale dell'Etna. Zeitschrift für Vulkanologie 3(1):59-61.

_____ 1924. L'attività dell'Etna nei primi anni del Secolo XX. Bulletin Volcanologique 1(1):13-25.

Ponte, G. 1910. Studi sull'eruzione etnea del 1910. Atti della Accademia Nazionale dei Lincei. Memorie, ser. 5, 8:663-694.

_____ 1913. Sulla indipendenza delle acque sotteranea dell'Etna dalle precipitazioni atmosferiche. Atti della Accademia Nazionale dei Lincei. Rendiconti, ser. 5, 22:502-507.

_____ 1914. Meccanismo delle eruzioni etnee. Zeitschrift für Vulkanologie 1(1):9-19.

_____ 1919. Il cratere centrale dell'Etna, suoi cambiamenti e sue eruzione. Atti della Accademia Gioenia di Scienze Naturali (Catania), ser. 5, 12(3):12.

_____ 1924. Le recenti eruzioni dell'Etna, Parte 7. I fenomeni eruttivi. Rivista Italiana di Vulcanologia 1:1-27.

_____ 1926. L'Etna dall'agosto 1923 a tutto il 1925. Bulletin Volcanologique 3(9, 10):219-222.

* _____ 1929a. L'eruzioni dell'Etna del novembre 1928 e l'Istituto Vulcanologico Etneo. Venice. 7 p. (Comitato Nazionale Italiano Geodetico-Geofisico. Bulletino no. 17)

_____ 1929b. La eruzione etnea del novembre 1928. Rivista di Fisica, Matematica, e Scienze Naturali 3(5):113-122.

_____ 1930. Le recenti eruzioni dell'Etna. (Nuove ricerche vulcanologiche) Bollettino della Società Geografica Italiana (Roma) 6:21-28.

_____ 1933. Attività del'Etna negli anni 1926, 1927 e 1928. Bulletin Volcanologique 5:73-79.

_____ 1936. Utilità practica degli studi vulcanologici sull'Etna. Bollettino delle Sedute dell'Accademia Gioenia di Scienze Naturali in Catania, ser. 3, 1:6-10.

_____ 1937. Rapporto riassuntivo dei fenomeni osservati sull'Etna dal 1934 al 1936. Bulletin Volcanologique, ser. 2, 1:193-200.

_____ 1949. Sull'eruzione etnea del 1950-51. Bulletin Volcanologique, ser. 2, 13:121-128.

Reck, H. 1928. Über die Tätigkeit von Etna und Vesuv im Herbst 1928. Zeitschrift der Deutschen Geologischen Gesellschaft 80:345-352.

Ricco, A. and S. Arcidiacono. 1904. L'eruzione dell'Etna nel 1892. Atti della Accademia Gioenia di Scienze Naturali (Catania), ser. 4, 17:51.

Rittmann, Alfredo. 1929. Der Ätna und seine Laven. Die Naturwissenschaften 17:84-100.

_____ 1958. Sulla determinazione quantitativa delle serie magmatische. Stromboli, Rivista di Vulcanologia, no. 6, p. 3-10.

Rodwell, G. F. 1878. Etna, a history of the mountain and its eruptions. London, C. Kegan Paul. 25 p.

Sapper, K. 1917. Beiträge zur Geographie der tätigen Vulkane. Zeitschrift für Vulkanologie 3(4):65-197.

Sieberg, A. 1913a. Bau und Bild des Ätna sowie seine Eruptionen der Jahre 1910 und 1911. Naturwissenschaftliche Wochenschrift 12(32):23.

_____ 1913b. Fliesserde am Gipfelkegel des Ätna. Beiträge zur Geophysik 12(2):162-176.

Silvestri, Orazio. 1865. Sulla eruzione dell'Etna del 1865: studii geologici e chemici. Nuovo Cimento 21:167-184.

_____ 1879. Un viaggio all'Etna. Torino, Loescher. 232 p.

Stella Starabba, F. 1913. Contributo allo studio del carbonati di sodio delle lave dell'Etna. Rivista di Mineralogia e Cristallografia Italiana (Padova) 42:19.

_____ 1933. Sulle lave dell'eruzione dell'Etna del 1928. Le variazioni della composizione chimica durante il periodo effusivo. Bulletin Volcanologique 5:56-69.

Tazieff, Haroun. 1951. L'Etna et son éruption actuelle. Bulletin de la Société Belge de Géologie, de Paleontologie, et d'Hydrologie (Bruxelles) 60:320-326.

Vinassa de Regny, P., A. Ricco, S. Arcidiacono, F. Stella Starabba, L. Taffara and O. de Fiore. 1912. L'eruzione etnea del 1910. Atti della Accademia Gioenia di Scienze Naturale (Catania), ser. 5, 4(20):53-57.

von Wolff, F. 1914. Der Vulkanismus. Stuttgart, F. Enke. 2 vols.

APPENDIX III

Lunisolar Influence on Eruptions

As another approach to volcano eruption prediction, several attempts have been made to relate the onset of volcanic eruptions to the increased crustal strains associated with earth tides at syzygy, perigee, perihelion, or combinations of these three. Most notable have been the analyses of Jagger (1920, 1931) on Hawaii, and Perret (1950) on Stromboli. Wood (1917) also reports effects from the nutation strain resulting from the inclination of the earth's rotational axis to the plane of the ecliptic and the plane of the moon's orbit. Jagger's and Wood's observations are based on the height of the Kilauea lava column and show a definite lunar semimonthly influence and a less pronounced semiannual control. Perret claims that the undefined quantity "volcanic activity" shows a pronounced increase at full and new moon. Perret also ventures a subjective opinion that activity on Mt. Etna is influenced in similar fashion.

The following lunar tables and Etna activity summary shown in Tables A-1 and A-2 and the bar graph shown in Figure A-1 provide an objective reinforcement of Perret's subjective views. Since, of necessity, data on the eruptive activity of a particular volcano accumulate very slowly, and since the "signal" under study will most certainly be obscured by "noise," many such analyses will be necessary before definite conclusions can be drawn.

Table A-1. Dates of the full moon, 1900-1960 (Chapman, 1968).

Year	Jan	Feb	March	April	May	June	July	Aug	Sept	Oct	Nov	Dec
1900	16	14	16	14	14	12	12	10	9	8	7	6
01	5	3	5	3	3	2	1, 31	29	28	27	26	25
02	24	22	24	22	22	20	20	19	17	17	15	15
03	13	12	13	12	11	10	9	8	6	6	4	4
04	3	1	2, 31	30	29	28	27	26	24	24	22	22
05	20	19	20	19	19	17	17	15	14	13	12	11
06	10	8	10	8	8	6	6	5	3	3	1	1, 30
07	29	27	29	27	27	25	25	23	22	21	20	20
08	18	17	17	16	15	14	13	12	10	10	9	9
09	6	5	6	5	5	3	3	1, 31	29	29	27	27
1910	25	24	25	24	23	22	22	20	19	18	17	16
11	15	13	15	13	13	11	11	9	8	7	6	6
12	4	3	3	2	1, 31	29	29	27	26	25	24	23
13	22	20	22	21	20	19	18	17	15	15	13	13
14	11	10	11	10	9	8	7	6	5	4	3	2
15	1, 30		1, 30	29	28	27	26	25	23	23	22	21
16	20	18	19	17	17	15	15	13	12	11	10	9
17	8	6	8	7	6	5	4	3	1	1, 30	29	28
18	27	25	27	25	25	23	23	22	20	20	18	18
19	16	15	16	15	14	13	12	11	9	9	8	7
1920	6	4	5	3	3	1	1, 30	29	27	27	25	25
21	23	22	24	22	22	20	20	18	17	16	15	14
22	13	11	13	11	11	9	9	8	6	6	4	4
23	2	1	2	1, 30	30	28	28	26	25	25	23	23
24	21	20	20	19	18	17	16	15	13	13	11	11
25	9	8	10	8	8	6	6	4	3	2	1, 30	30
26	28	27	28	27	26	25	25	23	22	21	20	19
27	18	16	18	16	16	14	14	12	11	11	9	9
28	7	6	6	5	4	3	2	1, 30	29	28	27	26
29	25	24	25	24	23	22	21	20	18	18	16	16
1930	14	13	14	13	12	11	11	9	8	7	6	5
31	4	2	4	2	2, 31	30	29	28	27	26	25	24
32	23	21	22	20	20	18	18	16	15	14	13	12
33	11	10	11	10	9	8	7	6	4	4	2	2, 31
34	30	28	30	28	28	27	26	25	23	23	21	21
35	19	18	19	18	17	16	15	14	13	12	11	10
36	9	7	8	6	6	4	4	2	1, 30	30	28	28
37	27	25	27	25	25	23	23	21	20	19	18	17
38	16	14	16	14	14	13	12	11	9	9	7	7
39	5	4	5	4	3	2	1, 31	30	28	28	26	26

(Continued)

Table A-1. Continued.

Year	Jan	Feb	March	April	May	June	July	Aug	Sept	Oct	Nov	Dec
1940	24	23	23	22	21	20	19	18	16	16	14	14
41	13	11	13	11	11	9	9	7	6	5	4	3
42	2, 31		2, 31	30	30	28	28	26	25	24	23	22
43	21	19	21	19	19	17	17	16	14	14	12	12
44	10	9	9	8	7	6	5	4	2	2, 31	30	30
45	28	27	28	27	26	25	24	23	21	21	19	19
46	17	16	17	16	16	14	14	12	11	10	9	8
47	7	5	7	5	5	3	3	2, 31	30	29	28	27
48	26	24	25	23	23	21	21	19	18	17	16	16
49	14	13	14	13	12	11	10	9	7	7	5	5
1950	3	2	3	2	2, 31	30	29	28	26	26	24	24
51	22	21	22	21	20	19	19	17	16	15	14	13
52	12	10	11	9	9	7	7	5	4	3	2	2, 31
53	30	28	30	28	28	26	26	24	23	22	21	20
54	19	17	19	18	17	16	15	14	12	12	10	10
55	8	7	8	7	6	5	5	3	2	1, 31	29	29
56	27	26	26	25	24	23	22	21	19	19	18	17
57	16	14	16	14	14	12	12	10	9	8	7	6
58	5	3	5	4	3	2	1, 31	29	28	27	26	25
59	24	22	24	22	22	21	20	19	17	17	15	15
1960	13	12	12	11	10	9	8	7	5	5	4	3

Note: These charts may be extrapolated forwards or backwards with good accuracy by application of the 19 year Metonic cycle.

Table A-2. Relation of onset of Etnean lava flows to syzygy.

| Date of eruption (E)	Date of closest full moon (F)	E-F	Date of eruption (E)	Date of closest full moon (F)	E-F
July 25, 1736	July 25	0	April 26, 1893	May 1	- 5
March 9, 1755	February 27	+10	April 29, 1908	April 16	+13
April 14, 1759	April 13	+ 1	March 23, 1910	March 25	- 2
April 19, 1759	April 13	+ 6	December 27, 1910	December 16	+11
February 5, 1763	January 30	+ 5	May 27, 1911	May 13	+14
June 20, 1763	June 26	- 6	September 9, 1911	September 8	+ 1
April 27, 1766	April 25	+ 2	November 13, 1913	November 13	0
May 18, 1780	May 20	- 2	November 29, 1918	November 18	+11
July 10, 1787	July 1	+ 9	June 16, 1923	June 28	-12
May 11, 1792	May 8	+ 3	February 8, 1929	January 25	+14
November 15, 1802	November 11	+ 4	December 4, 1929	December 16	-12
July 11, 1805	July 12	- 1	September 13, 1930	September 8	+ 5
March 27, 1809	March 31	- 4	September 17, 1930	September 8	+ 9
October 27, 1811	November 1	- 5	September 20, 1930	September 8	+12
May 27, 1819	June 7	-11	September 21, 1930	September 8	+13
March 4, 1831	February 27	+ 5	January 5, 1934	December 31	+ 5
October 31, 1832	November 8	- 9	March 20, 1936	March 8	+12
August 2, 1838	August 6	- 4	April 26, 1936	May 6	-10
November 27, 1842	November 18	+ 9	June 30, 1942	June 28	+ 2
November 17, 1843	November 7	+10	February 21, 1947	March 7	-14
August 20, 1852	August 31	-11	December 2, 1949	December 5	- 3
January 30, 1865	February 12	-13	November 25, 1950	November 24	+ 1
September 26, 1869	September 22	+ 4	July 30, 1953	July 26	+ 4
August 29, 1874	August 28	+ 1	June 29, 1955	July 5	- 6
May 26, 1879	June 5	-10	September 20, 1957	September 9	+11
March 22, 1882	April 3	-12	January 21, 1958	February 3	-13
March 22, 1883	March 24	- 2	April 19, 1958	May 3	-14
May 18, 1886	May 19	- 1	May 5, 1958	May 3	+ 2
July 8, 1892	July 11	- 3			

n = number of eruptive onsets
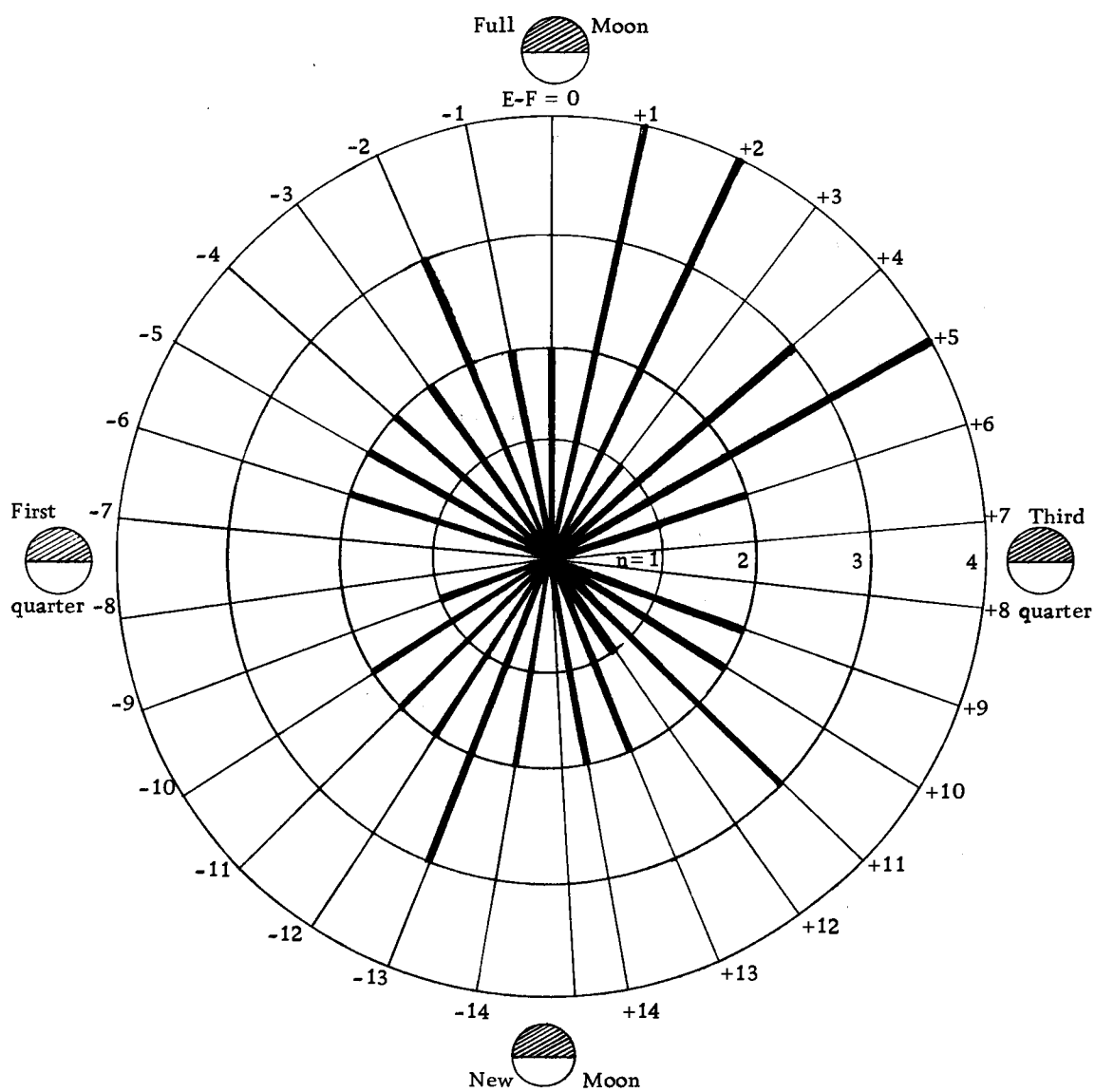
Figure A-I.   Distribution of eruptive onsets of Mt. Etna within the lunar month from 1736 to 1969 A. D.